KINETICS OF TRANSFORMATION OF METASTABLE SILVER-COPPER SOLID SOLUTIONS

Thesis by

Ronald Keith Linde

In Partial Fulfillment of the Requirements

For the Degree of

Doctor of Philosophy

California Institute of Technology

Pasadena, California

1964

(Submitted May 4, 1964)

$$\begin{vmatrix} T & i \\ -i & 0 \end{vmatrix} + \frac{2}{\sqrt{\pi}} \int_0^{\infty} e^{-x^2} dx$$

$$\binom{M}{1} \begin{vmatrix} \hat{\imath} & \hat{\jmath} & \hat{k} \\ A_x & A_y & A_z \\ I_x & I_y & I_z \end{vmatrix} \frac{\Gamma(N+1)}{\Gamma(N)} \lim_{h \to \infty} \left(1 + \frac{1}{h}\right)^h$$

ACKNOWLEDGEMENTS

It is a pleasure to thank Professor Pol Duwez for the untiring help and encouragement which he provided throughout the course of this work. The author also wishes to thank Professor F. S. Buffington for several fruitful discussions.

This writer is greatly indebted to his wife Maxine for her encouragement and for performing numerous computations and to John E. Brown for the preparation of many alloys and metallographic samples. William Satterthwaite and Robert Schaar aided in the performance of experiments and in the reduction of data. Frank Youngkin was responsible for photographic work.

ABSTRACT

Metastable solid solutions were obtained at compositions across the entire range from 0 at. % Ag;Cu to 100 at. % Ag;Cu by rapid-quenching from the liquid state. Lattice parameters were measured by x-ray diffraction in Debye-Scherrer powder cameras. The enthalpy of solution of the 75. 0 at. % Ag;Cu composition was determined calorimetrically and is discussed in relation to the predictions of existing theories.

The process of transformation of the metastable solid solutions into the equilibrium phases was studied by means of x-ray diffraction intensity measurements, electrical resistance measurements, and optical microscopy. Results are compared with those for an alloy quenched from the solid state at a composition which exists as a solid solution at elevated temperatures. Activation energies were computed and are shown to be compatible with a diffusion controlled growth process in which most of the nuclei are present very early in the process. A model for the transformation process is postulated and discussed in terms of experimental results.

Photographic materials on pages 26, 50, 51, 52, 55, 76, 77, 78, 105, and 107 are essential and will not reproduce clearly on Xerox copies. Photographic copies should be ordered.

TABLE OF CONTENTS

I. INTRODUCTION AND HISTORICAL BACKGROUND

The making and use of silver - copper alloys dates back to civilizations which existed well over two thousand years ago. Silver probably was originally alloyed with copper to achieve greater hardness in such items as jewelry, ornaments, and coins. Copper was also added in later times in order to conserve silver. In fact, by the third century A.D., Roman "silver" coins actually contained only about forty per cent silver by weight, the remainder being copper.[1] Although the silver-copper system was one of the first systems subjected to scientific investigation, it was not until the last half of the Nineteenth Century that such investigations were undertaken. The earliest determinations of the solid solubility of silver in copper were made by Matthiessen in 1863[2] and by Matthiessen and Vogt in 1865.[3] The liquidus curve was first published in 1875 by Roberts - Austen,[4] following a calorimetric determination. Since that time the equilibrium phase diagram has been the subject of much investigation, continuing as late as 1949.[5] The first observation of the increased solid solubility of silver in copper at elevated temperatures was recorded by Johansson and J. O. Linde in 1928 on the basis of electrical conductivity measurements.[6] Thus, it was realized that certain silver-copper alloys were age-hardenable. In the same year Norbury[7] studied the

physical properties of quenched and aged standard silver (92.5 wt. %Ag;Cu) and explained his results by the decomposition of the supersaturated solid solution. Although Wilm, using a 95.5 wt. %Al;4%Cu;0.5% Mg Alloy (Duralumin) is generally credited with having discovered age hardening in about 1906,[8],[9] it was not until 1919 that Merica, Waltenberg, and Scott[10] first recognized that solid phase precipitation which was made possible by decreasing solid solubility with temperature was an essential condition for age hardening. The aforementioned observations of Johansson and Linde and of Norbury were thus chronologically situated so as to arouse considerable interest in the silver-copper system. Studies of aging and precipitation in this system are too numerous to recount here, but pertinent references will be cited where appropriate in subsequent sections of this text.

Reference to Fig. 1 indicates that silver and copper form a eutectic system. At room temperature the solid solubilities of copper in silver and of silver in copper are limited to less than 0.1 atomic per cent. It is also evident that there is a miscibility gap extending from 4.9 at. %Ag;Cu to 85.9 at. %Ag;Cu at the eutectic temperature. These compositions constitute the limits of metastable solid solutions obtainable under ordinary conditions of classical quenching. With the development of a new rapid quench technique

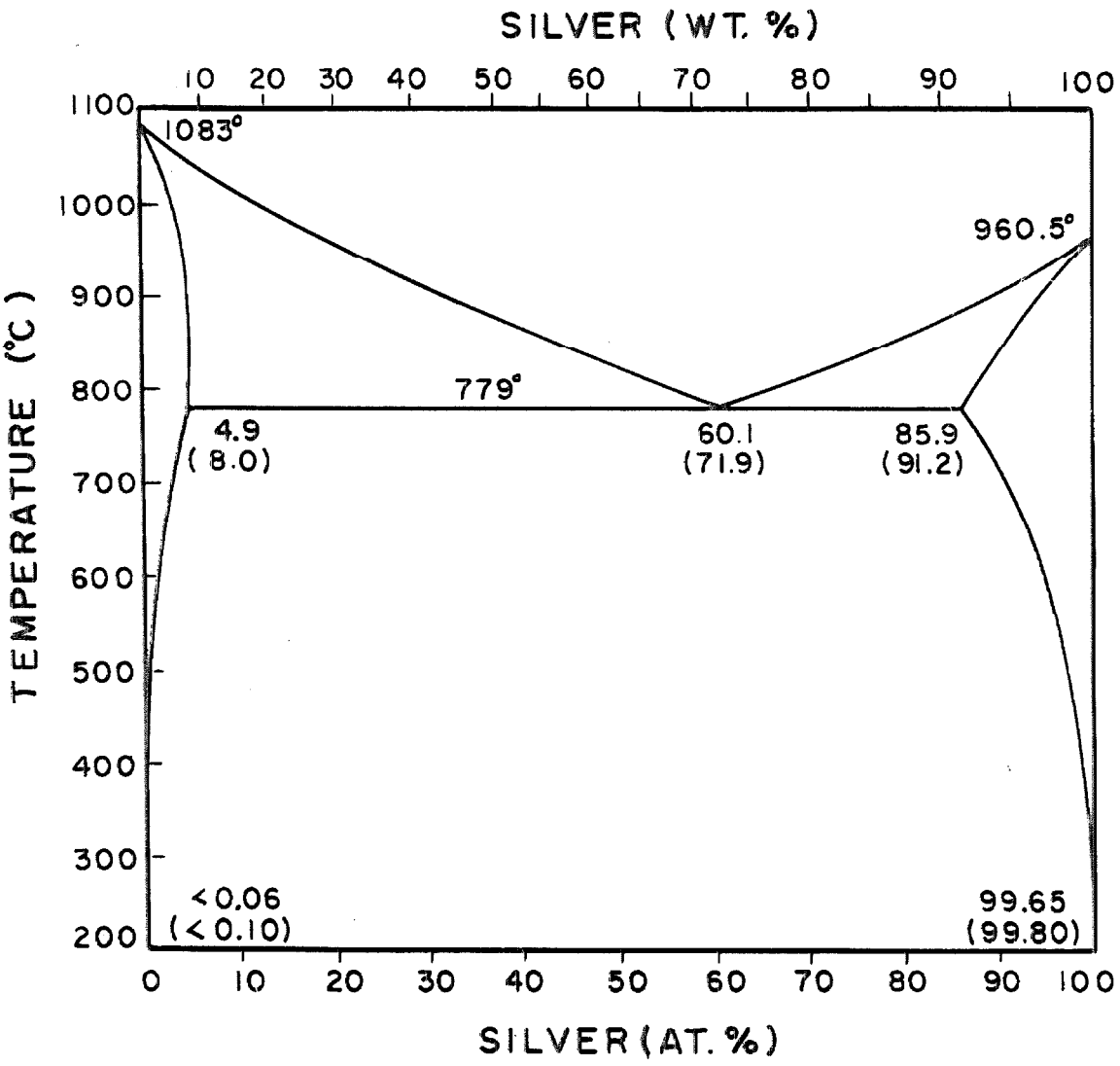

Figure 1. Equilibrium phase diagram of the Ag-Cu system, based upon data compiled by Hansen and Anderko.[11]

by Duwez, et.al., the possibility of extending these limits of solid solubility and, in fact, obtaining complete solubility at all compositions by quenching directly from the melt became a reality.[12] In 1961 Banerjee and Ahuja[13] successfully obtained single phase metastable solid solutions in Ag-Cu alloys in the composition ranges 0-15 at.% Ag;Cu and 80-100 at.% Ag;Cu by electrodeposition; in 1962 Pietrokowsky[14] obtained a single phase solid solution at the eutectic composition by a mechanical piston-and-anvil technique to be described later; and recently Mader, Widmer, d'Heurle, and Nowick[15] obtained complete solid solubility at all compositions by simultaneous vacuum evaporation of Ag and Cu, obtaining films with thicknesses ranging from 600 Å to 1000 Å. Comprehensive systematic studies have not been reported in (13), (14), or (15), however.

The production of such metastable alloys has opened up two avenues of research: 1) investigation of properties of the new metastable compositions, and 2) investigation of the transformation of the new metastable alloys to the stable state. Chapter II of this thesis is concerned with the first category and embodies both a reinvestigation of Klement's work on lattice parameters[16] and an estimation of the enthalpy of solid solution of the metastable 75.0 at.% Ag;Cu composition at room temperature. Chapters III and IV describe an experimental study of the transformation to

equilibrium of two metastable compositions: 75.0 at.% Ag;Cu and 60.1 at.% Ag;Cu (eutectic composition), while Chapter V embodies a theoretical discussion of the initial solidification process and of the subsequent transformation to equilibrium.

Methods for studying solid state transformations are numerous. Generally, they fall into the following main categories, which are considered separately:

Hardness: This is the method which has been most widely used in the study of silver-copper alloys. (See, for example, references (17) and (18).) In fact, hardness, rather than the process of transformation itself, has often been the primary property of interest.[19] In the present investigation hardness did not change appreciably with the degree of transformation, due probably to the overshadowing effect of the fine grain size involved. Thus hardness was not deemed a suitable parameter for studying the transformation.

Electrical Resistance: This parameter has been successfully used by several investigators, including the authors of (17) and (18), and was employed in the present investigation.

Thermoelectric Power: While thermoelectric power has been used as a tool in studies of other systems (see references (20) and (21), for example), its relationship to the degree of transformation is usually erratic and poorly understood. Thermoelectric power of the 75.0 at.% Ag;Cu alloy was measured to be about 43 μ V $/^{o}$K against

Constantan at room temperature, as expected, and did not vary appreciably with degree of transformation, thus making this an unsuitable parameter for the present study.

X-Ray Methods: Lattice parameter measurements are suitable in cases of continuous precipitation, as used, for example, by the authors of (22) and (23). Many other investigators have attempted to use lattice parameter measurements, but have not been able to trace kinetics satisfactorily, due to lack of continuous precipitation. Diffraction peak intensity measurements are suitable in the case of discontinuous precipitation, and were employed in the present investigation

Metallography: Many investigators, such as the authors of (24) and (25), have used metallography as a primary tool in the study of transformations. This approach found suitable application as an auxiliary tool in the present investigation.

Other Methods: Properties such as specific volume,[26] specific heat,[27] yield stress, ductility, and internal friction were deemed less reliable parameters under the conditions of the present study. Of course, magnetic properties are inappropriate for the alloy system under consideration, being limited in general to ferromagnetic alloys.

It should be noted that the metastable alloys showed no tendency to transform at room temperature, even after several months. This enabled some degree of freedom in handling alloys during the experiments upon which the remainder of this thesis is based.

II. PROPERTIES OF THE METASTABLE STATE

A. LATTICE PARAMETERS

The only attempt to measure lattice parameters of metastable Ag-Cu alloys rapid-quenched from the liquid state (as opposed to alloys quenched from the solid state) was made by Klement; [16] however, he reported that he was unable to suppress the formation of other silver-rich or copper-rich phases while working in the range of compositions which do not exist as a solid solution at equilibrium at any temperature (hereafter referred to as the extended metastable region). The development by Duwez and Willens of a new technique for rapid quenching of molten alloys [28] has enabled a reinvestigation of the problem by this author. A schematic diagram of the fast cooling apparatus is shown in Fig. 2. A specimen weighing about 50 mg. is melted in a vertical graphite crucible by induction heating. In the bottom of the crucible is a 0.8 mm. diameter hole. The molten alloy is retained in the crucible by surface tension until ejected by a pressure pulse supplied by a shock tube mounted above the crucible. Prior to melting of the alloy, the lower end of the shock tube is flushed with argon vented to atmospheric pressure. The shock wave is produced when a .003 in. mylar diaphragm is broken by subjecting it to pressure of about 800 psi by opening a valve leading to the helium-filled upper chamber of the shock tube.

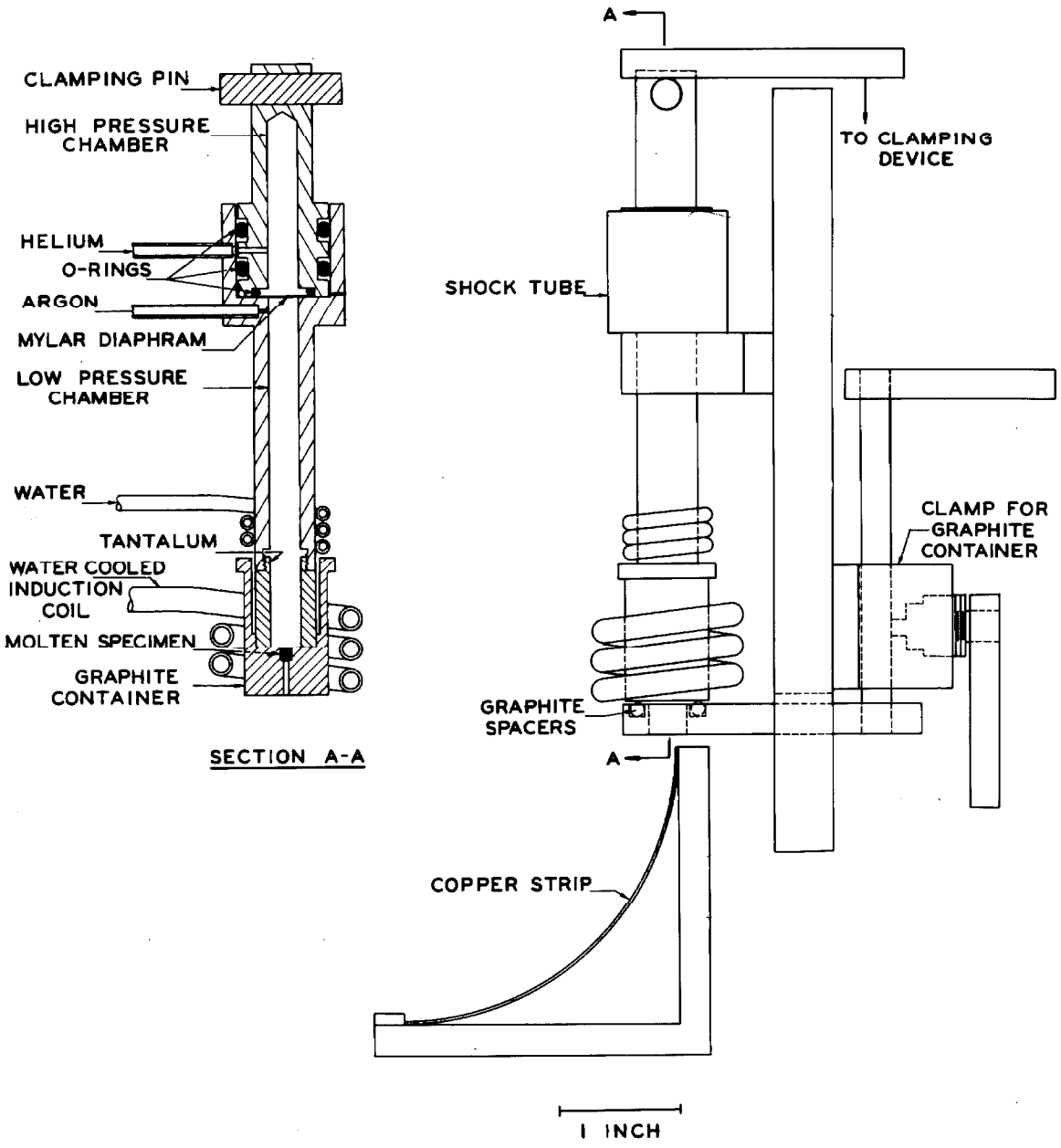

Figure 2. Schematic diagram of rapid-quenching apparatus. After Duwez and Willens.[28]

For this experiment the alloys were prepared from high purity silver ($\geq$ 99.99%) obtained from Englehard Industries and copper of purity > 99.999% obtained from Johnson, Matthey & Co., Ltd. Alloys were made in 3 g. to 5 g. heats, components being weighed accurately to 0.1 mg. In each case an initial melt was made by induction heating in an alumina crucible under an atmosphere of hydrogen. The melt was held at about 300° C above the melting point (as determined by an optical pyrometer) for approximately 2 minutes to insure good mixing. The resulting slug was weighed to check for possible losses (which amounted to < .02% by weight in all cases), and then remelted under an argon atmosphere and sucked through quartz tubes into 1 mm. wires. The wires were cleaned with acetone and cut into pieces of about 50 mg. each for insertion into the graphite crucibles. A piece of wire was then heated and shot by the above-described procedure from about 300° C above the melting point (as determined by an optical pyrometer) onto a copper strip roughened with No. 320-A sandpaper. The resulting metastable solid solution was in the form of thin discontinuous foils (of the order of 1 μ thick, with particles measuring from 1 μ to several millimeters in the transverse direction). A very crude estimate of cooling rates obtained would be of the order of 10^7 or 10^8 °C per second, based upon calculations given by Klement.[16]

The finer particles were shaken off the copper strip and

placed into a 0.3 mm. glass capillary tube, which was then mounted in a 114.6 mm. diameter Debye-Scherrer powder camera. Nickel-filtered copper $K\alpha$ radiation was used with $\lambda K\alpha_1 = 1.54050$ Å. Typical exposure times were 4-1/2 hrs. at settings of 45 KVP and 15 ma., using Ansco Superay 'C' double emulsion film.

Films were corrected for shrinkage, and lattice parameters were determined by extrapolation against the Nelson-Riley function. Experiments were repeated several times in each case to check reproducibility. Results are displayed in Table I. Figure 3 shows a comparison of these results with those of other investigators.

TABLE I

MEASURED LATTICE PARAMETERS OF Ag-Cu SOLID SOLUTIONS

Composition (at.% Ag)	Lattice Parameter (Å)
0	$3.6151 \pm .0003$
$12.50 \pm .05$	$3.6851 \pm .0015$
$25.00 \pm .05$	$3.7544 \pm .0010$
$37.50 \pm .1$	$3.8174 \pm .0008$
$50.00 \pm .1$	$3.8765 \pm .0010$
$62.50 \pm .1$	$3.9344 \begin{matrix} +.0010 \\ -.0005 \end{matrix}$
$75.00 \pm .05$	$3.9886 \pm .0010$
$87.50 \pm .05$	$4.0378 \pm .0003$
100	$4.0861 \pm .0003$

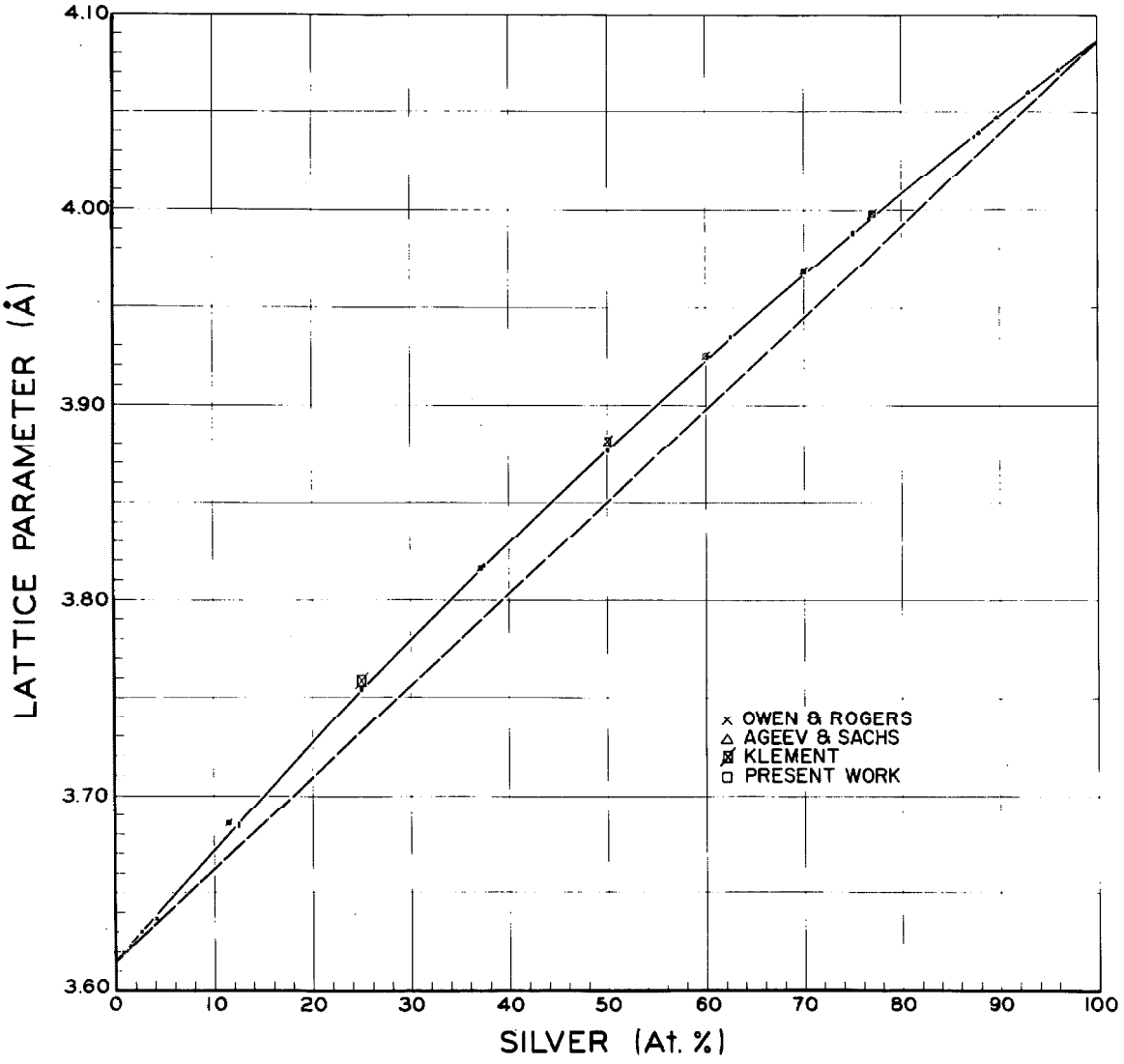

Figure 3. Lattice parameters in the Ag-Cu system.

The uncertainties in compositions listed in Table I were arbitrarily taken as plus or minus four times the change in composition which would result if all of the weight loss in the original melt were considered to come from the element present in smallest amount by weight.

The rectangles in Fig. 3 corresponding to Klement's work and to the present investigation represent the error limits claimed. For the solid state quenching region, the results of Owen and Rogers[29] and of Ageev and Sachs[30] are presented for comparison. Those of Megaw[31] and of Ageev, Hansen, and Sachs[32] were eliminated from the figure in the interest of clarity of presentation, but agreement was quite good in these cases also. The smooth curve was drawn solely on the basis of the present work.

Although lattice parameter plots are very convenient, it is more meaningful to consider the deviation of the atomic volume (in this case, the cube of the lattice parameter) from Vegard's law, rather than the deviation from linearity of just the lattice parameter. This is done in Fig. 4, using lattice parameter values measured in the present investigation.

The positive deviation from Vegard's volume law is not surprising, since an extrapolation of the solid solubility curves to $0\,^{o}K$ (see Fig. 1) implies that $2H_{AB} > (H_{AA} + H_{BB})$, where

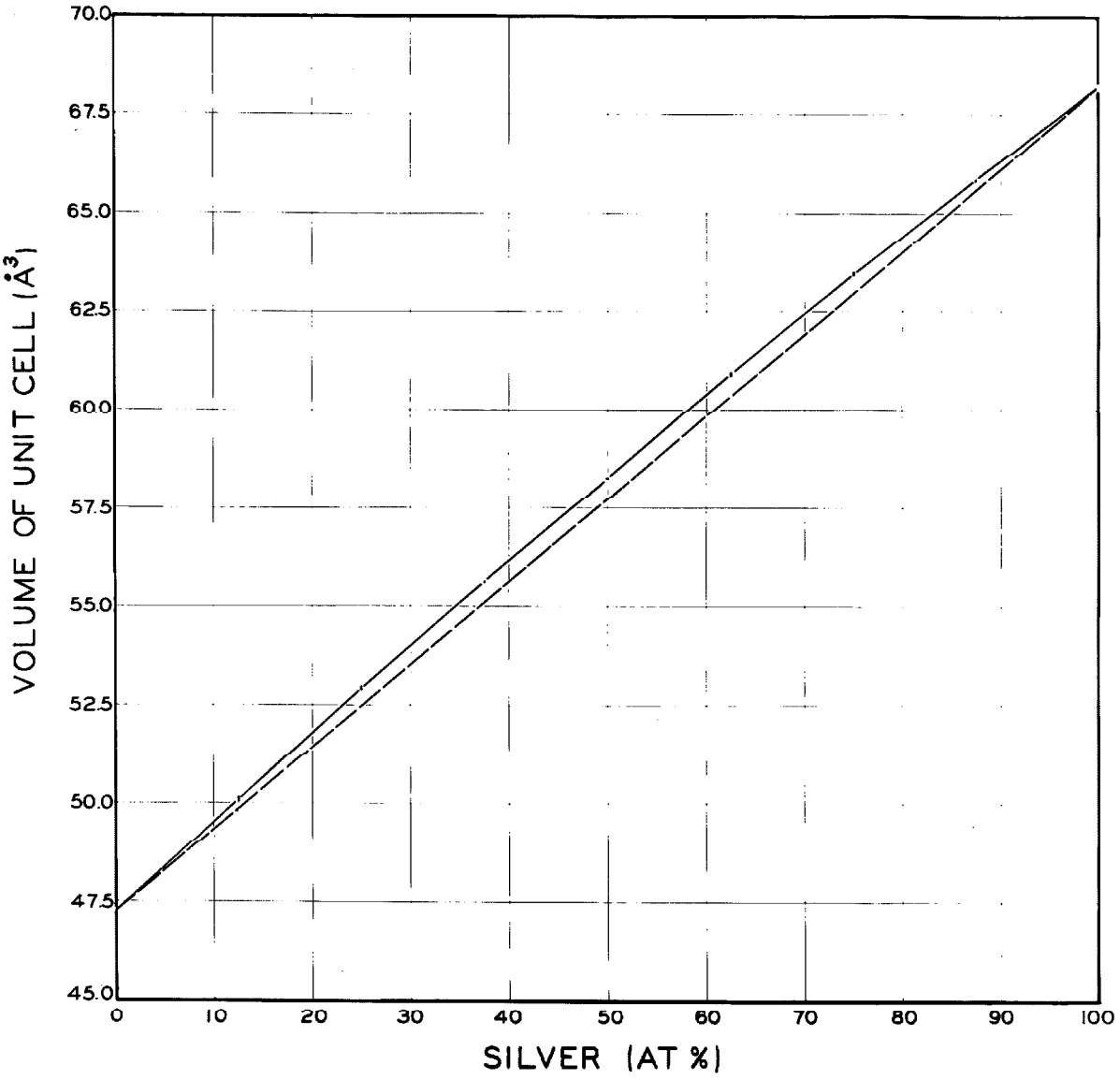

Figure 4. Deviation of atomic volume from Vegard's law, as measured for the Ag-Cu system.

H_{AB}, H_{AA}, and H_{BB} represent the magnitudes of the enthalpy associated with an A-B, an A-A, and a B-B bond, respectively. In cases where the above inequality holds it has been found that there is, in general, an effective repulsion between unlike atoms, resulting in an expansion of the lattice parameter. (The weaker the bond, the greater the interatomic spacing. [33]) The above statement is supported by the experimental results relating the molar volumes of crystals of some compounds to their heats of formation. (See for example, Kubaschewski and Evans. [34])

By the above reasoning, the relatively small magnitude of the deviation from Vegard's volume law evidenced in Fig. 4 leads one to expect a small enthalpy of solid solution, * which may be estimated from free energy considerations to be of the order of 1000 cal./g. mole. An investigation of this question comprises the second part of this chapter.

---

* The enthalpy of solution is the extra enthalpy associated with the existence of unlike neighbors after mixing. It should be noted that all enthalpies of solution referred to in this thesis are integral enthalpies of solution, defined as the enthalpy of solution per mole of solid solution. (In other words, per ($\frac{n}{100}$ moles of Ag + $\frac{100-n}{100}$ moles of Cu) for an n at. % Ag;Cu alloy.) Furthermore, the terms gram atom and gram mole may be used interchangeably, since they are identical for the case in point.

B. ENTHALPY OF SOLID SOLUTION

Since silver-copper forms a eutectic system (rather than exhibiting complete solid solubility at equilibrium), in contradiction to the prediction of semi-empirical rules of alloy phase formation (Hume-Rothery rules), and in view of the preceding discussion, one would expect the enthalpy of solid solution (as defined on the previous page) not to be very large, even in the region of extended metastable solid solubility. For the purpose of this study the 75.0 at.% Ag;Cu composition was chosen. Foils were prepared by the technique described in Section III-A. Half the foils were retained in the metastable condition, while half were heated at 205°C in an argon atmosphere for about 200 hours to insure transformation to the stable state. Foils were then cleaned (to remove oxides, etc.) by swabbing with a 28.46 wt.% HNO_3 solution, rinsed with distilled water, and then swabbed with acetone and allowed to dry in air.

Next, the foils were weighed into sample lots of 0.200 g. each. A small dewar flask (see Fig. 5) wrapped in asbestos and placed in a cardboard box to shield it from air currents was cleaned in the same manner as the foils. Then 25.16 ml. of a 28.46 wt.% HNO_3 solution (as determined by a 6.60 M KOH titration using a phenophthalein indicator, and checked by specific gravity measurements) was added to the dewar, which was maintained at $23.0 \pm 1/2$ °C, but held constant to within .01 °C during any given experiment. Two

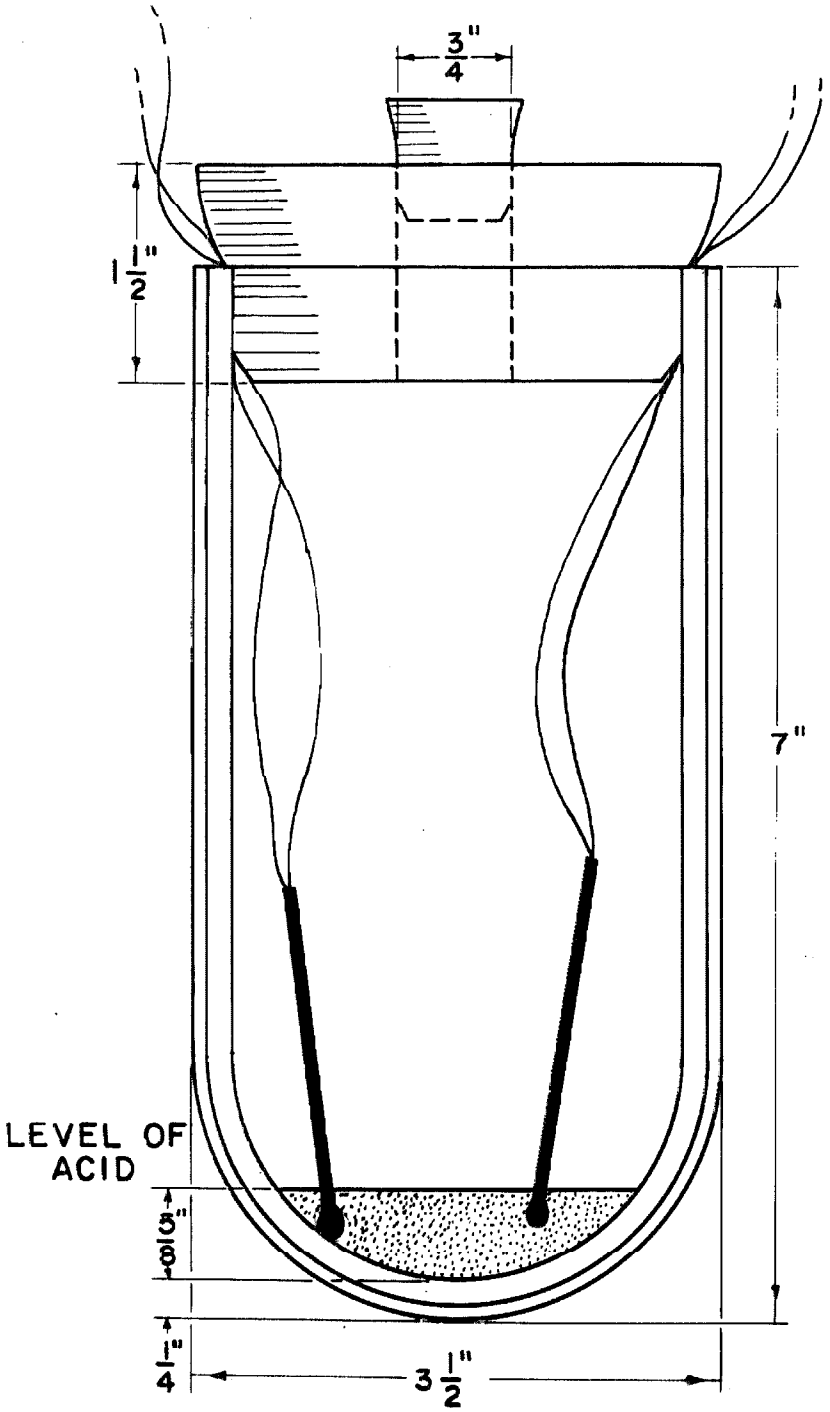

Figure 5. Method of measuring enthalpy of solid solution.

Fenwal GB 32P28 glass bead thermistors with temperature coefficients of 3.9% per ^{o}C at 23 ^{o}C were placed in the acid (one at the center of the dewar, one at the side), and their .012 in. diameter leads were brought out through the side of the cork at the top of the dewar. Samples were injected through a small stoppered hole in the top of the cork, as shown in Fig. 5.

As the foils were dissolved in the acid the rise in temperature, due primarily to the reactions[35]

$$Cu + 2H^{+} \rightarrow Cu^{++} + H_2\uparrow + 15,390 \text{ cal./g. mole}$$

and

$$Ag + H^{+} \rightarrow Ag^{+} + 1/2\,H_2\uparrow + 25,310 \text{ cal./g. mole},$$

was recorded by means of a Wheatstone bridge circuit (Fig. 6).

Now consider conducting two identical experiments of the type just described, one with a metastable sample, the other with a transformed sample. In the case of the metastable foils, additional energy corresponding to the enthalpy of solid solution should be released when the foil dissolves. Since the total proportion of atoms in grain boundaries and other high energy configurations is essentially the same for both types of foils (as determined by the sharpness of x-ray diffraction peaks and supported by photomicrographs in the case of grain boundaries), then if all experimental conditions are kept identical, the enthalpy of solid solution should be evidenced directly in the temperature rise of the acid solution. Tables of the

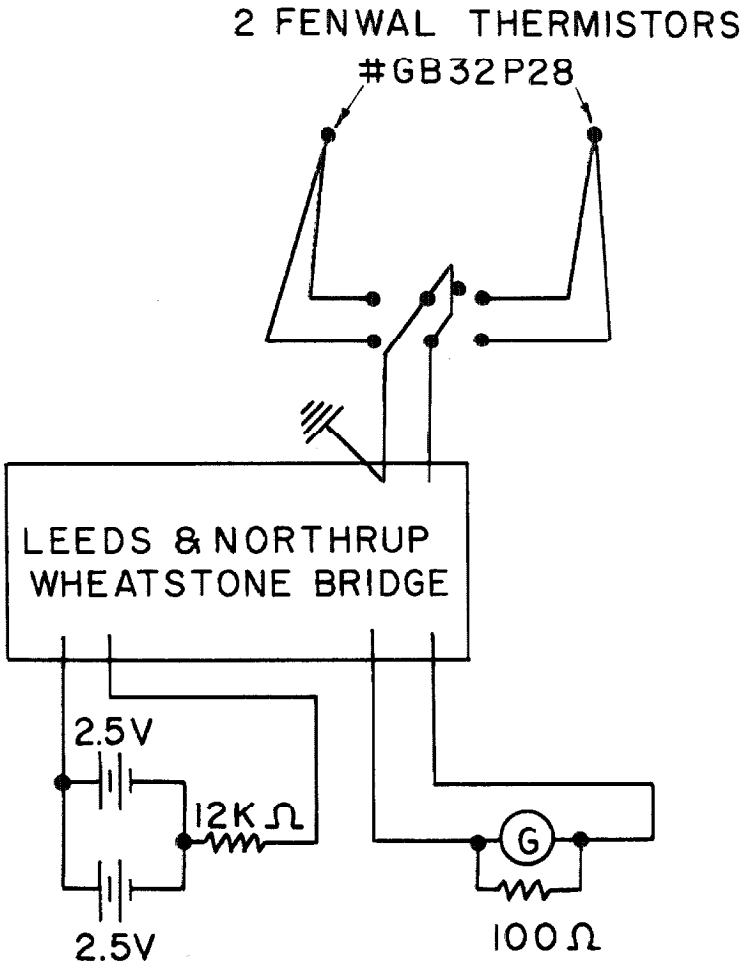

Figure 6. Electrical circuit for measuring enthalpy of solid solution.

heat capacities of various concentrations of nitric acid are readily available. (36)

The amount of hydrogen gas released should be the same in both cases, if the same weights of foils are used in both cases. Thus, the difference in temperature rise between the two cases, if multiplied by the heat capacity of the acid, should yield the enthalpy of solid solution for the quantity of foil used, provided that the heat capacities and heat losses are essentially the same for both cases. A record of temperature vs. time for a typical experiment (transformed foil) is shown in Fig. 7. The flat portion of the curve was used for calculations. Resistance values have been converted to equivalent temperature values for this presentation.

Results show an enthalpy of solid solution (ΔH) equal to 1150 ± 190 cal./g. mole, where the stated error limits are just the computed standard deviation of many trials. The experiments were repeated using 50.32 ml. of acid and 0.600 g. of foil, but keeping all other factors constant. Thus, while the volume of acid was doubled, the total surface area in contact with the inside of the dewar and the thermistor cases was increased by only about 60%. This change would tend to increase the temperature rise as compared with the original experiment (as is evident from a consideration of the heat capacities of the dewar walls and thermistor cases). The fact that the same value of ΔH was, indeed, obtained within the

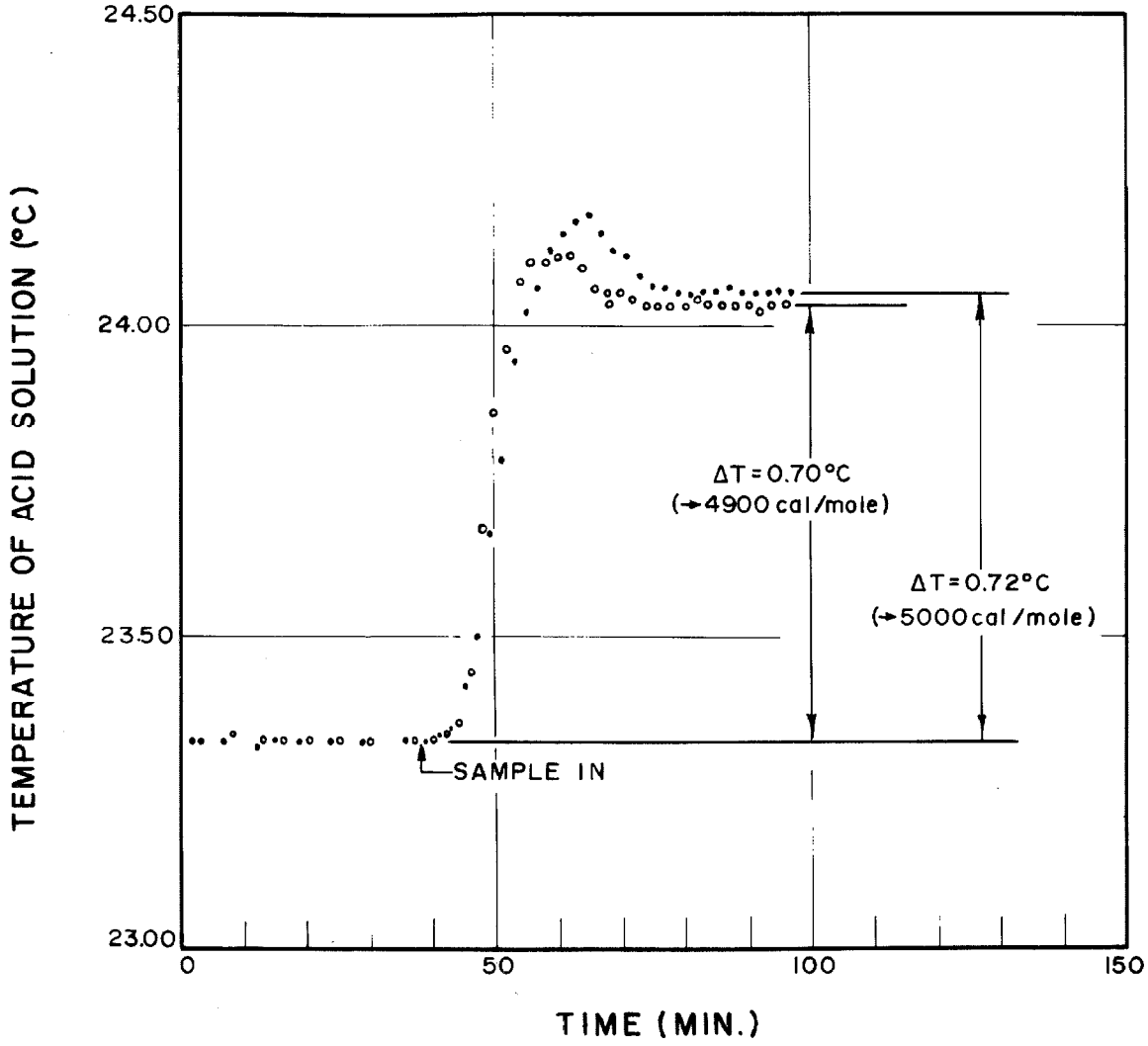

Figure 7. Temperature record for dissolution of transformed foil in acid solution.

sensitivity of the experiments demonstrated that heat losses of this nature could be neglected.

As far as other losses due to heat flow (conduction along dewar walls, convection of air, etc.) are concerned, the flatness of the curve of Fig. 7 after the initial mixing bears witness to the fact that this type of loss could not have been appreciable during the duration of the experiment. The effect of change in heat capacity of the acid upon dissolution of the foil was checked by performing the experiment with half as much foil and obtaining the same results within the limits of experimental accuracy. Due to the slow rate of heat loss it was possible in all cases to wait for natural mixing by convection currents to occur, without introducing additional energy by stirring, since a failure to stir all runs the same would introduce further error.

The above result of this section may be used to check various theoretical expressions for the prediction of enthalpies of solid solution. It should first be stated that the Neumann-Kopp rule has been assumed to apply in the first treatment discussed below. This rule, which has been well borne out experimentally in many cases [33], [34] and should not be a poor approximation for the Ag-Cu system, states that the heat capacity per mole of a compound or solid solution is very nearly equal to the sum of the heat capacities

of the constituents multiplied by their respective molar fractions. Moreover, this rule would be expected to apply best above the Debye temperatures of the constituents. The Debye temperature of Ag is 225 ^{o}K, while that of Cu is 339 ^{o}K, [37] which should not lead to appreciable deviations from the rule.

Scheil [38] has derived theoretical values for ΔH by means of a numerical integration technique using Simpson's rule. He developed an approximate expression of the form

$$\Delta H = -N_o \int_{N_o}^{1} \frac{RT \ln(1-N)}{N^2} dN,$$

where ΔH is the integral enthalpy of solid solution, N represents the concentration of the component in solution, N_o is the concentration at which ΔH is desired, T (^{o}K) is given as a function of N by the extrapolated solid solubility curves of the equilibrium phase diagram, and R is the gas constant. The approximation is not valid for $N_o \simeq 0$. For the 75.0 at.% Ag;Cu composition these calculations result in a value for ΔH of about 1110 cal./g. mole.

Hardy, [39] on the other hand, has developed a "sub-regular" solid solution model, in which the quantity $\left[2H_{AB} - (H_{AA} + H_{BB})\right]$ is allowed to vary linearly with concentration, and in which a temperature dependence is not excluded. It is assumed that the enthalpy of solution is given by an equation of the form

$$\Delta H = C_1 N_A^2 N_B + C_2 N_A N_B^2,$$

where N_A and N_B are the molar fractions of components A and B, respectively. The "constants" C_1 and C_2 are computed to be 6620

cal./g. mole and 4640 cal./g. mole, respectively, in the temperature range 873 ^{o}K - 1052 ^{o}K, when A represents Cu and B represents Ag. There is insufficient data available to compute C_1 and C_2 at lower temperatures; however, invocation of the Neumann - Kopp rule allows one to compare the results of Hardy's model with previously stated results. For the composition in question ΔH, as computed from Hardy's model, is 963 cal./g. mole. By analogy with other systems treated by Hardy, any temperature dependence is probably small, and in the direction of lower ΔH at lower temperatures.

It is thus evident that the result of the present work is in excellent agreement with the prediction of Scheil, while not being in wide disagreement with the expression developed by Hardy.

It is worth noting that Heumann [40] has computed the distortional energy (contribution to ΔH due to difference in sizes of Ag and Cu atoms) for the composition in question to be about 1230 cal./g. mole, so that it might appear that, in agreement with Heumann's conclusion, this represents by far the major factor in the enthalpy of solid solution, the other contribution (due to the formation of Ag-Cu bonds to replace Ag-Ag and Cu-Cu bonds, but excluding atomic size effects) being small. His model employed the assumptions of complete statistical randomness of substitution, short distances of action of atomic forces, and no change with alloying in the concentration of electrons contributing to the Fermi

energy. Also, solutions were assumed to be regular. Heumann's results are in sharp contrast with those of Oriani and Murphy. [41] These investigators concluded that

> " - - - energetics for introducing solute species are independent of rigidity of the phase, a large atom-size difference notwithstanding, "

based upon a comparison of their value of ΔH (liquid) for an 89 at.% Ag;Cu alloy with the value of ΔH (solid) obtained by Orr and Hultgren [42] for the same composition. Some doubt is cast upon their conclusion, however, because first of all, they implicitly assumed that the nondistortional part of ΔH has the same value for both the liquid and the solid state, and second of all, their conclusion was based upon data at only one point. Note that the magnitude of the difference between ΔH (solid) and ΔH (liquid) would be expected to be small for small concentrations. Results of what are considered by the present author to be the most reliable experimental studies reported to date, [27], [41], [43] taken in conjunction with the present investigation, indicate that the enthalpy of liquid solution is equal to roughly 40% of the enthalpy of solid solution, in general agreement with Scheil's [38] calculations.

In conclusion, it might be stated that the results of other investigators in the solid state quenching region are useful but limited in scope. Thus, an extension of the present work to a full range of compositions would undoubtedly prove to be of value.

III. EXPERIMENTAL TECHNIQUES FOR INVESTIGATION OF THE TRANSFORMATION TO EQUILIBRIUM

A. PREPARATION OF FOILS

For the purpose of studying the transformation to equilibrium, two compositions were chosen: 60.1 at.% Ag;Cu (eutectic composition), and 75.0 at.% Ag;Cu In order to produce metastable foils of size and thickness appropriate for accurate x-ray and electrical resistance measurements as well as for micrographic examination, a technique different from that used for the production of lattice parameter specimens had to be employed; therefore, a method based upon the apparatus of Pietrokowsky[14] was used.

Alloys were prepared in the manner described in Section II-A, with the exception that they were drawn into 2 mm. wires instead of 1 mm. wires. A piece of one of these wires, weighing about 0.5 g., was placed in a quartz nozzle and melted in a helium atmosphere by induction heating with a graphite susceptor surrounding the nozzle. (Refer to Fig. 8.) When a large drop (0.2 g. — 0.3 g.) of molten alloy was ejected from the nozzle by a pulse of helium, a photocell was deactivated by the blocking of a beam of light shining on the cell as the drop fell through the light beam path. This deactivation of the photocell in turn resulted in the activation of a solenoid which opened a valve, admitting high pressure gas to a chamber behind a driving

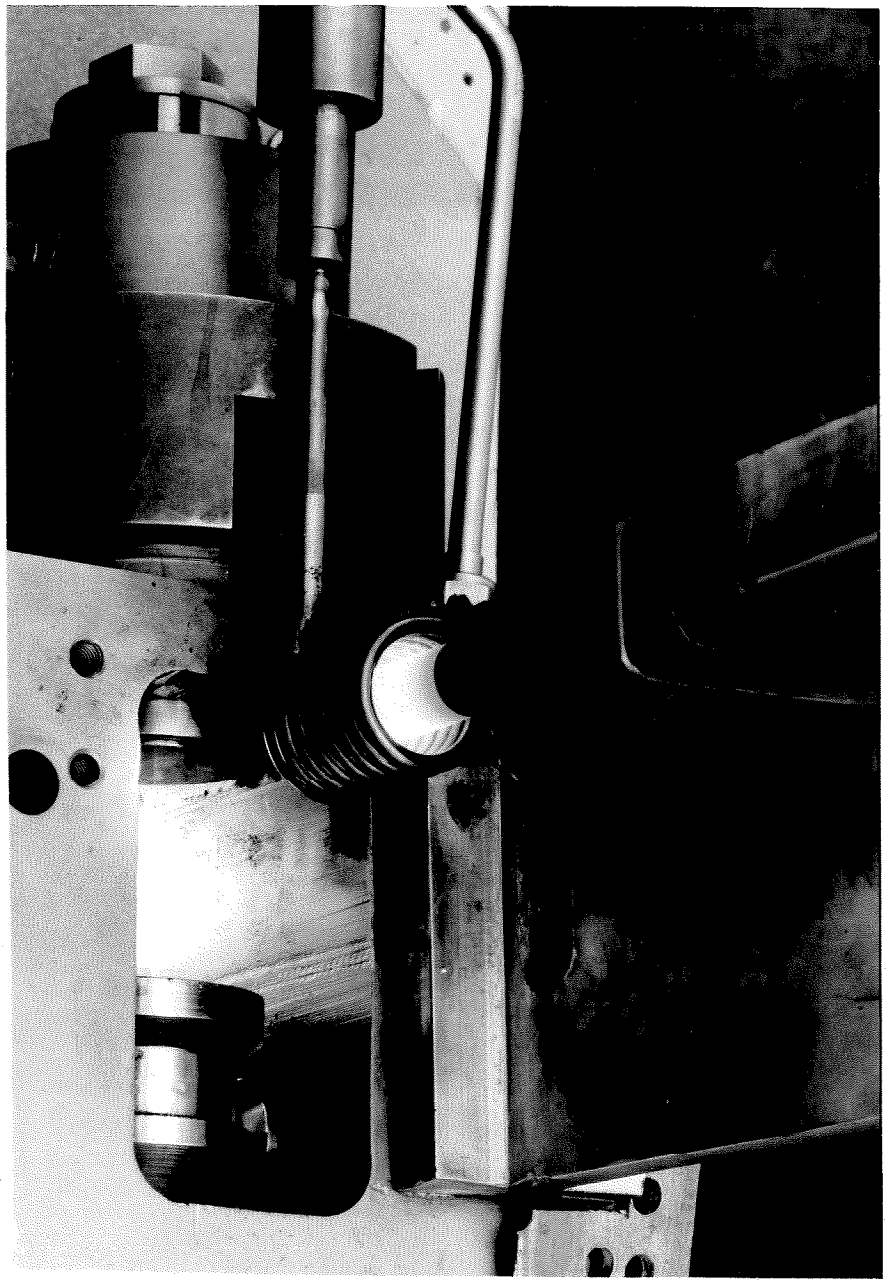

Figure 8. Apparatus for rapid quenching of foils appropriate to the study of the transformation to equilibrium.

anvil (piston). The freely falling drop of molten alloy was caught between this driving anvil and a stationary anvil, both anvils being made of highly polished copper. The resulting foils were approximately circular and measured about 1/4 in. to 7/8 in. in diameter and about .003 in. to .005 in. in thickness; they consistently exhibited essentially complete solid solubility of copper in silver at the 75.0 at.% Ag;Cu composition, and occasionally exhibited essentially complete solid solubility of copper in silver at the 60.1 at.% Ag;Cu composition. All foils were checked by x-ray diffraction. The thickness of foils could be varied by varying the driving pressure. Foils were then cut to the appropriate sizes for subsequent experiments by using a sharp pair of scissors. Independent chemical analysis performed on foils by Truesdail Laboratories, Los Angeles, California, confirmed the nominal compositions quoted to within the accuracy of their analysis (about $\pm$ 1/2%), but due to the negligible weight losses encountered in the melt (see Section II-A), it is felt that actual compositions are within much closer limits of the nominal compositions.

B. METALLOGRAPHIC TECHNIQUE

Metallography was used as an auxiliary tool in helping to support and interpret results of the x-ray and electrical resistance experiments. Metallographic samples were prepared by edge-mounting a foil between two 6 wt. % Be;Cu plates (. 020 in. x 3/8 in. x 5/8 in.) clamped together with a miniature alligator clip and mounted in Quickmount. Fig. 9 shows a sketch of a mounted sample.

Samples were polished using:

240, 320, 400, 600 mesh SiC particles
6 micron diamond on Buehler AB Nylon
0. 3 micron alumina on Buehler AB Nylon
Cer-Cre on Buehler AB microcloth

The most effective etching procedure was found to be:

Mix immediately before using:
10 parts NH_4OH (concentrated)
1 part H_2O_2 (30%)
5 parts H_2O
Swab for 5- 10 seconds

Photomicrographs were taken at 250, 550 and 1500 (oil immersion) magnifications using a Bausch and Lomb Research Metallograph. Polaroid Type 55 P/N positive-negative film was used.

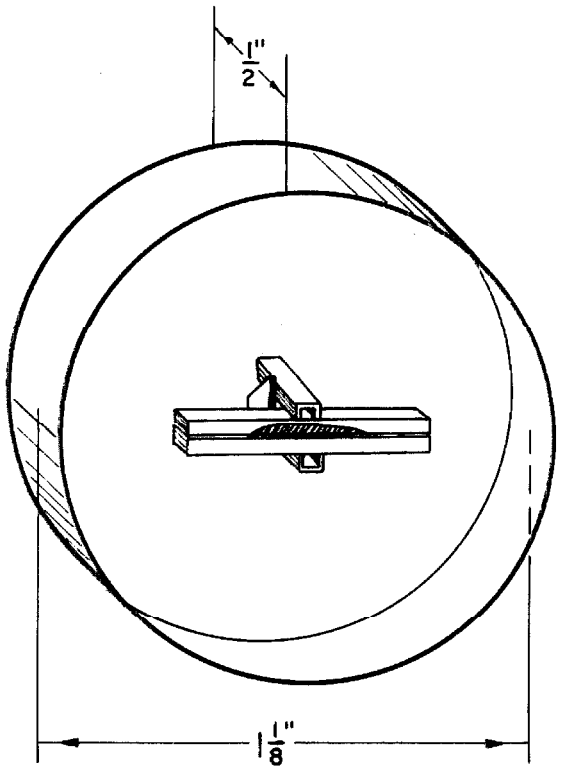

Figure 9. Edge-mounted metallographic sample.

C. X-RAY DIFFRACTION TECHNIQUES

As mentioned in Chapter I, x-ray diffraction may be used to study solid state phase transformations by either lattice parameter measurements or diffraction peak intensity measurements. In the present investigation preliminary experiments indicated that the lattice parameters of the phases did not change noticeably during the transformation, but rather that peaks corresponding to the metastable solid solution began to decrease in intensity, while peaks corresponding to the stable phases began to appear at their proper angular positions and to grow progressively in intensity. Thus it was deemed appropriate to study the process of transformation by measuring changes in peak intensities. The (111) peak of the metastable solid solution and the (111) peak of the Ag-rich phase were chosen for examination, since these peaks exhibited by far the greatest intensities. The overlap in the tails of these peaks necessitated the use of half-peak integrated intensities. The peaks were first assumed to be symmetrical about their centers, and then on a plot of intensity above background vs. diffraction angle 2θ, the peaks were traced out symmetrically in the region of overlap and subtracted from the total intensity at each angular position. The small remainder was considered to represent diffraction from regions in the process of transformation. The assumption of symmetry was checked by examining diffraction peaks from foils in the completely transformed condition.

These peaks were found to be symmetrical within the accuracy limitations imposed by other considerations.

The preparation of specimens proceeded in the following manner: Foils were produced as described in Section A of this chapter. Both sides of each foil were then checked on an x-ray diffractometer to verify essentially complete solid solubility. Foils were then trimmed to size and attached to a 1 - 3/8 in. x 1 - 3/8 in. x .05 in. plate of Pyrex glass by means of Armstrong A-12 epoxy cement. Although this cement required the time-consuming procedure of clamping the samples for twenty-four hours, it was found to produce the most satisfactory results of all cements which were tried. Samples were cleaned with a 5% solution of HCl, rinsed with water, and swabbed with acetone.

The peaks of interest were scanned with a Norelco diffractometer, using a step-scanning technique with steps of 0.05^{o}. A counting rate computer, with the aid of a chart recorder, plotted the reciprocal of the time required to accumulate 6,400 counts from a geiger counter at each angular position, this being a measure of the intensity of diffracted radiation at the angle in question. Typical step-scanning records taken during various stages of the transformation are shown in Figs. 10, 11, and 12. Ni filtered CuK_{α} radiation was used with tube settings of 45 KVP and 20 ma. Diffraction peak centers were determined for each record by replotting these

records onto a smooth curve in order to display the actual amount of symmetry of the peaks.

Preliminary experiments indicated that for practical rates of transformation the heat treatment of samples should be confined to the temperature range of 115 °C to 205 °C. The heat treatment of samples was accomplished by sealing the samples in argon-filled aluminum containers with stainless steel o-rings. The samples were first pressed between two additional pieces of Pyrex glass to serve as a further protection. Containers were then suspended in Fisher-wax baths of 8-1/4 qt. capacity. The wax was stirred, and the temperatures of the baths were controlled to within $\pm$ 0.2 °C of the nominally stated temperatures by means of Yellow Springs thermister probe controllers attached to 1000 watt resistance heaters at the bottoms of the baths. Although the temperatures were checked continually with ASTM No. 42C thermometers, accurate to within $\pm$ 0.1 °C, a special check was made using a Chromel-Alumel thermocouple attached to a foil. At each temperature a correction was made to allow for warm-up time in the baths. These correction factors were arrived at by recording temperature vs. time curves as determined by Chromel-Alumel thermocouples attached to foils placed in each bath. In each case the correction time was taken to be the time for the foil to come to within 0.5% of the desired temperature in degrees

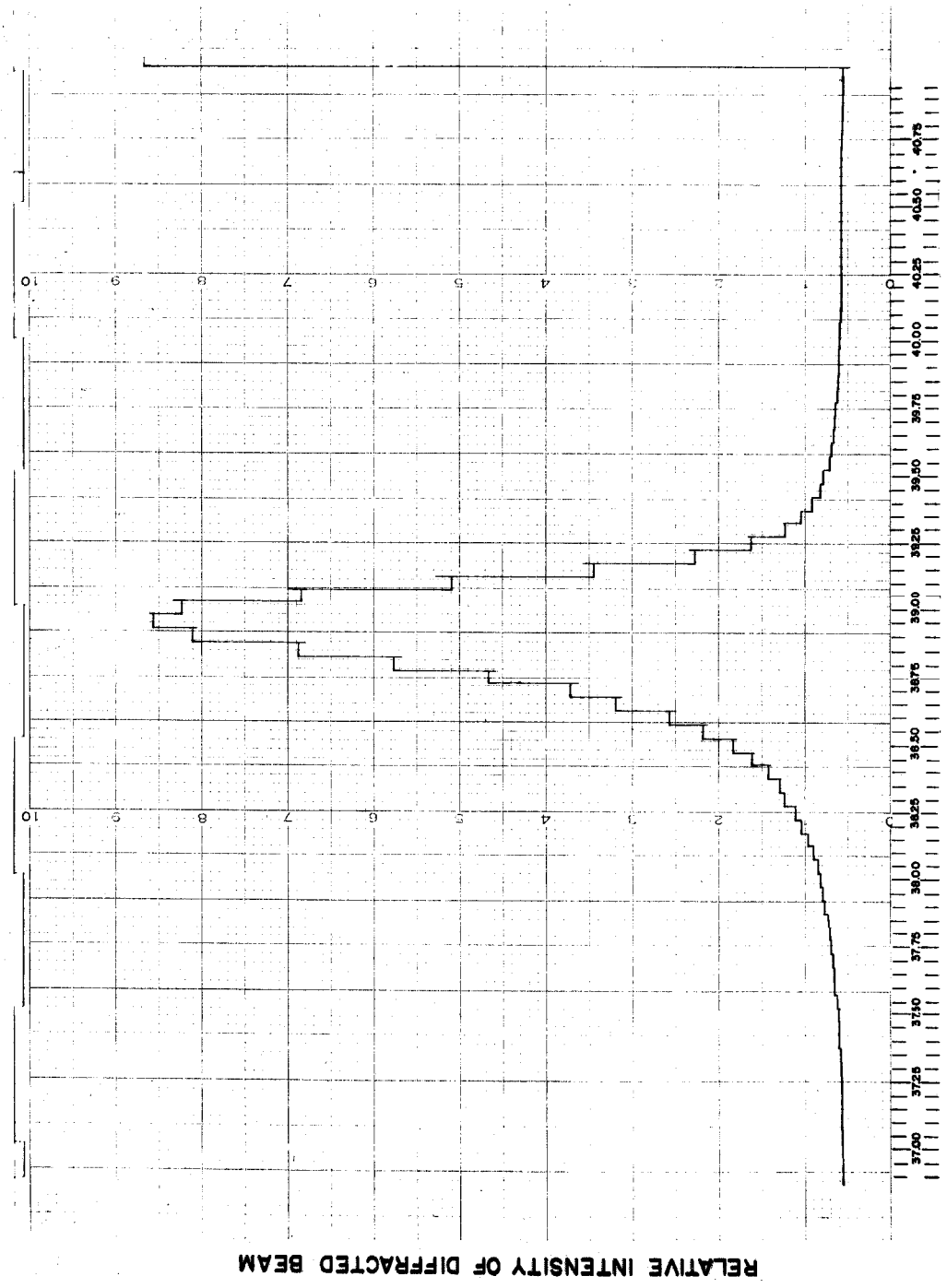

Figure 10. Step-scanning diffractometer record for 75.0 at.% Ag;Cu foil as quenched.

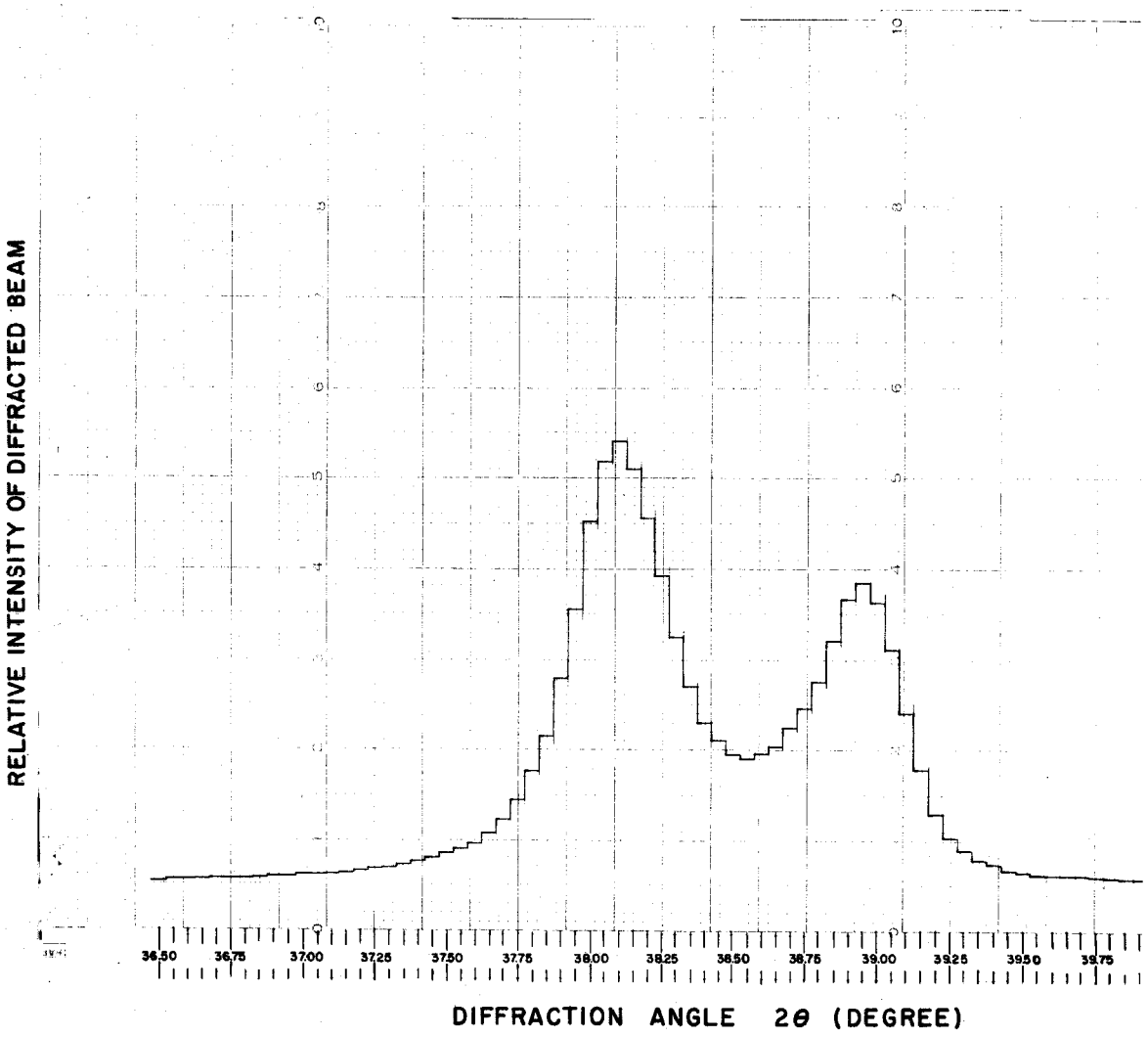

Figure 11. Step-scanning diffractometer record for 75.0 at.% Ag;Cu rapid-quenched foil held at 148.0 ^{o}C for 28.7 hours.

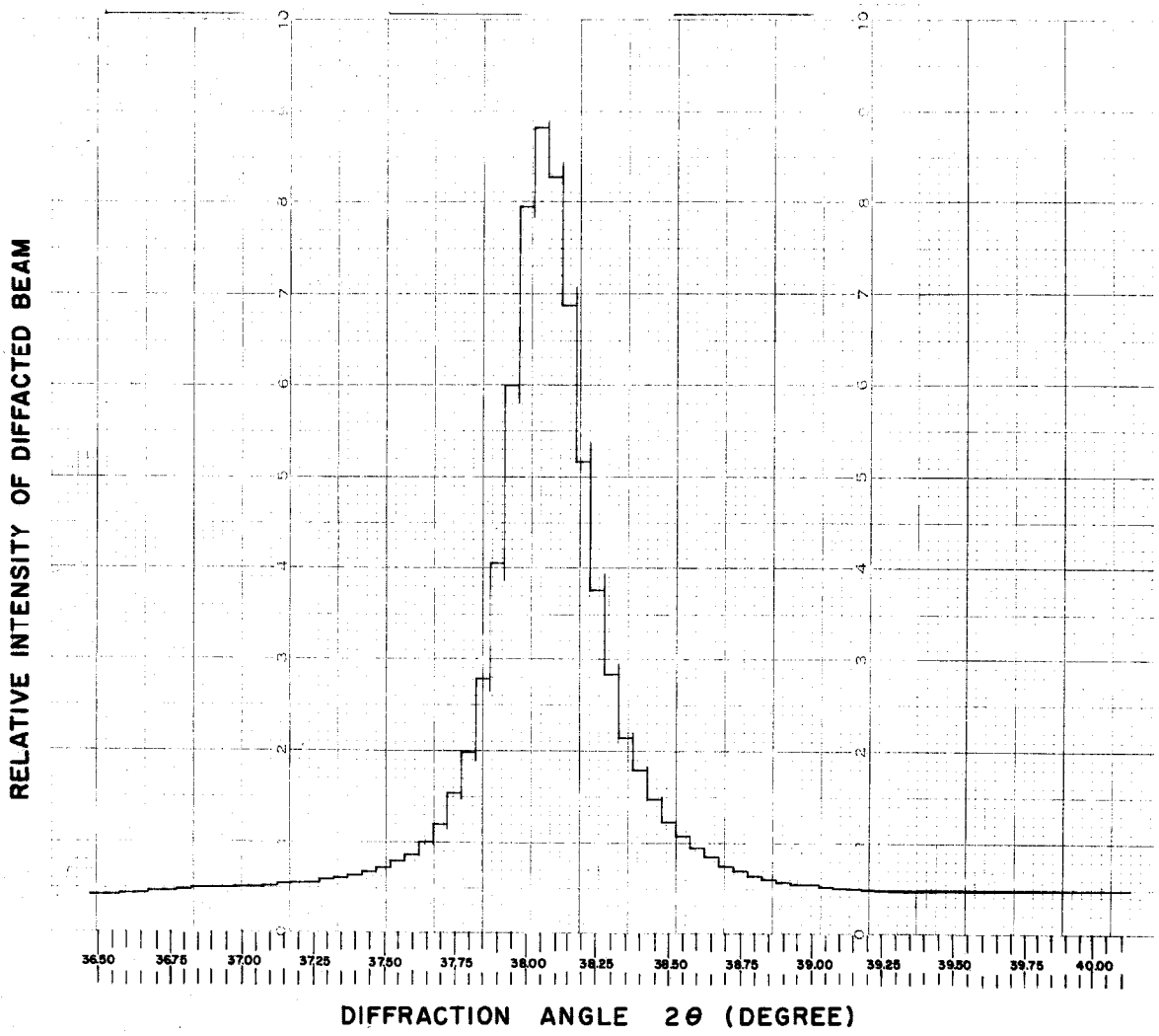

Figure 12. Step-scanning diffractometer record for 75.0 at. % Ag;Cu rapid-quenched foil held at 148 °C for 1630 hours.

Kelvin, which corresponded to about 2 ^{o}K below the final temperature. Table II presents a list of temperatures used, with corresponding correction times. Values of $10^3/T$ ($^{o}K^{-1}$) are also tabulated for future reference.

TABLE II

HEAT TREATMENT OF X-RAY SAMPLES

Temperature (^{o}C)	$10^3/T$ ($^{o}K^{-1}$)	Correction Time (min.)
116.0 $\pm$ .2	2.570 $\pm$ .001	7
136.0 $\pm$ .2	2.444 $\pm$ .001	9
148.0 $\pm$ .2	2.374 $\pm$ .001	9
162.0 $\pm$ .2	2.298 $\pm$ .001	10

These correction times were subtracted from the nominal times in determining the stated time of heat treatment. No correction was made for the time required for foils to cool below the 99-1/2% point after removal from the bath, since the containers were immediately plunged into water at 20 ^{o}C, resulting in a cooling time of only a few seconds.

D. ELECTRICAL RESISTANCE MEASUREMENT TECHNIQUES

In the case of electrical resistance measurements, it was decided to carry out all experiments (with one exception to be treated later) in liquid nitrogen because the percentage change of resistance with amount of transformation should be greater at low temperatures, since the effect of thermal scattering is less. Liquid nitrogen also provides a convenient constant temperature bath at -195.8°C (77.4°K) at 760 mm. Hg pressure. Using the Clausius-Clapeyron equation,

$$\log_{10} \frac{P_2}{P_1} = \frac{\Delta H_v}{2.303R} \left[\frac{T_2 - T_1}{T_1 T_2} \right],$$

with R=1.987 cal. per mole per °K, and for nitrogen the molar heat of vaporization ΔH_v equal to 1,338 cal./mole, [44] one finds that at 720 mm. Hg pressure the boiling point of nitrogen has only dropped to 77.0°K. The estimated temperature coefficient of resistivity at 77.4°K is not more than about 6×10^{-3} per °K in all cases, based upon measurements performed in the same manner as those of the constant heating rate experiment to be described. Fluctuations in temperature, rather than the actual magnitude of the temperature, are of major importance in this study, since only a very crude estimate of the actual magnitude of the resistivity is attempted. Therefore, fluctuations about the mean barometric pressure are the quantities of interest. Information obtained from

the U.S. Weather Bureau for the period over which experiments were carried out yields a maximum effective fluctuation in the temperature of about $\pm 1/2\ ^{o}K$ due to atmospheric conditions. This would result in a maximum error of $\pm 0.3\%$ in any individual measurement, which will have an even smaller effect in the final results due to the "smoothing out" effect of taking averages of results from several repetitions of each experiment and of subsequently drawing smooth best-fit curves as done later in this thesis. Therefore, corrections for barometric pressure fluctuations were not made.

Foils were cut into strips approximately 2.1 cm. long and 0.4 cm. wide. They were then cleaned in the manner previously described for x-ray samples to insure the removal of oxides and surface contamination so that good electrical contacts could be made. The foils were placed into brass holders as pictured in Fig. 13.

Electrical contacts were made with 1/16 in. diameter aluminum wire, insulation from the brass clamping assembly being provided by four transite blocks, two of them grooved to accommodate the aluminum wires. Prior to use, the aluminum wires were annealed at $250\ ^{o}C$ and cleaned with emery cloth and acetone. The purpose in annealing the aluminum wire was to enable the wire to flow plastically when the clamps were tightened. In this way good permanent electrical contacts could be made. Furthermore, this precluded the possibility of a large amount of plastic flow taking

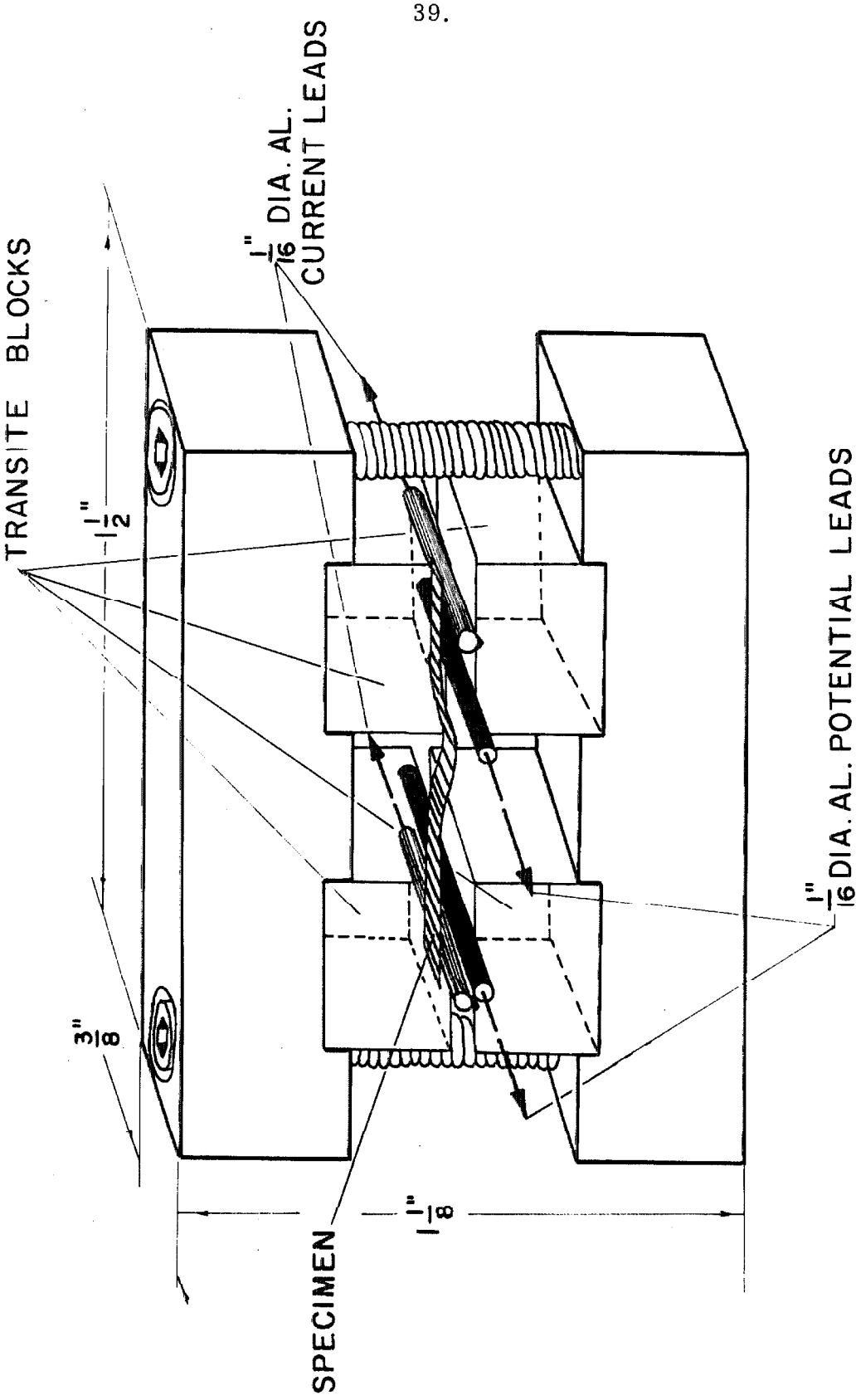

Figure 13. Holder assembly for electrical resistance samples.

place during the subsequent heat treatment of the foils, a situation which could appreciably change the effective contact positions. The "free length" of the foils was about 1.3 cm. in each case, a small amount of sag being allowed for thermal contraction.

Measurements on the first few foils were performed using a precision Kelvin bridge circuit (shown in Fig. 14), which cancels out the effects of contact and lead resistances, but most of the experiments were conducted using the inherently more accurate null circuit set-up of Fig. 15. In both circuits a potential drop was measured across the span of foil between the inner set of aluminum wires, while the outer set of aluminum wires was used to provide the main current conduction path.

In the Kelvin bridge circuit contact and lead resistances in the low resistance current path do not enter into the data, while contact and lead resistances in the high resistance current path are compensated for by opening the balance correction switch and adjusting the variable correction resistance until the galvanometer shows no deflection. The polarity reverse switch allows compensation for any thermal emf in the circuit.

The principle of the null circuit is that the unknown resistance is compared to the resistance of a known stable precision resistor (0.0100170 Ω abs.) by comparing the respective voltage drops across

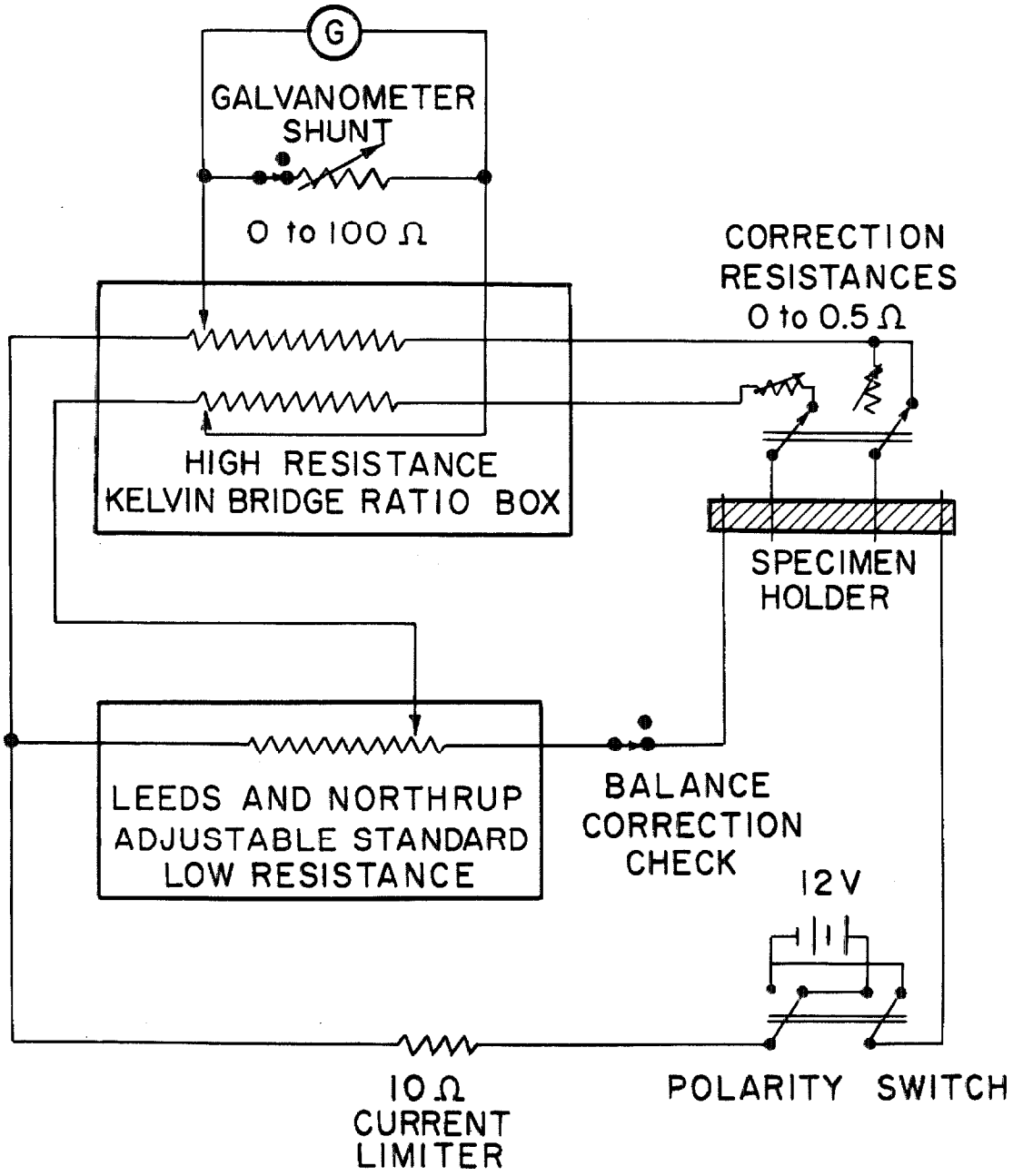

Figure 14. Precision Kelvin bridge circuit for measurement of electrical resistance.

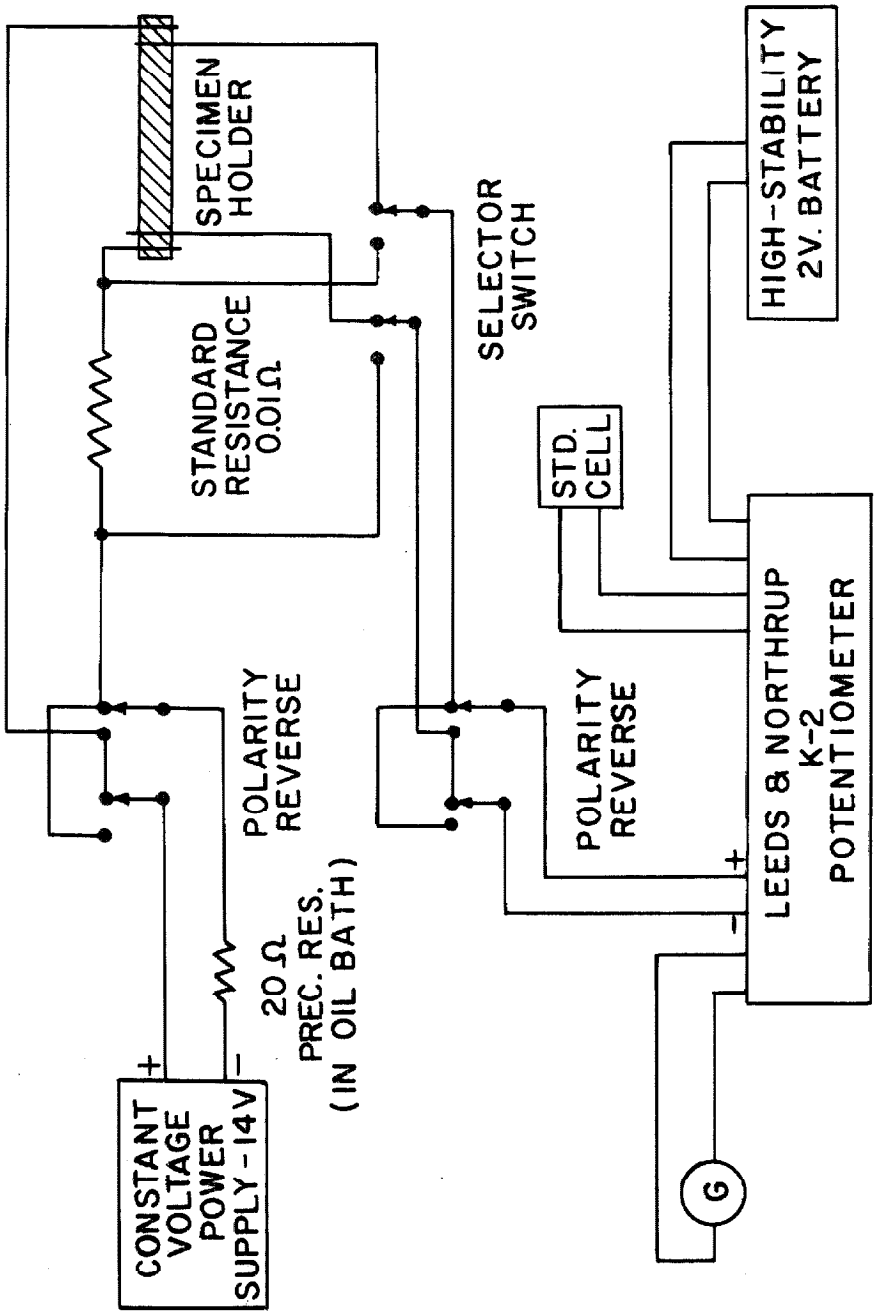

Figure 15. Null circuit for measurement of electrical resistance.

them when a constant current is applied. The unknown resistance is then determined. The 20Ω precision resistor shown in Fig. 15 converts the constant voltage source to a constant current source. It was placed in an oil bath to insure temperature stability. Adjustment for any thermal emf in the circuit was made simple by means of the polarity reverse switches.

In the Kelvin bridge method, a current of about 1.2 amps flowed through the foils, while in the null circuit method, a current of about 0.7 amps flowed through them, such high current levels being required in order to obtain appreciable voltage drops across the foils. The question then arises as to possible significant heating of the foils despite their large surface to volume ratios and their submersion in the liquid nitrogen. The fact that no significant heating occurred was confirmed by obtaining sensibly identical results when current values up to twice the above values were used on the same foils.

For heat treatment, samples were placed in argon-filled aluminum containers and suspended in the isothermal wax baths described in Section III-C. Correction times were determined in the same manner as described previously for the x-ray samples. Table III below indicates temperatures used, as well as correction times and values of $\frac{10^3}{T}$ ($^{o}K^{-1}$) for future reference.

TABLE III

HEAT TREATMENT OF ELECTRICAL RESISTANCE SAMPLES

Temperature (^{o}C)	$10^{3}/T$ ($^{o}K^{-1}$)	Correction Time (min.)
116.0 $\pm$ .2	2.570 $\pm$ .001	11
126.0 $\pm$ .2	2.505 $\pm$ .001	12
136.0 $\pm$ .2	2.444 $\pm$ .001	13
148.0 $\pm$ .2	2.374 $\pm$ .001	14
162.0 $\pm$ .2	2.298 $\pm$ .001	15
205.5 $\pm$ .2	2.098 $\pm$ .001	18-1/2

In order to determine whether or not quenched-in defects [45] played a major role in the transformation, an 88.0 at.% Ag;Cu alloy was studied, since metastable solid solutions are obtainable at this composition by quenching from the solid state. Foils were cut in half; one half of each foil was retained in the metastable state, while the other half was sprinkled with alumina powder to avoid the possibility of foils later sintering. About thirty half-foils were then placed in a rectangular protective steel shell with the two largest faces open and sealed in an evacuated quartz tube along with a titanium getter (see Fig. 16). This tube was then suspended in a vertical tube furnace, with a 1 lb steel bar above it, and heated to 785 $\pm$ 5 ^{o}C in about 20 min. as determined by a double Pt-Pt 10% Rh thermocouple placed just above the quartz tube. The foils were held at this temperature for 40 min. The assembly was then dropped from

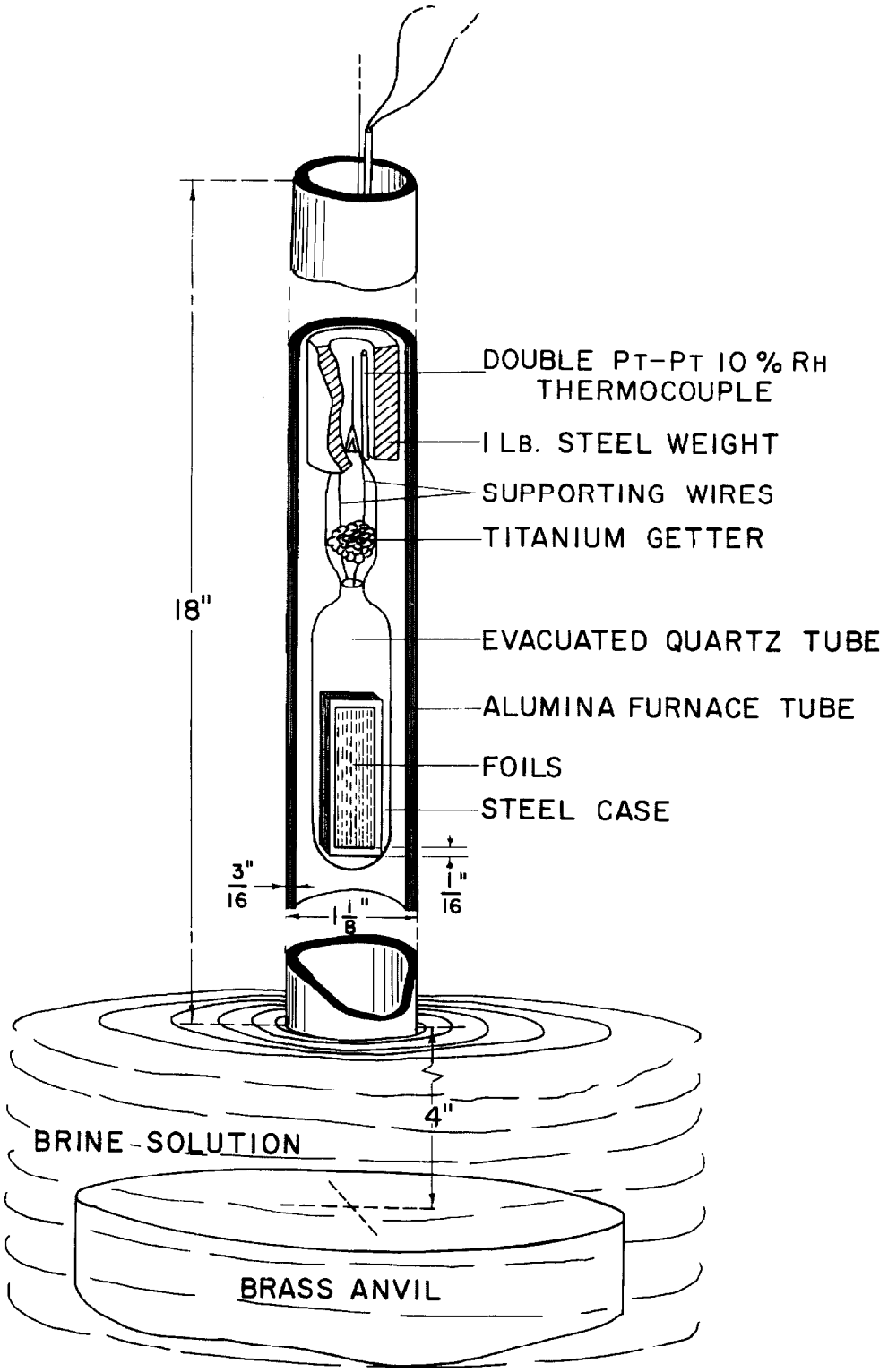

Figure 16. Apparatus for solid state quenching.

790±5 °C into a 26% (saturated) solution of NaCl in water at 24 °C. The bottom of the quartz tube was immediately broken on impact with a brass anvil at the bottom of the brine container, and the foils were exposed to the brine solution. Brine was chosen as the quenching medium in order to minimize the vapor layer through which heat transfer has to take place. [47] A crude estimate of the initial cooling rate would be 10^3 or 10^4 °C per sec. [47] as compared with a very crude estimate of 10^6 °C per sec. for the rapid-quenched foils. Several foils were then heat-treated at 162.0 °C and 205.5 °C in the manner described previously, resulting in the transformation to equilibrium. In each case both halves of the same foil were heat-treated together.

Finally, a constant heating rate experiment was performed using the mounting technique shown in Fig. 17. A 75.0 at.% Ag;Cu foil was milled to the shape indicated and mounted between copper blocks on a transite base. The copper blocks provided electrical contacts to which copper wires were attached to take the place of the outer pair of aluminum wires of Fig. 13. The inner aluminum wires were replaced by .05 in. diameter copper wires spot-welded to the tabs on the foil. The assembly was placed in an argon-filled Pyrex tube within a uniform temperature furnace, and a constant heating rate of 25 °C per hr. was applied to heat the foil from 21 °C to 352 °C. An argon flow was maintained throughout the duration of

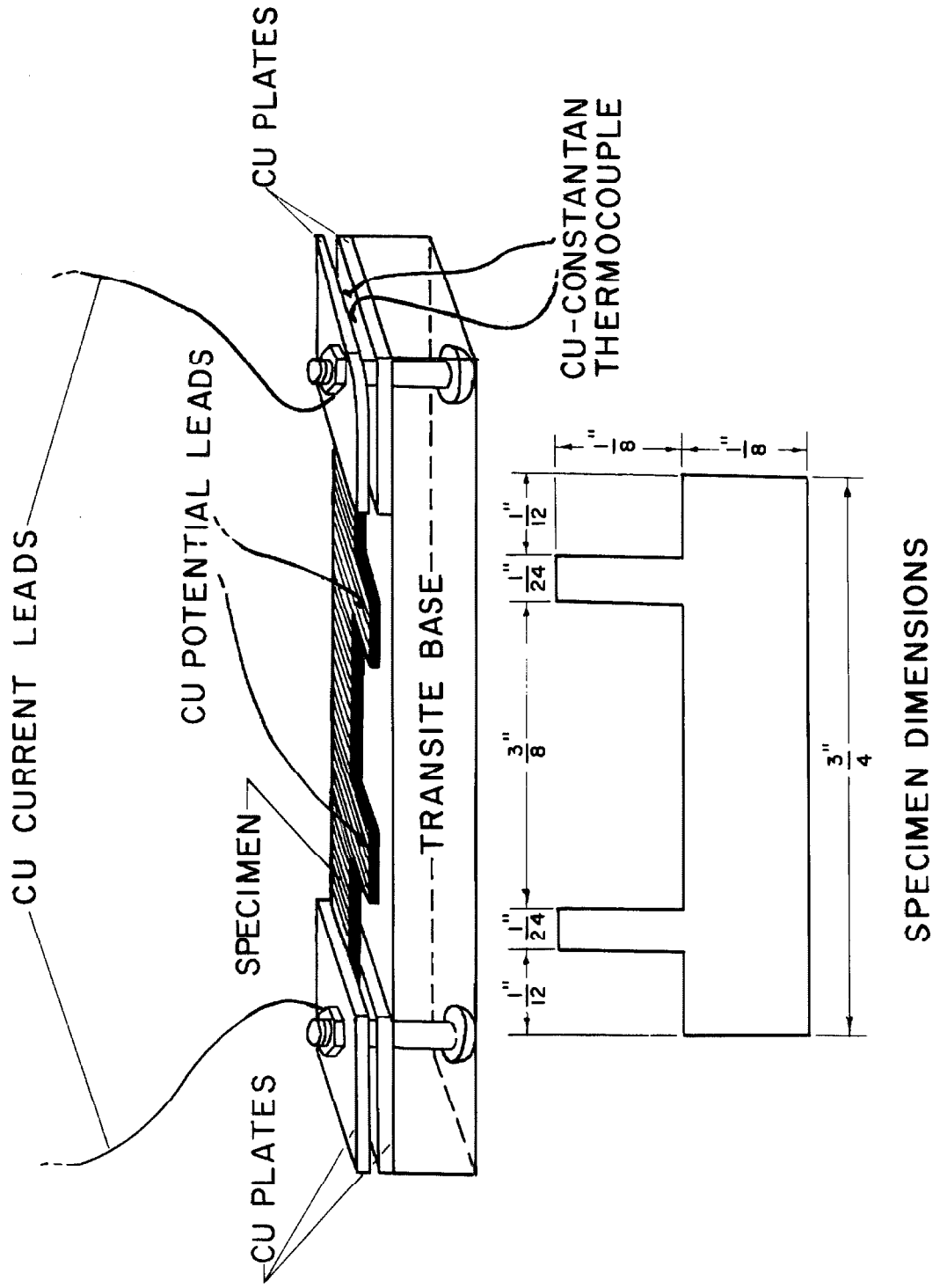

Figure 17. Method of mounting foil for constant heating rate experiment.

the experiment. Temperatures were continuously recorded from a copper-Constantan thermocouple pressed between the copper blocks. Electrical measurements were made using the null circuit of Fig. 15.

After the foil was completely transformed, the change in resistance of the foil as the furnace cooled down at the rate of $25\,^{o}C$ per hr. was recorded over the whole temperature range from $352\,^{o}C$ to $21\,^{o}C$ so that the original data could be adjusted for the temperature coefficient of resistivity. It should be noted that the time required to make a measurement was about 3 min., which is very small compared with the time required in this experiment for appreciable changes in the amount of transformation.

IV. EXPERIMENTAL RESULTS OF THE INVESTIGATION OF THE TRANSFORMATION TO EQUILIBRIUM

A. MICROSTRUCTURE OF QUENCHED FOILS

Fig. 18 shows a typical sample in the as-quenched condition. It is evident that there are two structural constituents present. These are referred to as "columnar" and "fine grained," respectively, in subsequent discussions. From this figure one might predict that foils of thickness less than about .002 in. would be obtainable in the entirely columnar form. This supposition is, indeed, borne out, as may be seen by reference to Fig. 19. Thin foils of pure copper and of pure silver also yielded columnar structures.

Occasionally foils contained a third structural constituent (see Fig. 20), which will henceforth be referred to as "coarse grained." The coarse grained structure, whenever it appeared, was always present between the columnar region and the fine grained region.

A question may be raised as to whether or not the fine grained and coarse grained structures are truly single phase solid solutions, since x-ray diffractometer checks may reveal only the more rapidly cooled sections near the surface (columnar structure). To settle this question, a portion of a foil which showed the columnar structure on only one side and which had particularly large regions of the fine and coarse grained structures was chosen. (See Fig. 20.)

(a) (b) (c)

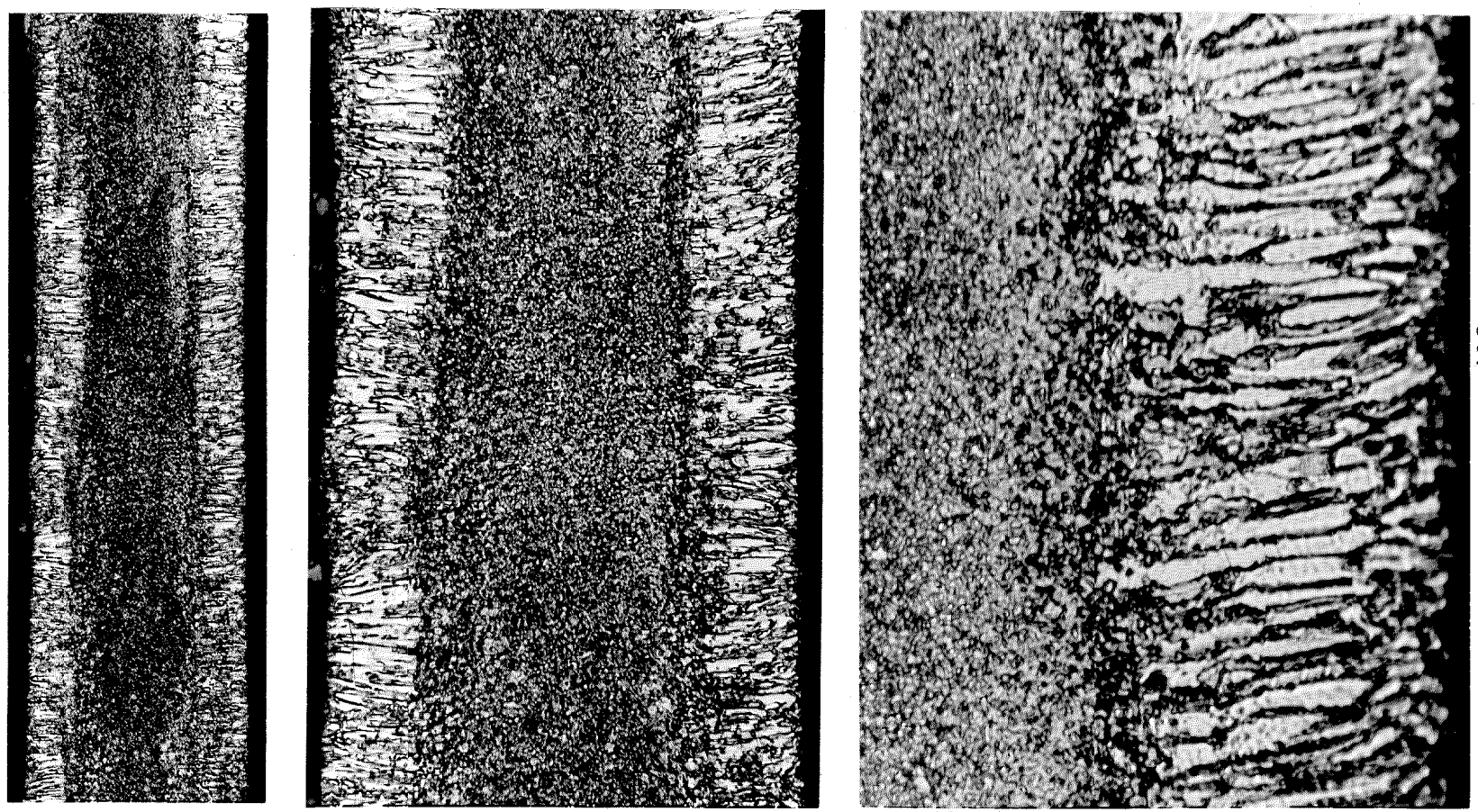

Figure 18. 75.0 at .% Ag;Cu foil as quenched: a) 250x, b) 550x, c) 1500x.

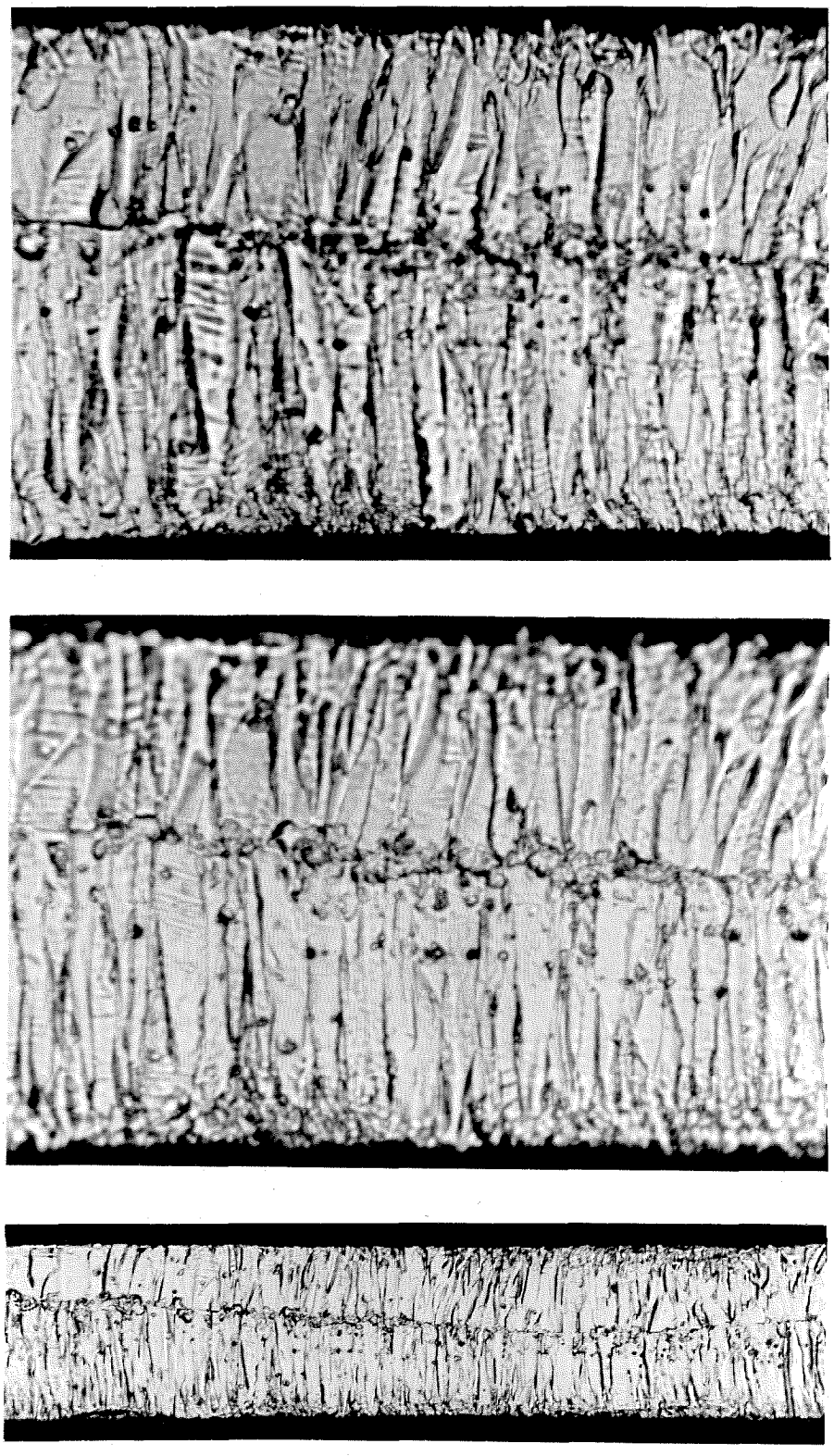

Figure 19. 75.0 at.% Ag;Cu foil as quenched: a) 550x, b) 1500x focused on center, c) 1500x focused on edges.

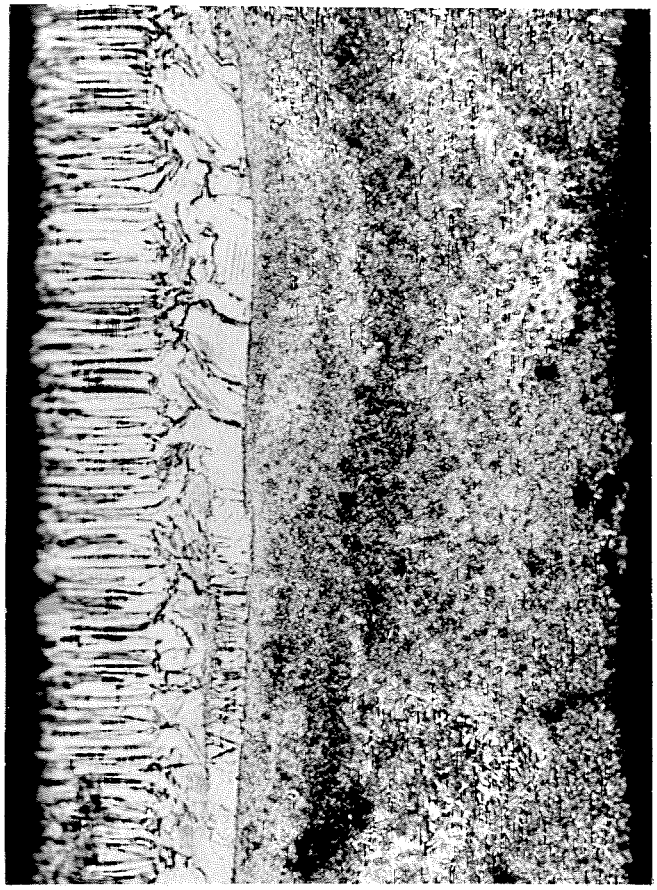

Figure 20 . 75.0 at.% Ag;Cu foil as quenched. 550x.

Such a situation could be brought about by a region of higher thermal resistance at one of the anvils, resulting in slower cooling in some portions of the foil. In fact, it is quite possible that cooling in the fine grained region took place mainly by heat transfer through the foil to the opposite anvil.

The exact position at which the photomicrograph was taken was marked, and the foil removed by dissolving the mount. A pin-hole x-ray transmission photograph was taken using Zr filtered MoKα radiation with a wave length of 0.71069Å. A Picker x-ray unit was used with .0020 in. pinholes, and Ansco Superay 'C' double emulsion film was placed 5.00 cm. from the pinhole from which the beam emerged. The sample was placed so that the area of interest intercepted half of the beam, as evidenced by the shadow in the resulting diffraction pattern shown in Fig. 21 . Exposure time was 86 hours at 40 KVP, 15 ma. It is evident that only a single set of diffraction rings is present, indicating a single phase. The above exposure was made with the fine grained structure surface facing toward the film, and thus contributing more strongly to the diffraction pattern. A similar exposure taken with the columnar structure surface toward the film yielded a pattern with rings in exactly the same positions, indicating the same phase.

It might be noted in passing that the continuity of the rings in both exposures indicates no marked degree of preferred orientation, in contrast with the results of other investigators (such as Weinberg

and Chalmers [47]) studying dendritic growth of pure metals. The occasional spots visible on the print correspond to individual grains in particularly strongly diffracting orientations. This lack of appreciable preferred orientation is not considered to be peculiar to the Ag-Cu system, but is thought rather to result from the rapid cooling rate. Foils of pure Cu and of pure Ag showed varying amounts of preferred orientation when examined.

To this author's knowledge, no studies of the variation in the amount of preferred orientation with changes in growth rate of dendrites have been performed. The availability of the present quenching technique and the observations just cited would indicate that this might be an interesting area for further research.

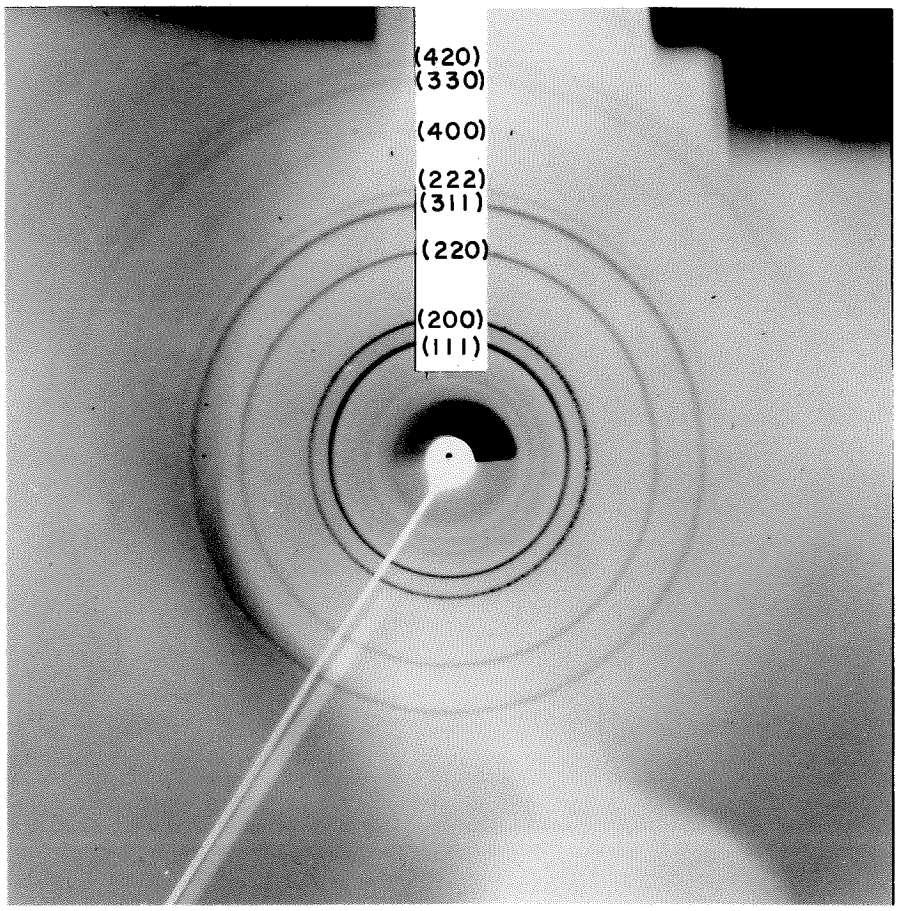

Figure 21. X-ray transmission pattern of region of foil shown in Fig. 20.

B. X-RAY STUDY OF THE TRANSFORMATION

The variation of location of x-ray diffraction peak maxima with degree of transformation for a typical foil is shown in Fig. 22. The constancy of position of these diffraction peaks indicates that the transformation (in the temperature range of 116 °C to 205 °C, at least) occurs by a process of essentially discontinuous precipitation, wherein small regions transform completely while the rest of the matrix remains unchanged, and this process continues until the entire matrix is finally transformed.

The transformation curves are shown in Figs. 23 and 24 for the 60.1 at.% Ag;Cu and the 75.0 at.% Ag;Cu compositions, respectively. For these figures the per cent transformed was computed as I/I_o, where I is the intensity of the metastable solid solution (111) peak at time t, and I_o is the initial intensity of this peak. In the case of the Ag (111) peak, the per cent transformed listed in Tables IV and V was computed as $\frac{I-I_i}{I_o-I_i}$, where I_i is the initial intensity of the peak. This small initial intensity, as evidenced in the asymmetric peak of Fig. 10 and observed also for the (200) and peaks of higher index, serves as direct evidence of the presence of at least segregates, even in the columnar regions of the as-quenched foils, since the asymmetry was detected even for entirely columnar foils.

The curves of Figs. 23 and 24 are typical of a nucleation and growth process; the possibility that most of the stable-phase nuclei

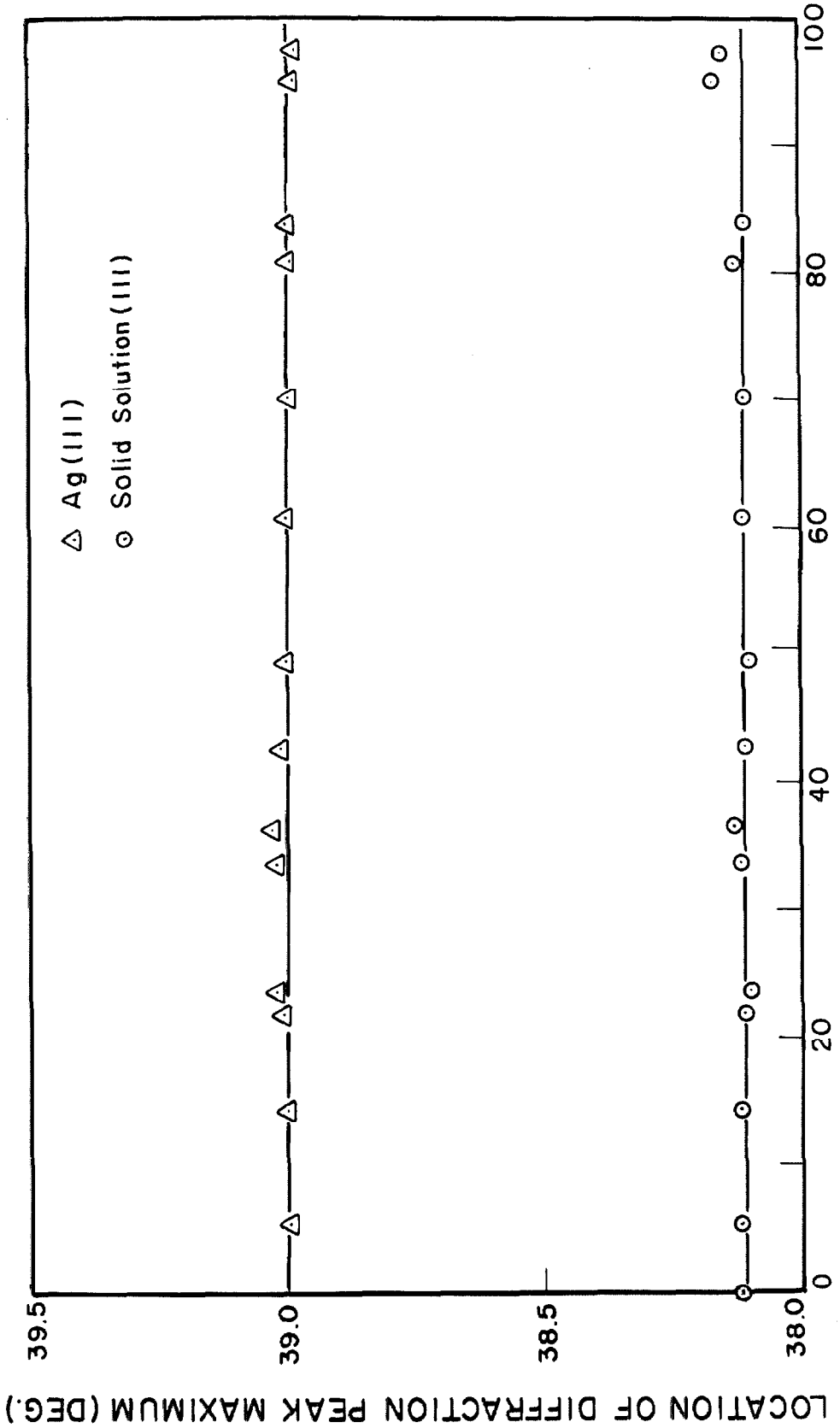

Figure 22. Shift in diffraction peak maxima with degree of transformation for the temperature range 116 ^{o}C to 205 ^{o}C. Composition shown is 75.0 at.% Ag;Cu.

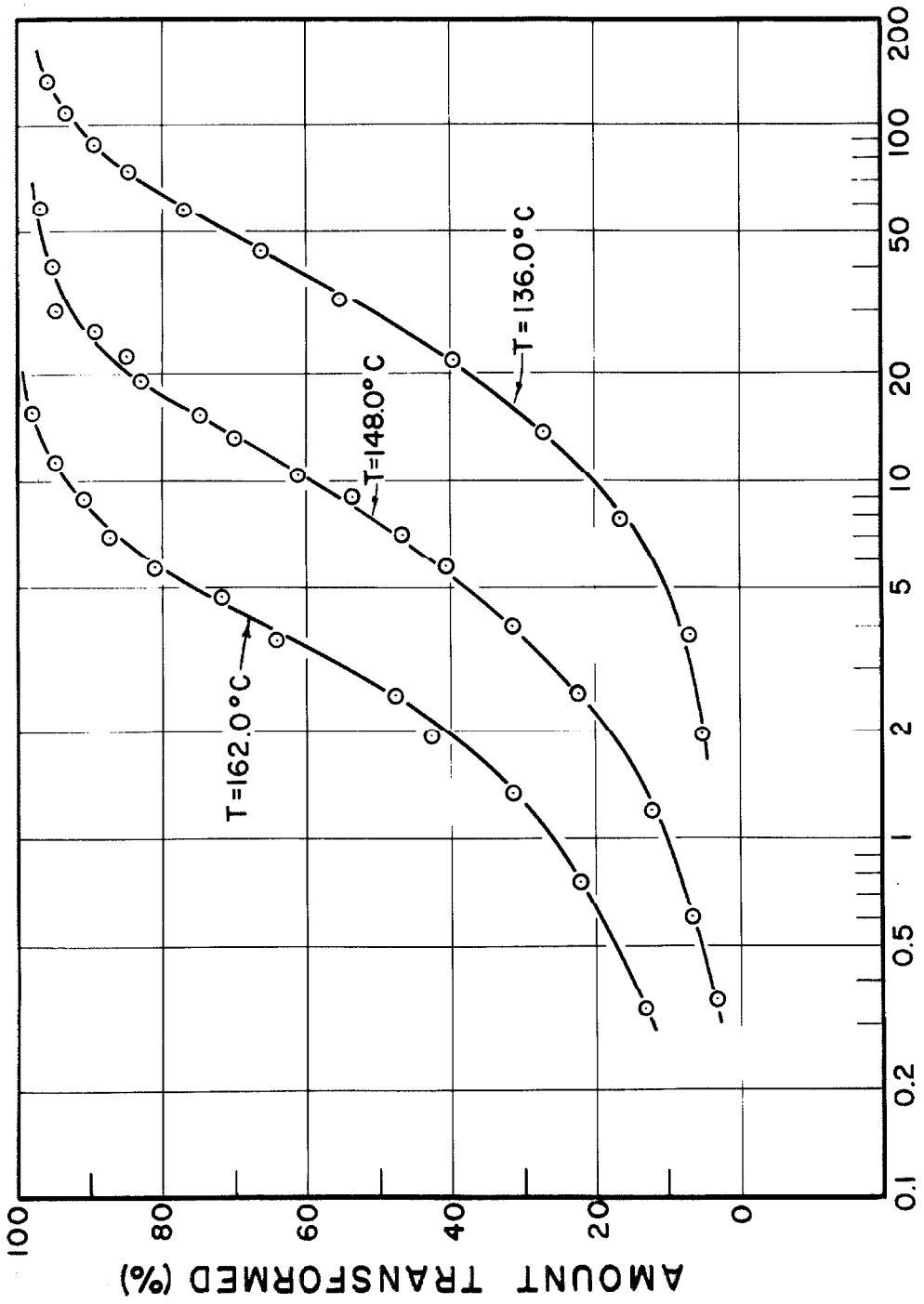

Figure 23. Experimental transformation curves as determined by x-ray analysis for the 60.1 at. % Ag;Cu alloy.

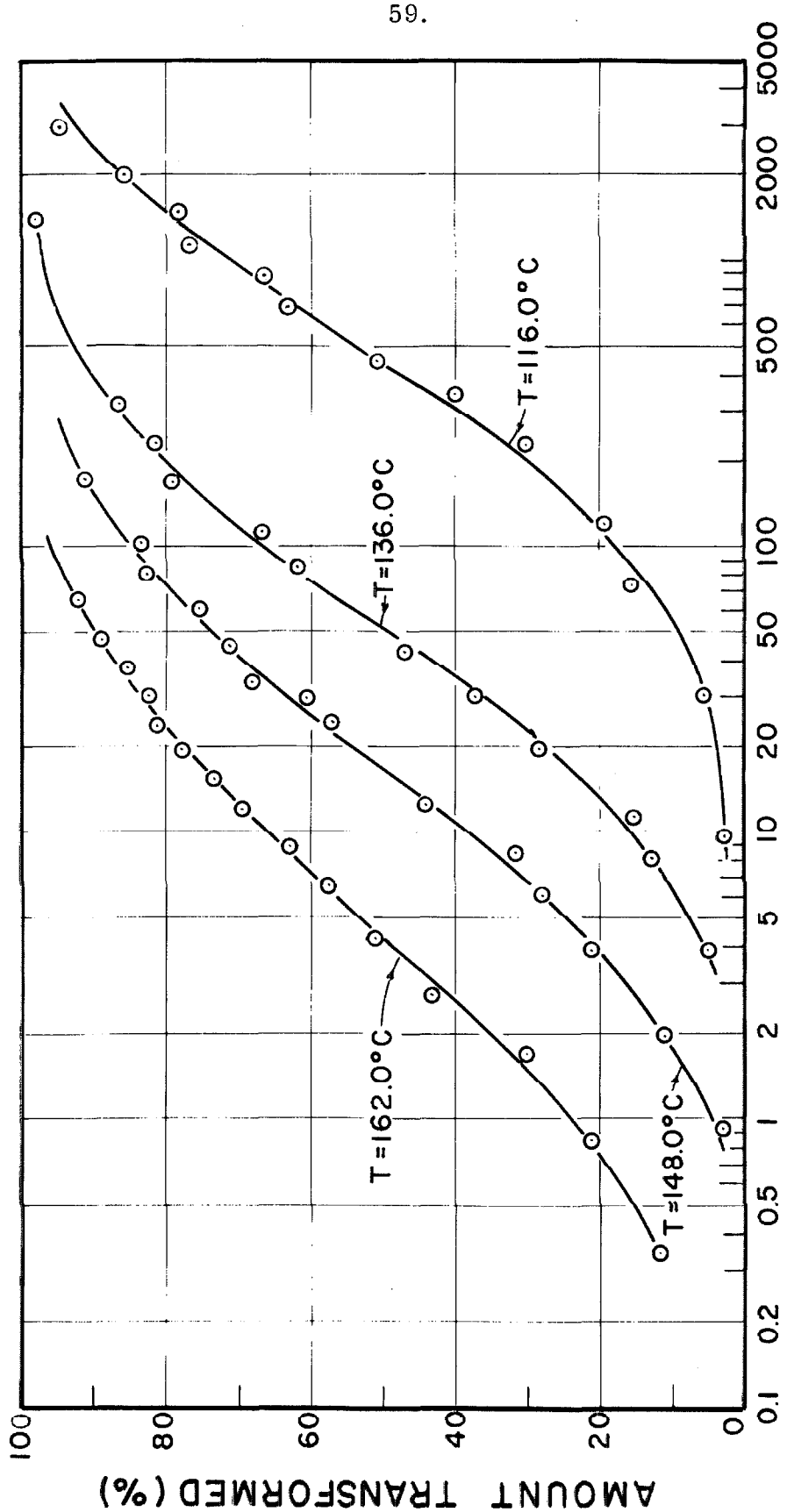

Figure 24. Experimental transformation curves as determined by x-ray analysis for the 75.0 at.% Ag;Cu alloy.

were present in the as-quenched condition will be discussed further in Chapter V.

For diffusion controlled processes, one may generally assume an expression of the form

$$P = C e^{-Q/RT},$$

where P is the transformation rate, T is the absolute temperature (^{o}K), Q is the so-called "activation energy," R is the gas constant = 1.987 cal. / ^{o}K, and C is a constant with respect to temperature. From this expression one can compute the value of Q from a measurement of the slope of a plot of ln P vs. (1/T), by assuming Q to be independent of temperature over the temperature range considered. Thus,

$$Q = -R \frac{d(\ln P)}{d(1/T)} = -(2.303) R \frac{d(\log_{10} P)}{d(1/T)}.$$

P was taken to be the time required for a specific per cent transformation. The resulting graphs are shown in Figs. 25 and 26. The validity of the foregoing procedure is dependent upon the mean distance between the surfaces of precipitating particles remaining reasonably constant over the temperature range considered, [48], [49] a reasonable assumption in view of the discussion to be presented later and the good straight line fits obtained.

Although results of calculations of Q from both the metastable solid solution peaks and the stable Ag-rich peaks have been compiled, only the former have been shown in Figs. 25 and 26, since these results are considered to be more reliable. However, results from

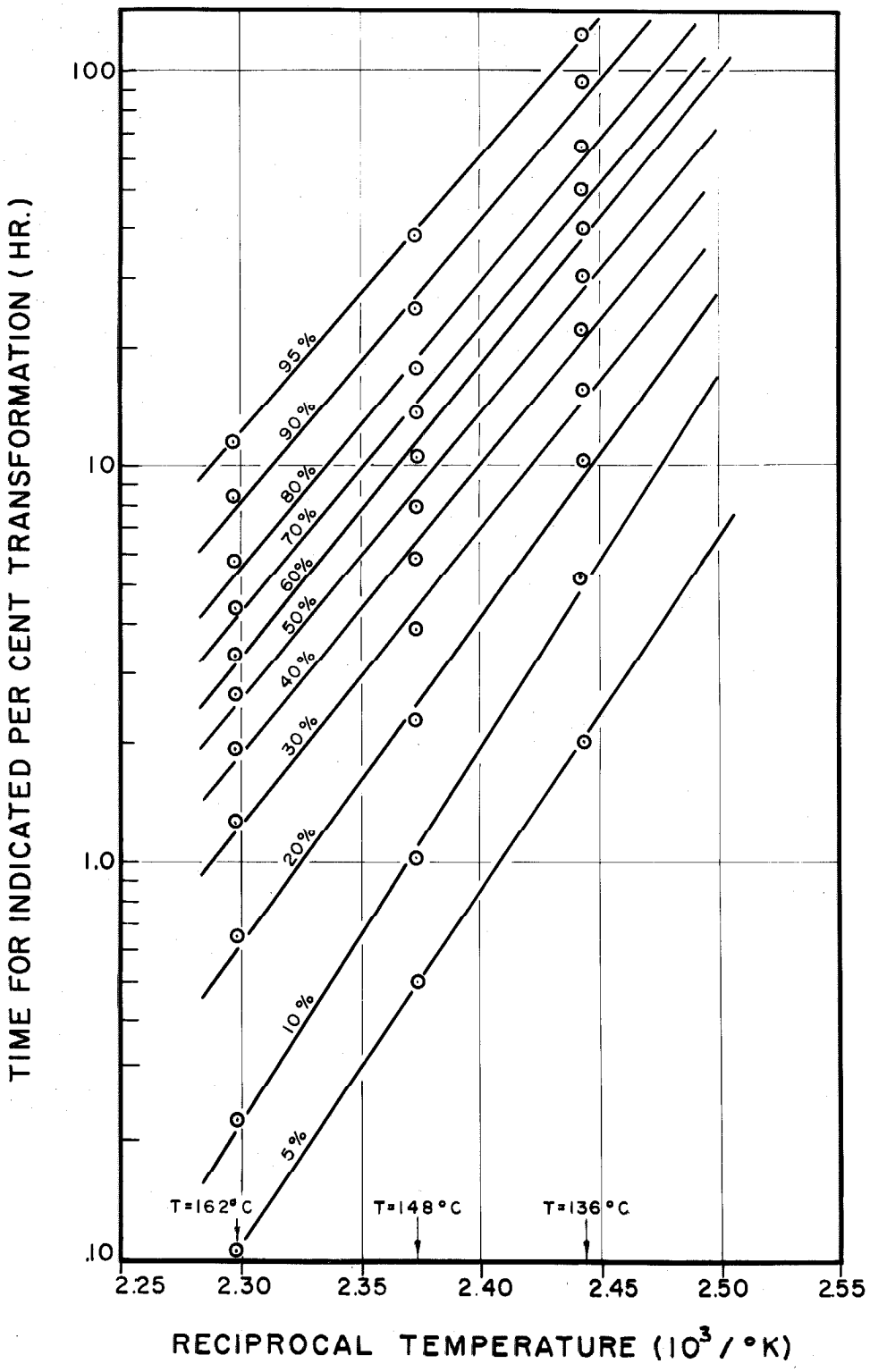

Figure 25. Graph for the determination of Q by x-ray measurements for the 60.1 at. % Ag;Cu alloy.

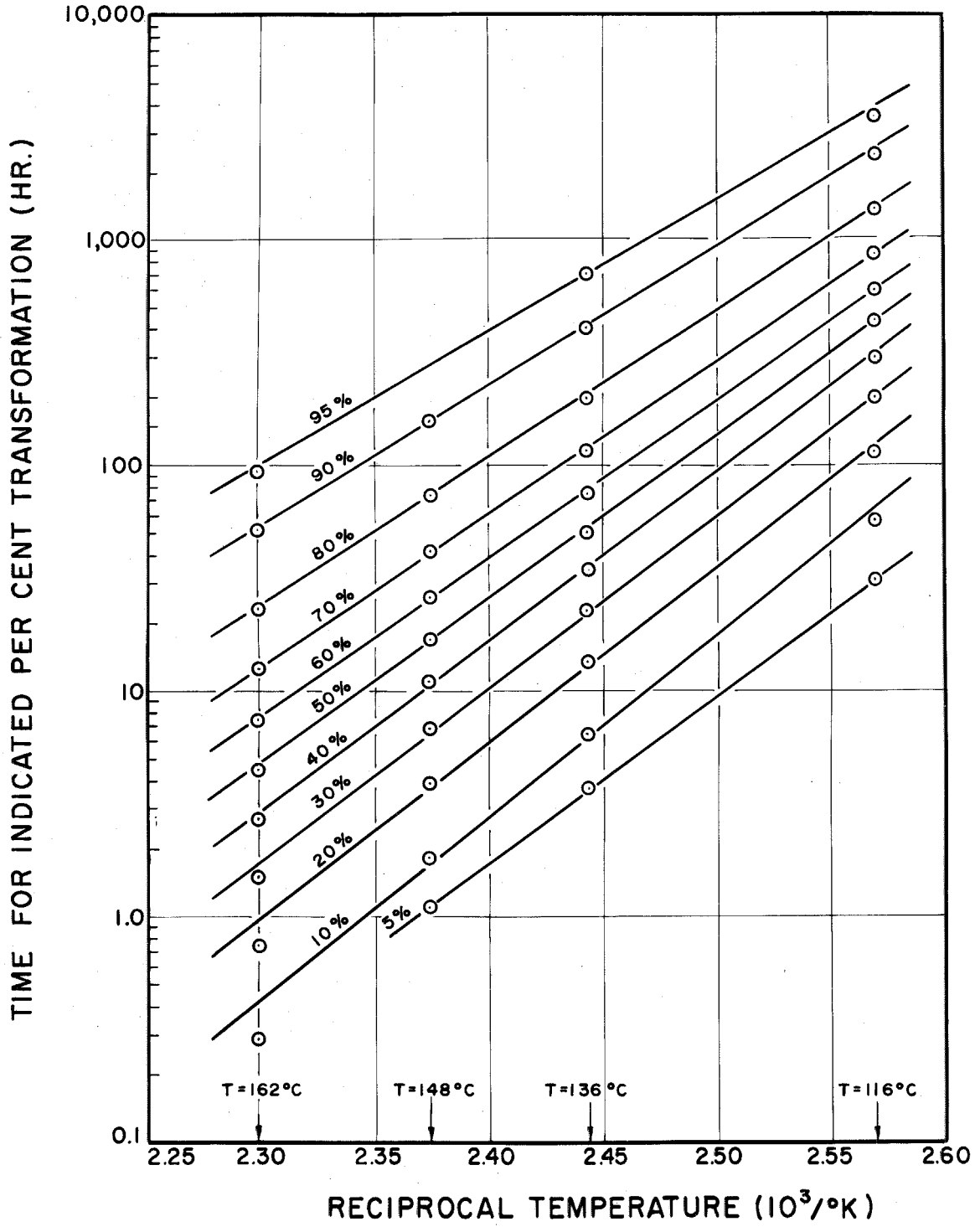

Figure 26. Graph for the determination of Q by x-ray measurements for the 75.0 at.% Ag;Cu alloy.

the Ag-rich peaks have been tabulated along with those from the metastable solid solution peaks and presented as supporting evidence in Tables IV and V.

TABLE IV

ACTIVATION ENERGY FOR TRANSFORMATION OF THE 60.1 at. % Ag;Cu ALLOY AS COMPUTED FROM X-RAY DATA

Amount Transformed (%)	Activation Energy, Q (cal./g. mole) Calculated From: Solid Solution (111) Peak	Ag (111) Peak
5	41,200 ± 9000	
10	43,100 ± 7000	
20	37,500 ± 7000	38,400 ± 7000
30	34,100 ± 7000	33,400 ± 7000
40	33,600 ± 4500	33,800 ± 7000
50	33,600 ± 2500	33,100 ± 7000
60	33,800 ± 2500	31,500 ± 9000
70	34,300 ± 2500	30,400 ± 11,000
80	33,400 ± 2500	28,300 ± 11,000
90	32,700 ± 4500	29,400 ± 11,000
95	32,000 ± 7000	

TABLE V

ACTIVATION ENERGY FOR TRANSFORMATION OF THE 75.0 at. % Ag;Cu ALLOY AS COMPUTED FROM X-RAY DATA

Amount Transformed (%)	Activation Energy Q (cal. /g. mole) Calculated From: Solid Solution (111) Peak	Ag (111) Peak
5	37,800 ± 7000	33,800 ± 10,000
10	36,600 ± 7000	39,800 ± 10,000
20	35,900 ± 4500	41,200 ± 4000
30	35,900 ± 2000	37,500 ± 4000
40	34,500 ± 2000	36,600 ± 4000
50	33,100 ± 2000	35,200 ± 4000
60	33,400 ± 2000	35,900 ± 4000
70	31,100 ± 2000	35,000 ± 6000
80	30,400 ± 2000	33,600 ± 8000
90	29,000 ± 4500	32,700 ± 10,000
95	28,600 ± 7000	35,900 ± 10,000

For each composition a weighted average of the activation energies tabulated above was determined. In the case of the 60.1 at.% Ag;Cu alloy only three temperatures were used due to the great difficulty encountered in producing essentially single-phase foils at this composition by the piston-and-anvil technique. In view of this situation, a greater expected error was assigned to the resulting weighted-average activation energy.

Values obtained by the above procedures were:

Composition (at. % Ag)	Activation Energy, Q (cal. /g. mole)
60.1	$33,600 \pm 2500$
75.0	$33,100 \pm 2000$

For the purposes of comparison and later reference, Table VI contains activation energies for diffusion processes. In cases where more than one value is reported in the literature the value which is considered by this author to be the most reliable has been quoted, although the conclusions drawn in Chapter V would not be changed by the choice of other values available in the literature.

TABLE VI

ACTIVATION ENERGIES FOR RELATED DIFFUSION PROCESSES

Process	Q (cal./g. mole)	Reference
Volume Diffusion:		
Ag in Ag (630-935 °C)	44,090 ± 180	Tomizuka and Sonder[50]
Ag in 98.25 at.% Ag;Cu (750-850 °C)	44,800 ± 2000	Hoffman, et. al. [51]
Ag in 95.84 at.% Ag;Cu (750-900 °C)	46,600 ± 2000	Hoffman, et. al. [51]
Ag in 93.44 at.% Ag;Cu (700-850 °C)	43,500 ± 2000	Hoffman, et. al. [51]
Ag in 1 at.% Ag;Cu (717-867 °C)	35,600 ± 3000	Kubaschewski [52]
Ag in 0.1 at.% Ag;Cu (700-900 °C)	33,200 ± 500	Gertsriken and Revo[53]
Ag in Cu (700-900°C)	38,600 ± 500	Gertsriken and Revo [53]
Cu in Ag (716-944 °C)	46,100 ± 920	Sawatsky and Jaumot [54]
Cu in 98 at.% Ag;Cu (760-895 °C)	24,800*	Seith and Peretti[55]
Cu in Cu (685-1062 °C)	47,140	Kuper, et. al.[56]

* The value given by Seith and Peretti (1936) is subject to question, but it is the only available value at the stated composition, so that no comparisons can be made.

TABLE VI (continued)

Process	Q (cal./g. mole)	Reference
Grain Boundary Diffusion (polycrystalline specimens, random orientations of grains):		
Ag in Ag (355-480 °C)	20,000 ± 2000	Turnbull and Hoffman[57], [58]
Ag in 0.1 at.% Ag;Cu (250-450 °C)	17,050 ± 500	Gertsriken and Revo[53]
Ag in Cu (250-450 °C)	17,200 ± 500	Gertsriken and Revo[53]

It might be noted that Margolin [59] and Mishima [60], [61] have determined activation energies for precipitation hardening of solid solutions of Ag in Cu. Their results are substantially lower than the volume diffusion activation energies shown in Table VI. Precipitation hardening is, however, a complicated process, and there is no reason to expect a direct relationship between the activation energy for precipitation hardening and the activation energy for diffusion.

C. ELECTRICAL RESISTANCE STUDY OF THE TRANSFORMATION

Transformation curves for the 75.0 at.% Ag;Cu alloy are shown in Fig. 27, where R is the resistance at time t, and R_o is the initial resistance. Each point plotted represents the average of several determinations using different samples. With the aid of these plots a weighted-average activation energy of 31,600$\pm$2000 cal./g. mole for the process was determined by the same method as in Section B of this chapter. Results are presented in Table VII. It may be seen that these results agree rather well with those obtained by x-ray diffraction peak intensity measurements.

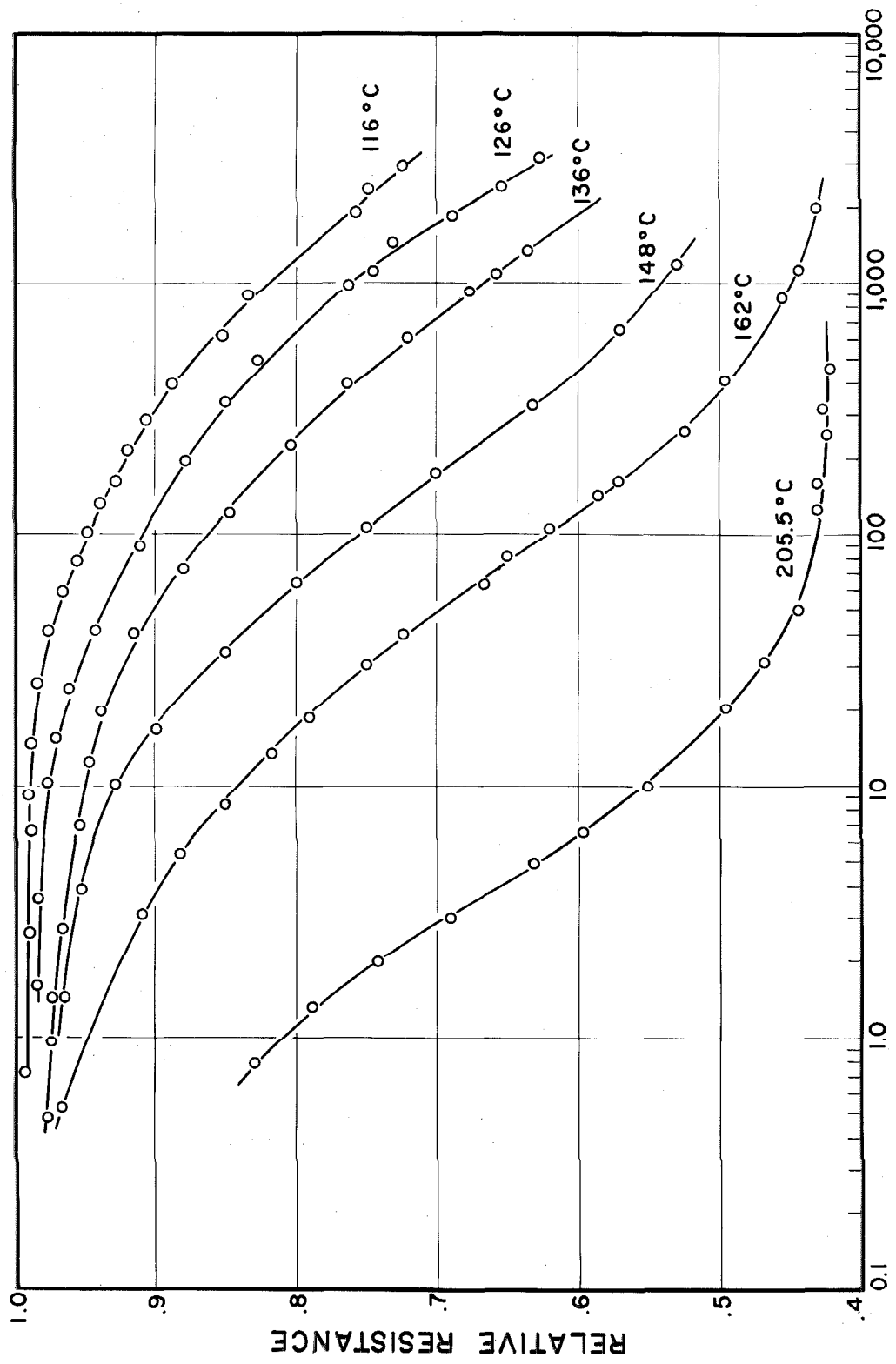

Figure 27. Experimentally determined variation of electrical resistance with amount of heat treatment of 75.0 at.% Ag;Cu foils.

TABLE VII

ACTIVATION ENERGY FOR TRANSFORMATION OF THE 75.0 at. % Ag;Cu ALLOY AS DETERMINED BY ELECTRICAL RESISTANCE MEASUREMENTS

Relative Resistance, R/R_o	Activation Energy, Q (cal./g. mole)
.95	33,300 $\pm$ 2000
.90	31,900 $\pm$ 1000
.85	31,900 $\pm$ 2000
.80	31,200 $\pm$ 1000
.75	30,700 $\pm$ 1000
.70	31,400 $\pm$ 3000
.65	32,100 $\pm$ 2000
.60	31,200 $\pm$ 3000
.55	31,200 $\pm$ 5000

In the above table, values of per cent transformed are not listed since there was no simple unbiased way of correlating relative resistance with per cent transformed. This problem stems from two major causes. The most important cause is the combined effects of grain boundaries, lattice defects, and strain, which will be discussed below. The second cause is the fact that the resistivity of a mixture of two phases cannot be taken as just the weighted average of the resistivities of the two phases. Rather, it lies somewhere

between this value and the reciprocal of the weighted average of the conductivities of the two phases, and might be expected to change within these limits during the transformation. However, this effect should not prevent comparisons between the same R/R_o values for different temperatures, provided that the grain boundary, lattice defect, and strain effects do not vary appreciably within the temperature range considered.

The accuracy of electrical resistivity determinations was limited by the nonuniform thickness of the foils. The approximate resistivity of the metastable foils is 3.4×10^{-6} Ω cm. at liquid nitrogen temperatures, as compared with an approximate resistivity of 1.4×10^{-6} Ω cm. for these foils after transformation. This latter value is about four times as large as might be expected for large-grained samples, as may be inferred from data for pure metals,[62] assuming an approximately linear variation of resistivity with relative amounts of the two phases.

Composite results of experiments conducted on the 88.0 at.% Ag;Cu foils are shown in Figs. 28 and 29 in order to enable a comparison between the transformation process of foils rapid-quenched from the liquid state and the transformation process of foils quenched from the solid state. Unfortunately, the larger grain sizes of the foils quenched from the solid state (see Fig. 30) complicates the question of the role played by quenched-in defects in the foils.

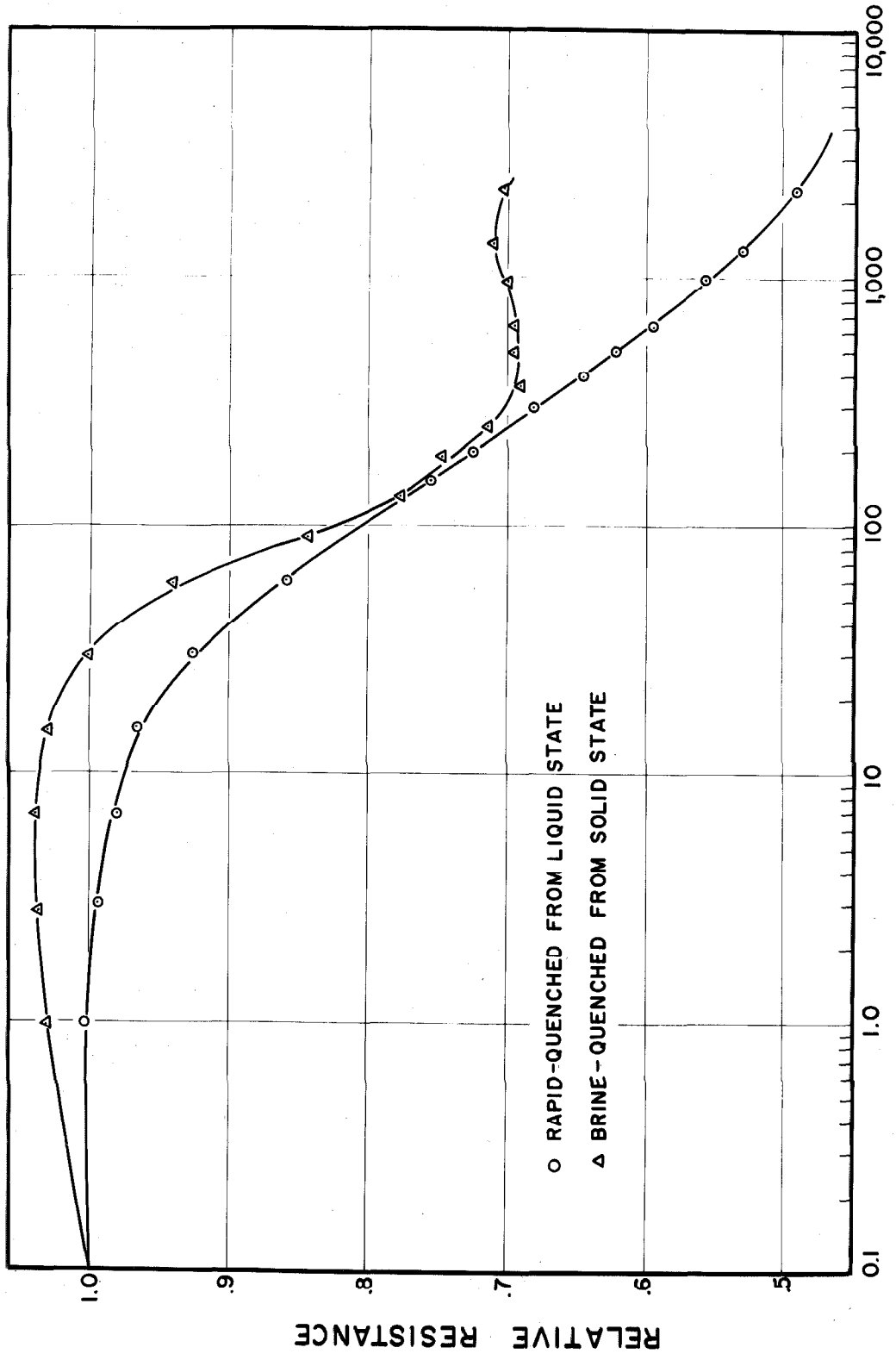

Figure 28. Comparison of transformation of rapid-quenched and solid-state quenched foils by electrical resistance measurements. Heat treatment at 162.0 ^{o}C.

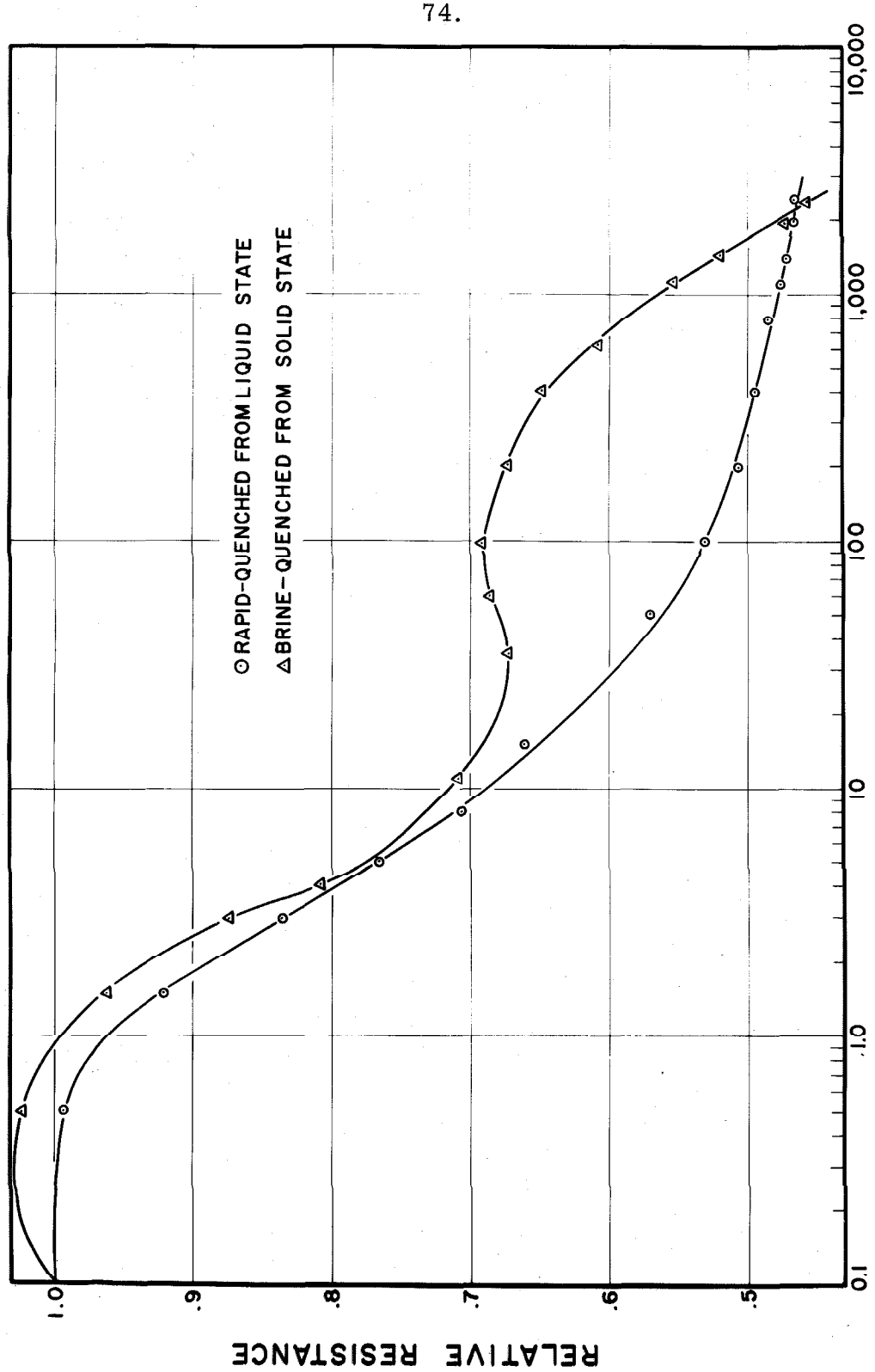

Figure 29. Comparison of transformation of rapid-quenched and solid-state quenched foils by electrical resistance measurements. Heat treatment at 205.5°C.

Momentarily neglecting the initial portions, the curves of Figs. 28 and 29 can be explained on the basis of grain size considerations. The reader is referred to the photomicrographs in Figs. 30 - 34 and to the ensuing discussion. No photomicrographs of rapid-quenched foils of the 88.0 at.% Ag;Cu composition are shown because they were found to be indistinguishable from photomicrographs of 75.0 at.% Ag;Cu foils at corresponding stages in the transformation.

Reference to Figs. 30 - 34 shows that after 5 hrs. at 162.0°C precipitation is visible in only a few (presumably more highly strained) grains. After 100 hr. precipitation is visibly pronounced in most of the grains. The absence of visible evidence of precipitation in the remainder of the grains is evidently just an orientation effect, as was evidenced by heavier etching. After 300 hr. the microstructure has attained an appearance which does not change even after further heat treatment consisting of an additional 1000 hr. at 205.5°C. Precipitation is essentially complete after 300 hr. at 162.0°C, as far as can be told by the metallographic examination performed.

The initial rise in electrical resistance of the foils quenched from the solid state is in direct agreement with the results of Cohen[18] and is due to the pre-precipitation phenomenon found by other investigators and discussed in Chapter V. This effect obscures the effect of fewer quenched-in defects in foils quenched from the solid state when comparisons with rapid-quenched foils are attempted.

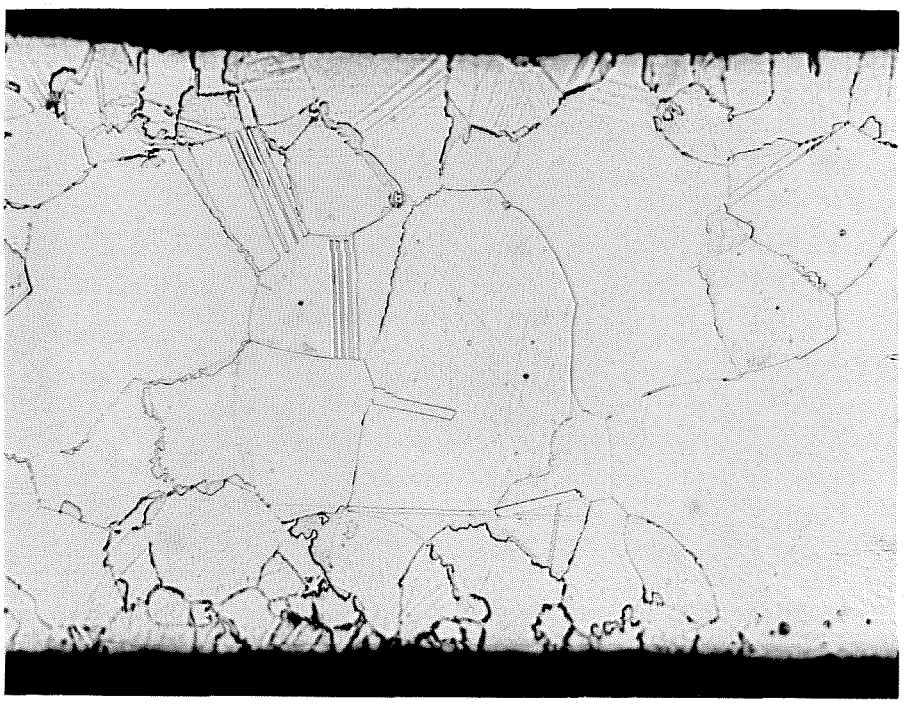

Figure 30. Part of an 88.0 at.% Ag;Cu foil as quenched in brine from 790$\pm$5°C. 550x.

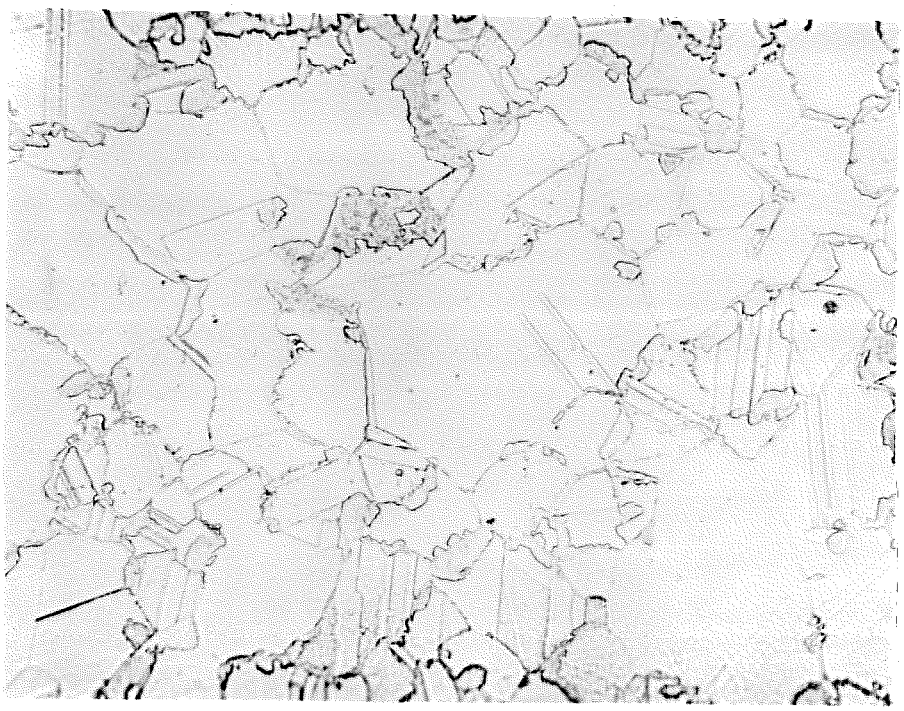

Figure 31. Part of an 88.0 at.% Ag;Cu foil quenched in brine from 790$\pm$5°C, then held for 5 hr. at 162.0°C. 550x.

(a)

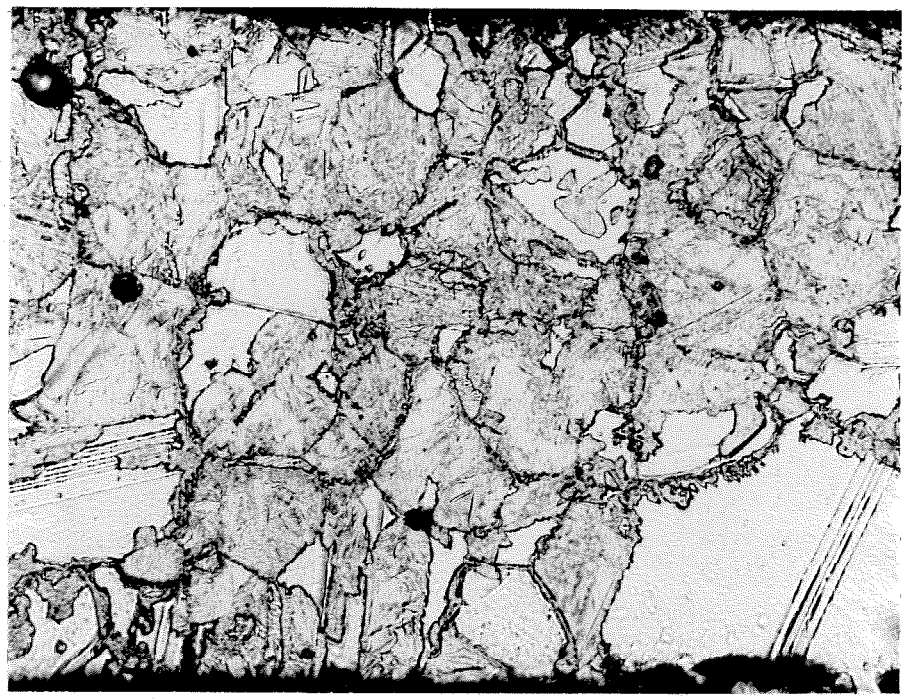

(b)

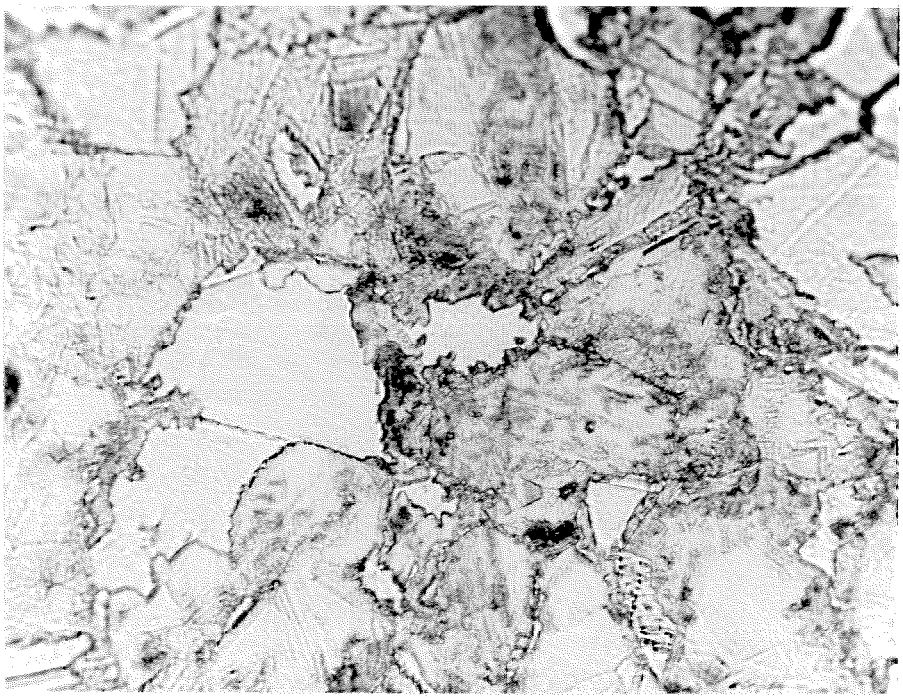

Figure 32. Part of an 88.0 at.% Ag;Cu foil quenched in brine from 790+ 5°C, then held for 100 hr. at 162.0°C: a) 550x, b)1500x.

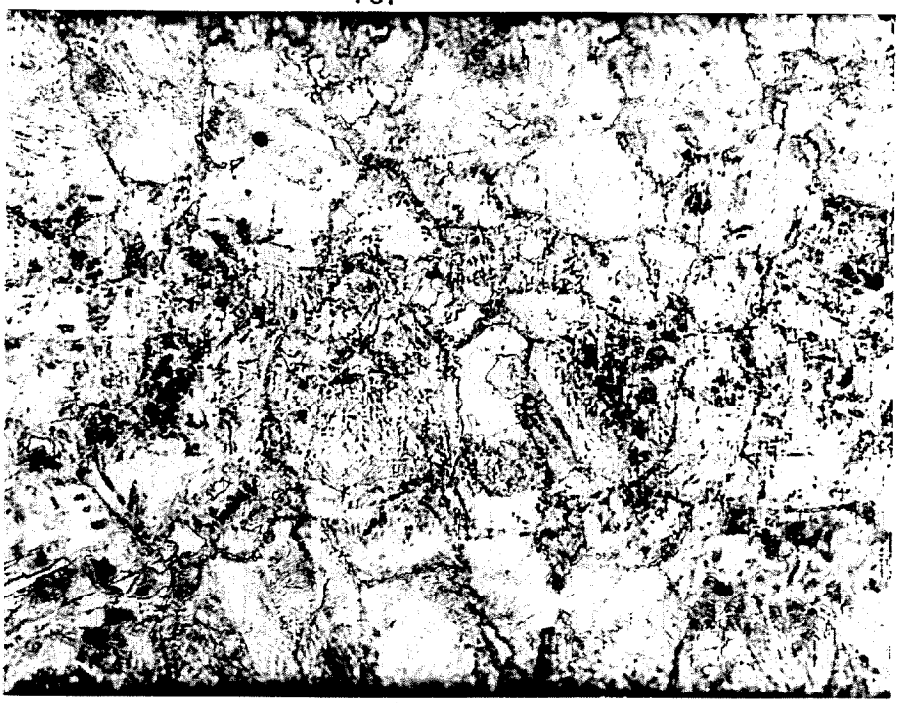

Figure 33. Part of an 88.0 at.% Ag;Cu foil quenched in brine from 790 ± 5 °C, then held for 300 hr. at 162.0 °C. 550x

Figure 34. Part of an 88.0 at.% Ag;Cu foil quenched in brine from 790 ± 5 °C, then held for 1000 hr. at 162.0 °C. 1500x.

The incubation period associated with pre-precipitation in foils quenched from the solid state accounts for the shape of the resistance curves of these foils up to the region approaching the plateau. When the plateau is approached, most of the precipitation has already taken place, as is evidenced by the photomicrographs just discussed and by a comparison of the time scales of Figs. 24 and 27 for the 75.0 at.% Ag;Cu composition. The effects of electron scattering by lattice imperfections and distortions in foils quenched from the solid state evidently exceed those for the rapid-quenched foils at this stage in the transformation. (Most of this increase in electron scattering takes place in the grain boundaries.) Soon thereafter, any decrease in resistance is balanced by, and even overshadowed by, these grain boundary effects. Eventually, the reduction of intergranular strains and the grain growth due to feeding on adjacent grains of the same phase (resulting in a reduction of grain boundary volume) are sufficient to reduce the relative resistance of foils quenched from the solid state below that of rapid-quenched foils. This indicates that the net relative increase in grain boundary volume and intergranular strains is greater in the rapid-quenched foils, presumably due to the much greater number of nuclei which were present to grow. Also, the rapid-quenched foils have grains so small that strains due to stresses exerted by adjacent grains affect a much greater proportion of the atoms in a given grain, a situation which could be a major cause of the above results.

To illustrate the approximate magnitude of grain size effects, it should be pointed out that a comparison of the resistivities of rapid-quenched and solid-state quenched metastable foils (computed as previously described) shows ρ(solid-state quenched) $\simeq$ 1.6×10^{-6} Ω cm., while ρ(rapid-quenched) $\simeq 2.4 \times 10^{-6}$ Ω cm. at liquid nitrogen temperatures. To show that this difference was not due mainly to quenched-in defects, electrical resistances of rapid-quenched foils which had been completely transformed at 162°C (a temperature low enough to insure no appreciable grain growth) were measured. The samples were then removed from their holders (Fig. 13), heated to about 500 °C in an evacuated quartz tube, and held at this temperature for several hours to promote grain growth without appreciably changing the amount of solid solubility. Photomicrographs indicated grain sizes less than, but comparable to, that of foils as quenched from the solid state. The foils were replaced in their holders and their electrical resistances remeasured. In all cases, resistances had dropped to between 55% and 70% of their previous values.

Thus, while the role of quenched-in defects in increasing the transformation rate of rapid-quenched foils cannot be ruled out entirely, there is within the limits of the present investigation no experimental evidence to support any such role. This subject will be discussed in greater detail in Chapter V.

The continuing drop in electrical resistance after x-ray measurements have indicated complete transformation may be caused by the following: 1) greater sensitivity of electrical resistance measurements to the last few per cent of transformation, which involves regions too small to contribute much to x-ray diffraction peaks but which increase the electrical resistance by virtue of their small size, and 2) breaking away of semicoherent precipitates (to be discussed in Chapter V), resulting in a reduction of coherency strains, and thus a reduction in electrical resistance.

The process of grain growth and/or relief of nonuniform elastic strain in the rapid-quenched foils is evidenced by a continual sharpening of the x-ray diffraction peaks from typical widths of 7×10^{-3} radians at half maximum intensity when essentially complete transformation has taken place according to x-ray results, to typical widths of 5×10^{-3} radians after the electrical resistance curves have leveled out. Further grain growth is essentially stopped (at the temperatures involved), since the driving force for this process is much less after the initial coalescence of micrograins.

The extra broadening B (radians) due to small grain size is given by the well-known Scherrer formula,

$$B = \frac{0.9\lambda}{t \cos\theta},$$

where λ is the wavelength of the incident radiation, θ is the diffraction angle, and t is the thickness of the diffracting grain. Thus,

there is no appreciable extra broadening due to grains thicker than about 10^4 Å. The extra broadening b (radians) due to nonuniform elastic strain is given by

$$b = \Delta(2\theta) = -2\frac{\Delta d}{d}\tan\theta,$$

where d is the interplanar spacing for the planes in question, so that the maximum tensile or compressive strain is $\simeq \frac{\Delta d}{2d}$, and thus no appreciable broadening occurs for strains less than about 10^{-4}. It should be mentioned here that some of the broadening of the as-quenched solid solution (111) peak (Fig. 10) may be caused by small fluctuations of composition about the mean.

It has been indicated above (on the basis of Fig. 29) that the net effect of grain boundaries and strain in increasing the electrical resistance of transformed foils is greater than the net effect of quenched-in defects, grain boundaries, and strain in increasing the electrical resistance of rapid-quenched metastable foils. This does not imply, however, that the relative number of atoms in such high energy configurations is very large. Thus, even though electrical resistance measurements are sensitive to these configurations, the results of this chapter cast no doubts upon the measured ΔH values in Chapter II within the error limits stated there.

The fact that the activation energy for transformation of the 75.0 at.% Ag;Cu alloy computed in this section agrees so well with the activation energy computed from x-ray diffraction data indicates

that the effects discussed above are nearly the same for all temperatures in the range considered. These effects might be expected to be slightly more important at the lower temperatures, resulting in a slightly lower value for Q as computed from electrical resistance data, as was indeed found to be the case.

Results of the constant heating rate experiment are shown in Fig. 35. Values obtained for the temperature coefficient of resistivity (referred to 21 ^{o}C as a base) were 2.00×10^{-3} per ^{o}C for the metastable solid solution over the temperature range 21 ^{o}C to 120 ^{o}C, and 3.24×10^{-3} per ^{o}C for the transformed foils over the temperature range 21 ^{o}C to 352 ^{o}C. In obtaining the graph of Fig. 35 a linearly weighted average of these temperature coefficients was used in the steeply sloped portion of the curve. The general characteristics of a similar curve obtained by Mader, et, al.[15] indicate that the transformation process of their vacuum deposited films (referred to in Chapter I) is probably of the same type as that of the present investigation.

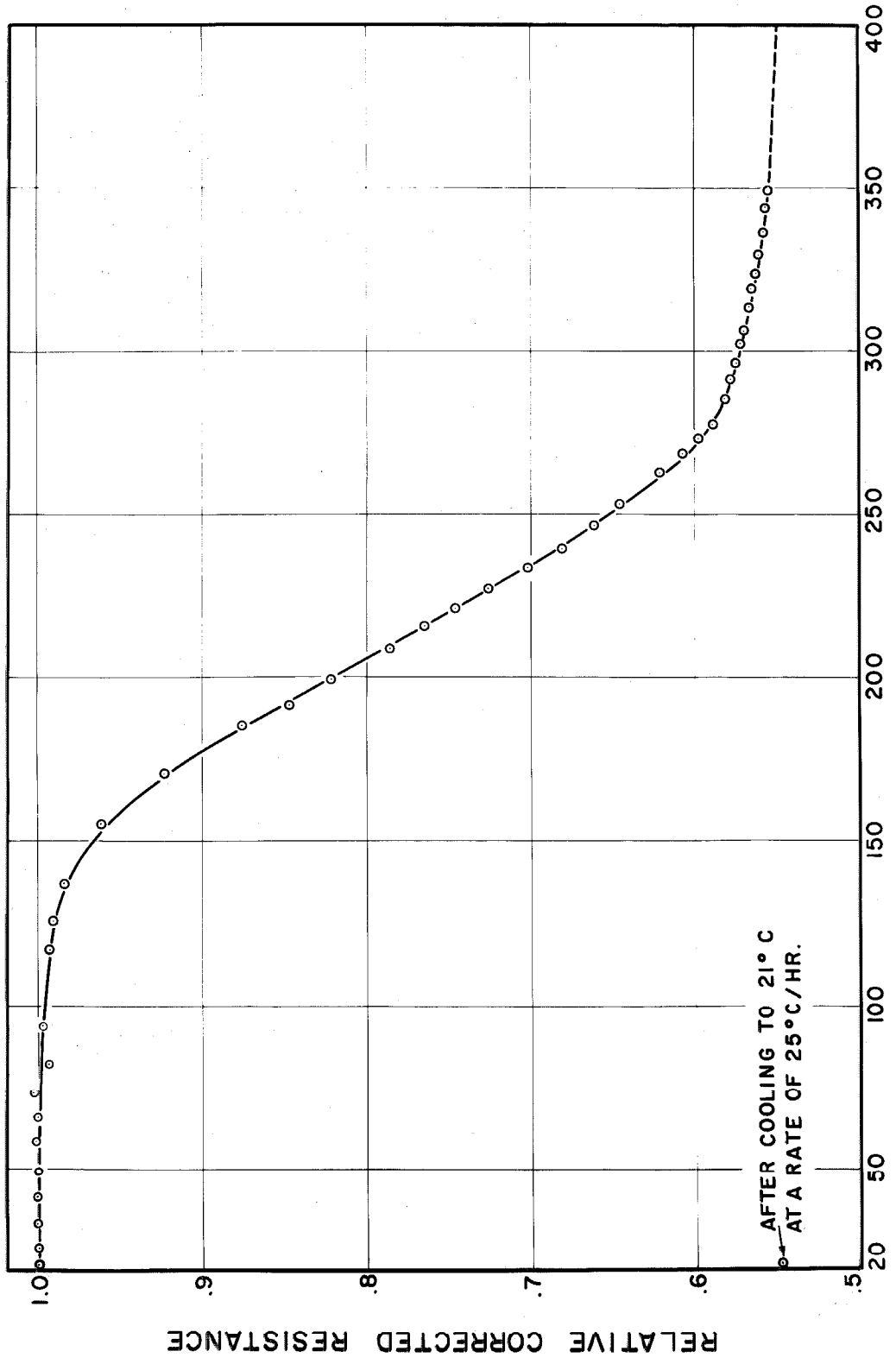

Figure 35. Change in electrical resistance during heating at constant rate of 25 °C/hr. Readings have been corrected to allow for the temperature coefficient of resistivity.

IV. DISCUSSION OF THE SOLIDIFICATION AND TRANSFORMATION PROCESSES

A. NUCLEATION AND SOLIDIFICATION

In this section a model for the solidification process of rapid-quenched foils will be discussed, and the observed microstructure will be explained. The presence of quenched-in stable-phase nuclei will also be considered. However, before proceeding to this discussion, some general remarks about nucleation are in order.

Any solid state precipitation process involving changes of composition of phases begins with the formation of nuclei or segregates. The mechanism of nucleation is still the subject of much discussion, but certain aspects of the process are evident. In a metastable state (quenched solid or supercooled liquid) the total free energy of the system is greater than it would be in the stable state. This excess free energy, then, provides the driving force for the precipitation of the stable phase (s). A nucleus may form in solid alloys when concentration fluctuations produce a cluster of atoms of lower total free energy than that of the original composition. The change in chemical free energy per unit volume of the nucleus is denoted by ΔF_V. In the case of a supercooled liquid, ΔF_V represents the difference in chemical free energy per unit volume between the liquid and the solid nucleus. The quantity ΔF_V is necessarily negative for nucle-

ation to occur.

It is evident that there will also be a positive contribution to the total free energy change (ΔF) due to the existence of an interface between the nucleus and the matrix of the parent phase. This may be termed a surface free energy per unit area of the surface of the nucleus and be denoted by ΔF_s.

For solid state precipitation there is still another positive term in ΔF due to the strain which occurs when the nucleus must be fitted into a region of different specific volume, resulting in distortion of the lattice. This contribution is denoted by ΔF_e per unit volume, but can be neglected for nucleation from the liquid state.

Consider precipitation of a solid from a supercooled liquid. If ΔF_v and ΔF_s were the only important factors, then the shape of the nuclei would be that which will minimize the surface-to-volume ratio, since ΔF_v is negative and ΔF_s is positive. This shape is a sphere. Then if r is the radius of the sphere,

$$\Delta F = \frac{4}{3}\pi r^3 \Delta F_v + 4\pi r^2 \Delta F_s,$$

and the critical radius r_c for formation of a stable nucleus is the value of r for which any increase in the radius makes $\frac{\partial(\Delta F)}{\partial r}$ become negative. For this case Klement[16] has suggested (on the basis of related results of many investigators) that

r_c (metastable solid solution) $\geq$ 1.15 r_c (equilibrium phase) (1)

for equiatomic Ag-Cu alloys. There is, however, an additional factor to be considered: namely, the heat of fusion. If heat is released upon solidification, then the temperature of the nucleus is increased, and thus the magnitude of ΔF_v is decreased, resulting in an increase of the critical radius. Furthermore, since removal of heat is fastest for a thin plate nucleus (highest surface to volume ratio), the most probable nucleus shape should deviate from the spherical form, becoming oblate. However, the ΔH calculations and discussion of Chapter II indicate that deviations from the spherical shape should not differ greatly between the metastable and equilibrium phase nuclei.

With the support of Equation 1, Klement showed that diffusion rates in the liquid would be large enough to enable formation of these equilibrium nuclei during the time required for solidification. Thus, one would expect that many of the nuclei of the copper-rich and silver-rich phases are formed during the initial solidification. The subsequent preferential growth of the metastable phase is then envisaged as the result of the metastable lattice's being able to assimilate atoms at random, while the stable lattice can grow only by selectively assimilating atoms from the melt.

The possibility of spontaneous segregation (no activation energy required) immediately after solidification should also not be ignored. The spinodal curve of Hardy [49] (Fig. 36) is a plot of the equation $\frac{\partial^2 F_V}{\partial C^2} = 0$ for the Ag-Cu system. All compositions (C) at temperatures which fall below this curve can undergo segregation spontaneously. These segregates could act as preferred nucleation sites due to their concentration differences.

Because of the high cooling rates involved it is quite possible that nucleation is primarily homogeneous. The case of heterogeneous nucleation will be dealt with at the end of this section. According to Turnbull, [63] the degree of undercooling necessary for homogeneous nucleation for a great number of metals is about 17% to 20% of the melting temperature (^{o}K), with 20% representing the approximate limit for metallic systems up to the present time [16]. For pure Ag and pure Cu the values are 18.4% and 17.4%, respectively. Furthermore, calculations made in the manner described below indicate that homogeneous nucleation rates for the alloys in question increase by about one order of magnitude for every additional 5 ^{o}C undercooling near the 20% limit. Thus, even for cooling rates somewhat greater than those estimated for the foils, the undercooling would fall far short of 30% (equivalent to undercooling to 736 ^{o}K for the 75 at% Ag;Cu alloy).

Turnbull and Fisher [64] have shown that the rate of homogeneous nucleation R' of a solid from a liquid when compositional changes are not involved may be expressed as

$$R' \simeq (N\,k\,T\,/h) \cdot \exp\left[-(\Delta f + \Delta F_c)/k\,T \right] \quad (2)$$

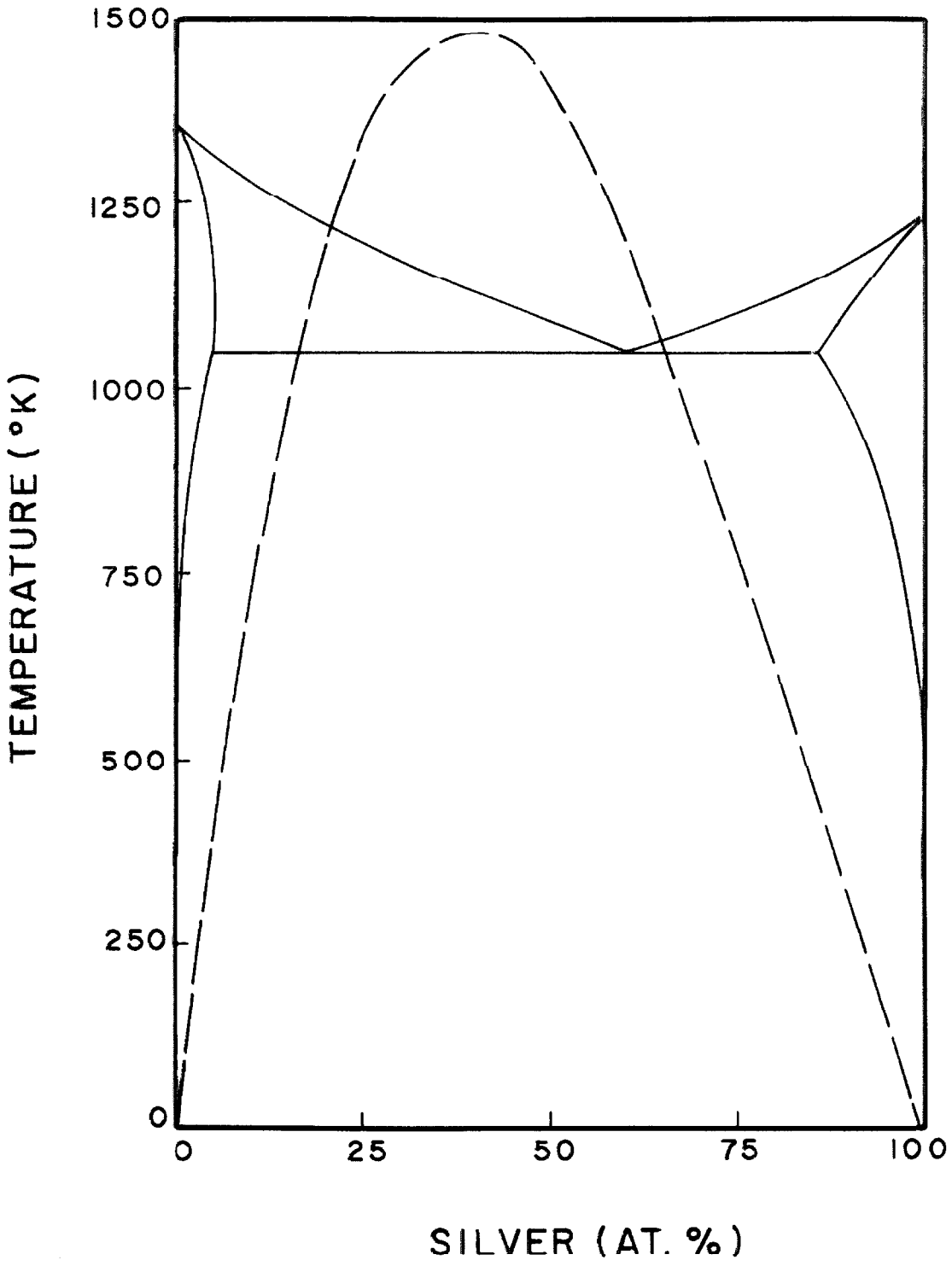

Figure 36. Calculated spinodal curve. After Hardy and Heal. [49]

nuclei per mole per second to an order of magnitude. In the above expression, Δf is the free energy of activation for diffusion of atoms moving a fraction of an atomic distance across an interface to join a new lattice, N is Avagadro's number, k is Boltzmann's constant, h is Planck's constant, and ΔF_c is the value of ΔF at $r = r_c$. The critical radius r_c, in turn, can be calculated from the condition, $\left.\frac{\partial(\Delta F)}{\partial r}\right|_{r_c} = 0$. Unfortunately, reliable values of Δf and ΔF_c are not available, so that even if the above formula is capable of good predictions of nucleation rates, the calculated values are likely to be in error by several orders of magnitude. It is possible, however, to obtain a reasonable idea of relative rates near the maximum and of the approximate temperature at which this maximum occurs by using the approximate expression for ΔF_c as a function of T derived in the Appendix.

The value of Δf is generally taken to be the activation energy for viscous flow, which in the case of Ag at 1400 °C is 4,820 cal./g. mole.[65] For the present calculation, values of Δf equal to 0, 5000, and 10,000 cal./g. mole were used as a basis for comparison. The results are plotted in Fig. 37, which is a graph of Equation 2 on an arbitary linear scale. It should be pointed out that the maximum of each peak in Fig. 37 has been set at 100, even though the difference in heights between the peak for $\Delta f = 0$ and the peak for $\Delta f = 10,000$ cal./g. mole is as much as four orders of

magnitude. Great caution must be used in interpreting this graph because although the linear scale used demonstrates the desired results, the uncertainty in absolute magnitudes involved is such that the upper temperature at which the nucleation rate actually drops to an insignificant value is unknown. It is certain, however, that this temperature is well above the temperature at which it appears to happen in Fig. 37 by virtue of the scale used there.

The point to be drawn from the foregoing development is that (as shown in Fig. 37) with the present degree of undercooling the maximum rate of homogeneous nucleation could not have been reached. Thus, it is evident that the microstructures observed cannot be explained on the basis of an increased nucleation rate in the more slowly cooled portions of the foils. In view of this conclusion, the solidification process may be envisioned as proceeding in the following manner: When the globule of molten metal is caught between the anvils, the degree of undercooling is so great that nucleation takes place at a very rapid rate. As the solid-liquid interface moves toward the center of the foil, there is not much growth in the transverse directions due to impingement as a result of the great number of nuclei initially formed. Columnar growth is further favored by the conditions for removal of the latent heat of fusion upon solidification.

Of course, some nucleation would take place throughout all

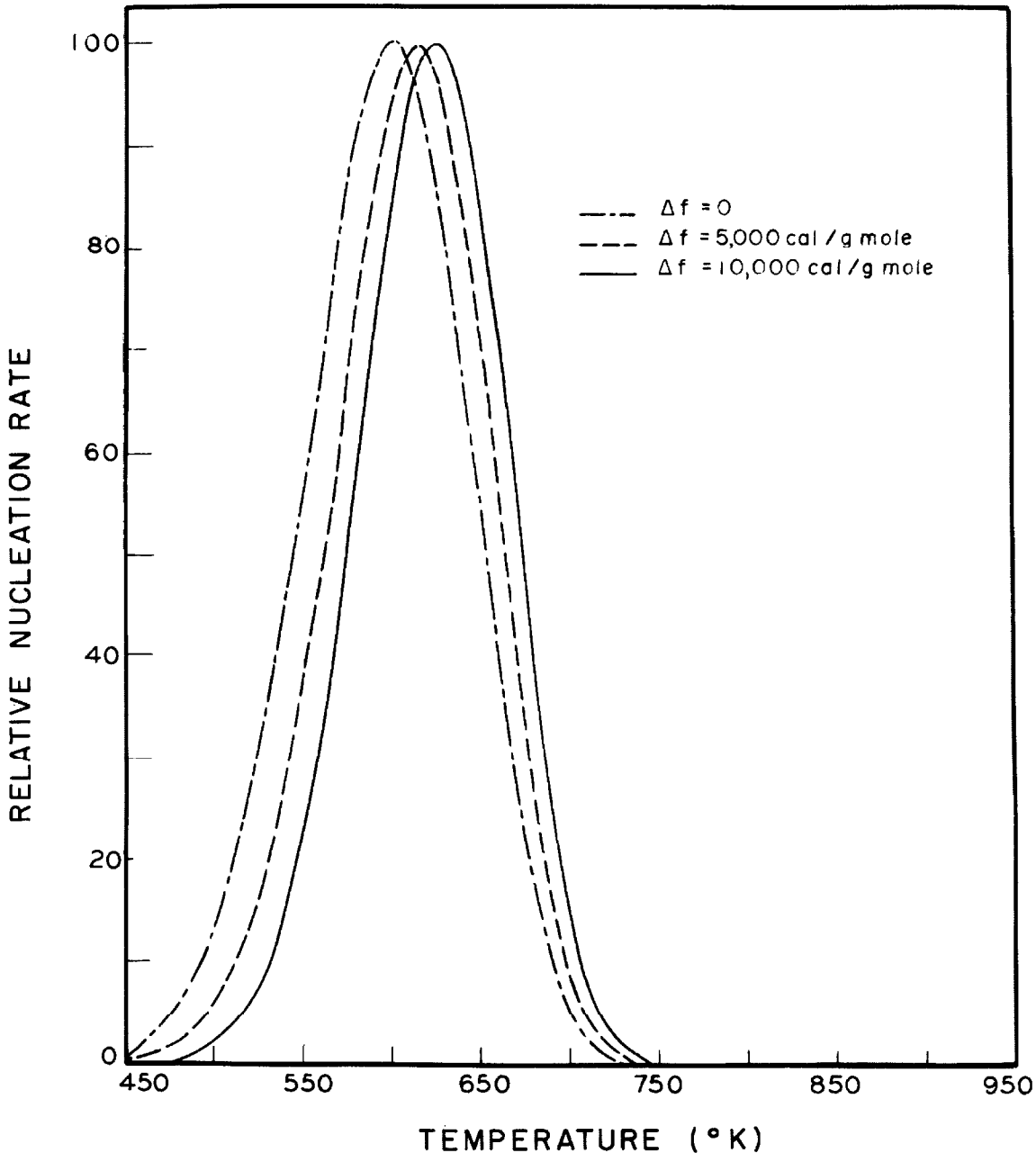

Figure 37. Relative nucleation rates as computed from Equation 2.

parts of the liquid before solidification could occur entirely by growth of the nuclei at the outer surfaces of the foil. However, for columnar growth it has been found that the rate of growth (checked for undercoolings up to about 18%) varies approximately as the square of the undercooling, [66], [67], [68] so that the columnar growth could quite possibly be responsible for solidification of the outer regions of the foil before enough time has elapsed for nucleation and growth of other nuclei to solidify much of the foil. Once columnar growth begins, it should proceed at a rate governed by the thermal conductivity of the solid, but independent of the external cooling conditions.

The amount of undercooling will, of course, decrease from the surface to the center of the foil (due both to the rate of heat transfer to the anvils and to the release of the heat of fusion from solidified portions), which in turn decreases the nucleation rate. By the time columnar grains have extended about .001 in., enough nucleation has evidently taken place in the central portion of the foil to prevent the further growth of the columnar grains. The nuclei are probably so numerous in this region that not much growth is required to complete the process of solidification. The situation shown in Fig. 20 is one in which some coarser grains are present between the columnar structure and the fine-grained structure. This

configuration could be caused by cooling conditions in this intermediate region of the foil which enable a few nuclei to form in this region and start to grow before the columnar grains can penetrate that far into the foil. Then, due to impingement, further growth must proceed from these noncolumnar grains and extend into regions where liquid is still present. The above arguments predict that foils thinner than about .002 in. should be obtainable in the entirely columnar form, as was experimentally borne out (see Fig. 19).

The foregoing development was based upon the assumption of homogeneous nucleation. In the case of heterogeneous nucleation the above picture of the solidification process would not be changed, but would be perhaps even more strongly supported because there would be more nucleating sites at the anvils than in the interior of the liquid and because the amount of undercooling would be even less than for homogeneous nucleation. Any shift of the maximum nucleation rate to higher temperatures would not be enough to alter the above conclusions.

B. TRANSFORMATION TO EQUILIBRIUM

On the basis of experimental results obtained in this investigation, a model for the transformation process will be developed in this section with the aid of transformation equations proposed by other investigators.

In view of the discussion of the preceding section, it is reasonable to expect that many of the nuclei of the Ag-rich and Cu-rich phases and perhaps Ag-rich and Cu-rich segregates are present in the as-quenched foils. This conclusion is supported by the asymmetrical peak of Fig. 10. It is evident that nucleation rates for these two stable phases are significant at the temperatures in question, because for slightly slower cooling rates the appearance of these phases in appreciable amounts cannot be suppressed. However, if the cooling rate is rapid enough, the growth of stable-phase nuclei after formation can be severaly limited, as suggested in the previous section of this chapter. In addition, one would expect dislocations to be present in the foils due, first of all, to the plastic flow which might occur as a result of the solidification of the last liquid regions between existing grains. (The grains will be placed in tension due to the volume contraction of about 4% [69] upon solidification.) Probably by far the most important sources of dislocations are the "accidents" which occur upon solidification. Dislocations are generally favored sites for nucleation in

the same sense that grain boundaries are. Furthermore, the segregation of Cu atoms to the compression side and Ag atoms to the tension side of edge dislocations could provide favorable concentration fluctuations for nucleation. Perhaps of greater importance is the fact that, as Suzuki [70] has pointed out, in face-centered cubic crystals ordinary dislocations are unstable and split into two partial dislocations* separated by a stacking fault about two atomic planes in thickness and having a concentration of solute atoms different from that of the average matrix. This configuration, too, would provide favorable concentration fluctuations for nucleation. In any case, the formation of any additional nuclei, although thought to be unnecessary, would take place very early in the transformation process. Homogeneous segregation would be unnecessary. This point could be further explored by electron microscopy.

The precipitation process for the transformation to equilibrium of rapid-quenched foils, in contrast to that of foils quenched from the solid state, is not conceived as involving a "pre-precipitation" stage in which atoms of one species would preferentially segregate to a particular crystallographic plane in an otherwise

---

*The formation of such partial dislocations would be due to reactions of the type, $\frac{a}{2}$ $(1\,0\,\bar{1}) \rightarrow \frac{a}{6}(11\bar{2}) + \frac{a}{6}(2\,\bar{1}\,\bar{1})$, as shown by Heidenreich and Shockley[71].

"perfect" matrix, forming sheets only a few atoms thick (formation of Guinier-Preston zones). These sheets have been thought by other investigators to act as nuclei for the plate-like precipitates observed in the so-called Widmanstätten structures.[72], [73]

Nabarro[74] has shown that for the Ag-Cu system the strain energy associated with a particle of precipitate is so large that the precipitate must form in flat plates. He further concluded that the atomic size difference is so great that any nucleus must either break away immediately from the parent lattice or redissolve, since the elastic strain energy needed to maintain coherence with the parent lattice would be greater than the chemical free energy decrease associated with the precipitation. There has been some disagreement as to the habit plane of these precipitates. (Compare, for example, references (72), (75), (76).) Calculations by Barrett,[77] however, confirm Geisler's point of view [76] that the habit plane is the (100) plane in precipitation from both Ag-rich and Cu-rich alloys.

In the present investigation of rapid-quenched foils it is believed that the above-described process does not play a significant role, but rather that growth of quenched-in nuclei is the predominant mechanism. To this end, a determination of the average shape of precipitates is in order; thus, an attempt was made to fit the experimental data with a transformation equation. Two types of transfor-

mation equations were considered, as described below.

The first type of equation used was of the same form as one developed by Johnson and Mehl [78] and later used by Wert [48] and by Wert and Zener, [79] who developed it further in the study of precipitation of C and N from α — Fe. Following the development by Wert, the initial rate of transformation may be written as

$$\frac{dW(t)}{dt} = f(t),$$

where W (t) is the fraction of material transformed, and f (t) is an as yet undetermined function of time. Due to depletion (and eventually impingement) there will be an effective interference between particles of precipitate, causing the rate of transformation to decrease, and this decrease is assumed to be directly proportional to the amount already transformed; hence,

$$\frac{dW(t)}{dt} = \left[1 - W(t)\right] f(t),$$

which has the solution

$$W(t) = 1 - \exp\left[-\int_0^t f(t)\, dt\right].$$

The explicit form used was

$$\frac{\Delta C(t)}{C_o} = 1 - \exp\left[-\left(\frac{t}{\tau}\right)^n\right], \qquad (3)$$

where $\Delta C(t)$ is the total number of solute atoms present in transformed regions, C_o is the initial number of solute atoms, and τ is a constant with respect to time but is a function of C_o, the absolute temperature T, and perhaps some other undetermined factors. The symbol n represents some number independent of C_o and T.

Rewriting the above equation,

$$\log \ln \frac{C_o}{C(t)} = n \log t - n \log \tau , \qquad (4)$$

where C (t) is the amount of solute in the untransformed phase, so that

$$C_o = C(t) + \Delta C(t).$$

Using Equation 4 one may determine n and τ directly from a log-log plot of $\ln\left[\frac{C_o}{C(t)}\right]$ vs. t. In this plot the slope of the resulting line is n, while the intercept at $\ln\left[\frac{C_o}{C(t)}\right] = 1$ is τ .

Zener [80] has shown that if the rate of growth of a particle of a second phase in a matrix of infinite extent is controlled by diffusion, then the time dependence of the transformation rate is a predictable function of the precipitate particle shape. For a spherical precipitate he has shown that the radius increases as $t^{1/2}$; hence the volume V_{sphere} is proportional to $(t - t')^{3/2}$, where t' is the time at which the nucleus was formed. In the case of a cylindrical precipitate he has shown that the radius increases as $t^{1/2}$, while the length increases as t, so that $V_{cylinder}$ is proportional to $(t - t')^2$. For a disk he has shown that the thickness increases as $t^{1/2}$, while the radius increases linearly with time, since the growth conditions at the advancing edge of the disk remain constant (no effective depletion of atoms of a given type), so that V_{disk} is proportional to $(t - t')^{5/2}$.

If $t \ll \tau$, then Equation 3 may be rewritten as

$$\frac{\Delta C(t)}{C_o} = \left(\frac{t}{\tau}\right)^n . \qquad (5)$$

If use is now made of the previous conclusion that essentially all the nuclei were present in the initial quench or soon thereafter, then $t' \simeq 0$ and Equation 5 is in just the right form for interpretation in the light of Zener's conclusions.

The quantities n and τ of Equations 3 - 5 were determined from Figs. 38 and 39, which show plots based upon substitution of x-ray diffraction data from the present investigation into Equation 4. It was assumed that the measured relative peak intensity varied linearly with the amount of transformation. Using the notation of Chapter IV, I_o/I was used for $C_o/C(t)$ in the x-ray measurements (solid solution (111) peak). When $\frac{R_o - R_f}{R(t)}$ was used for $C_o/C(t)$ in the electrical resistance measurements, with the final resistance R_f being determined from the plots of samples carried to completion (shown in Fig. 27), straight lines were also obtained; however, it is difficult to attach any real significance to them, since there is no unbiased way to relate values of $\frac{R_o - R_f}{R(t)}$ to specific amounts of transformation.

Although it would have been very interesting to compare the results of this analysis for rapid-quenched foils with those of foils quenched from the solid state, this was not deemed possible under the present conditions, due to the previously referred to spurious grain size effects, especially in the case of the foils quenched from the solid state. The results of the foregoing analysis are shown

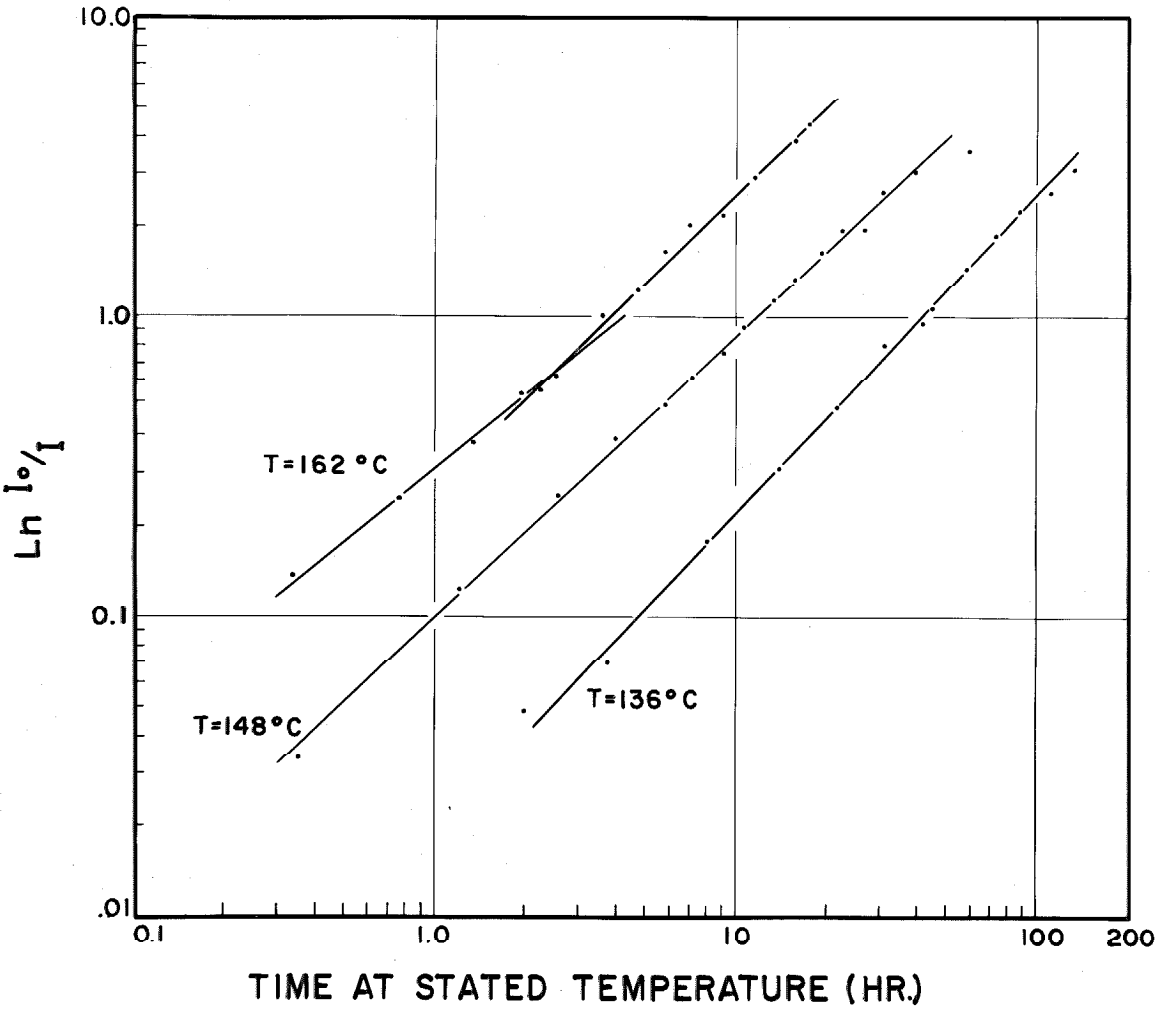

Figure 38. Determination of n and τ of Equations 3 - 5 for the 60.1 at.% Ag;Cu composition, using x-ray diffraction data.

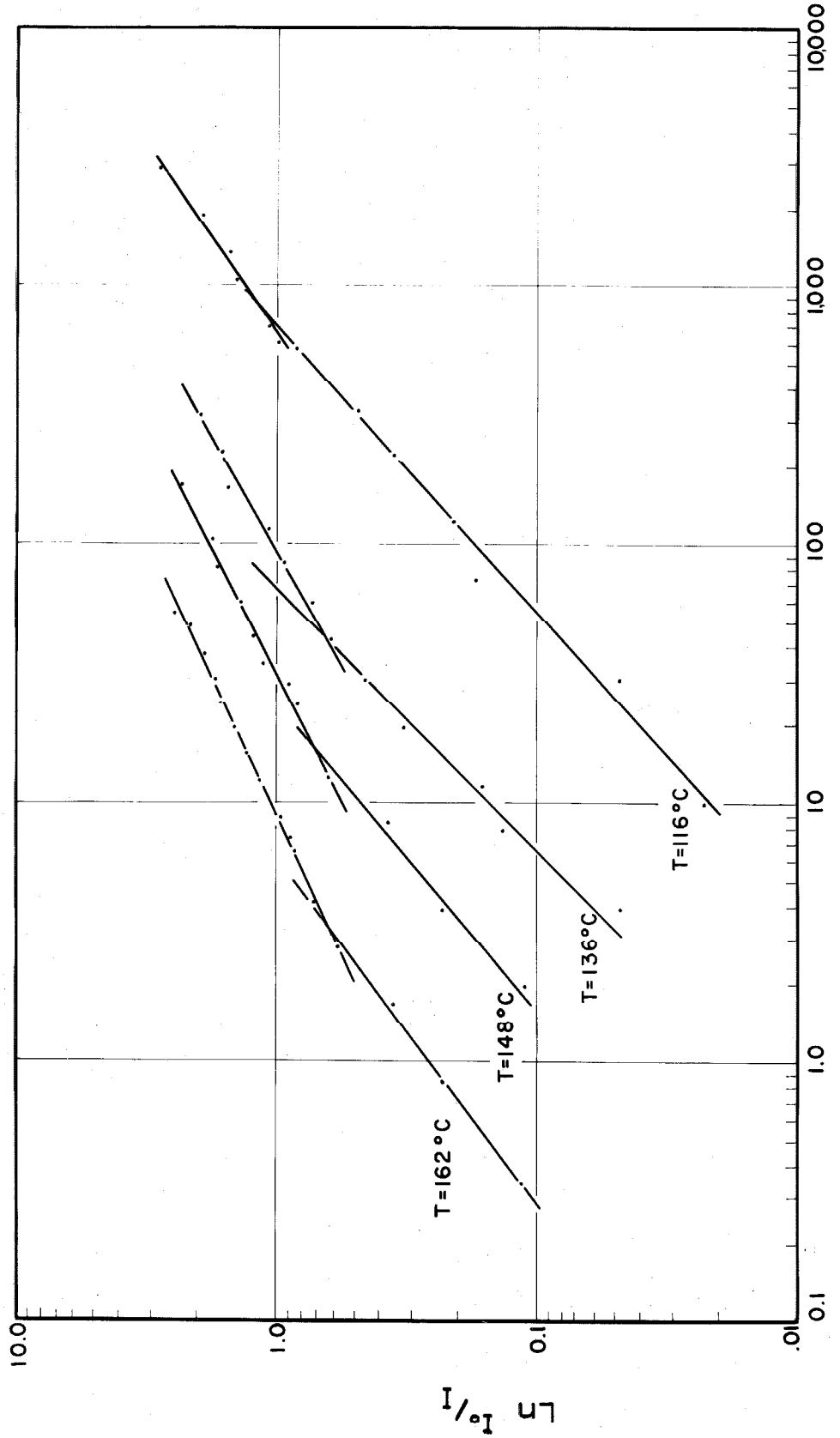

Figure 39. Determination of n and τ of Equations 3 - 5 for the 75.0 at.% Ag;Cu composition, using x-ray diffraction data.

in Table VIII.

TABLE VIII

PARAMETERS IN EQUATIONS 3 - 5 DETERMINED FROM FIGURES 38 AND 39.

Composition (at.% Ag)	Temperature (°C)	τ (hr.)	n ($t \ll \tau$)	n ($t \gtrsim \tau$)
60.1	136.0 ± .2	40.3	.94	.94
60.1	148.0 ± .2	11.4	1.06	1.06
60.1	162.0 ± .2	4.1	1.30	1.02
	Average:		1.10	1.01
75.0	116.0 ± .2	662.	1.11	1.44
75.0	136.0 ± .2	67.3	1.01	1.76
75.0	148.0 ± .2	24.0	1.16	1.94
75.0	162.0 ± .2	6.0	1.33	2.13
	Average:		1.15	1.34

The small value of n obtained does not appear at first sight to fit the analysis presented in the previous discussion. The fairly good straight line fits, however, indicate that the transformation can be represented by Equation 3 with the above parameters. The analysis of Zener, however, cannot be applied because the process of transformation is such that depletion becomes important very early in the small transforming regions due to the large number of nuclei participating in the discontinuous precipitation. Zener's assumption of a nucleus in an infinite matrix is not satisfied here,

even for $t \ll \tau$. This view is supported by the fact that $n\,(t \gtrsim \tau) \simeq n\,(t \ll \tau)$, as may be seen in Table VIII.

The growth of quenched-in nuclei strains the surrounding grains and contributes to a catastrophic breakdown of coherency. Any nuclei formed as a result of segregation within the grains (such as at dislocations) would contribute to catastrophic breakdown due to lattice coherency strains. Thus, nuclei are inhibited from starting to grow, due to the strain energy involved, but once growth starts in a region, it can go rapidly to completion. This breakdown may result in many small-angle boundaries and semicoherent boundaries, which would have an appreciable effect on electron scattering in the electrical resistivity measurements. After long anneal, there is some growth of sub-grains at the expense of others, with the result that the new grain boundaries become more well defined as evidenced by the loss of columnar appearance of grains in the photomicrographs of Fig. 40. This process relieves inter-subgranular strains and semicoherency strains. The grain boundaries may also be made more visible by the migration of dislocations to grain boundaries upon annealing. It is worthy of note that this loss of columnar appearance does not take place until long after complete transformation has taken place, a situation which is in accord with the above discussion. The reader is referred

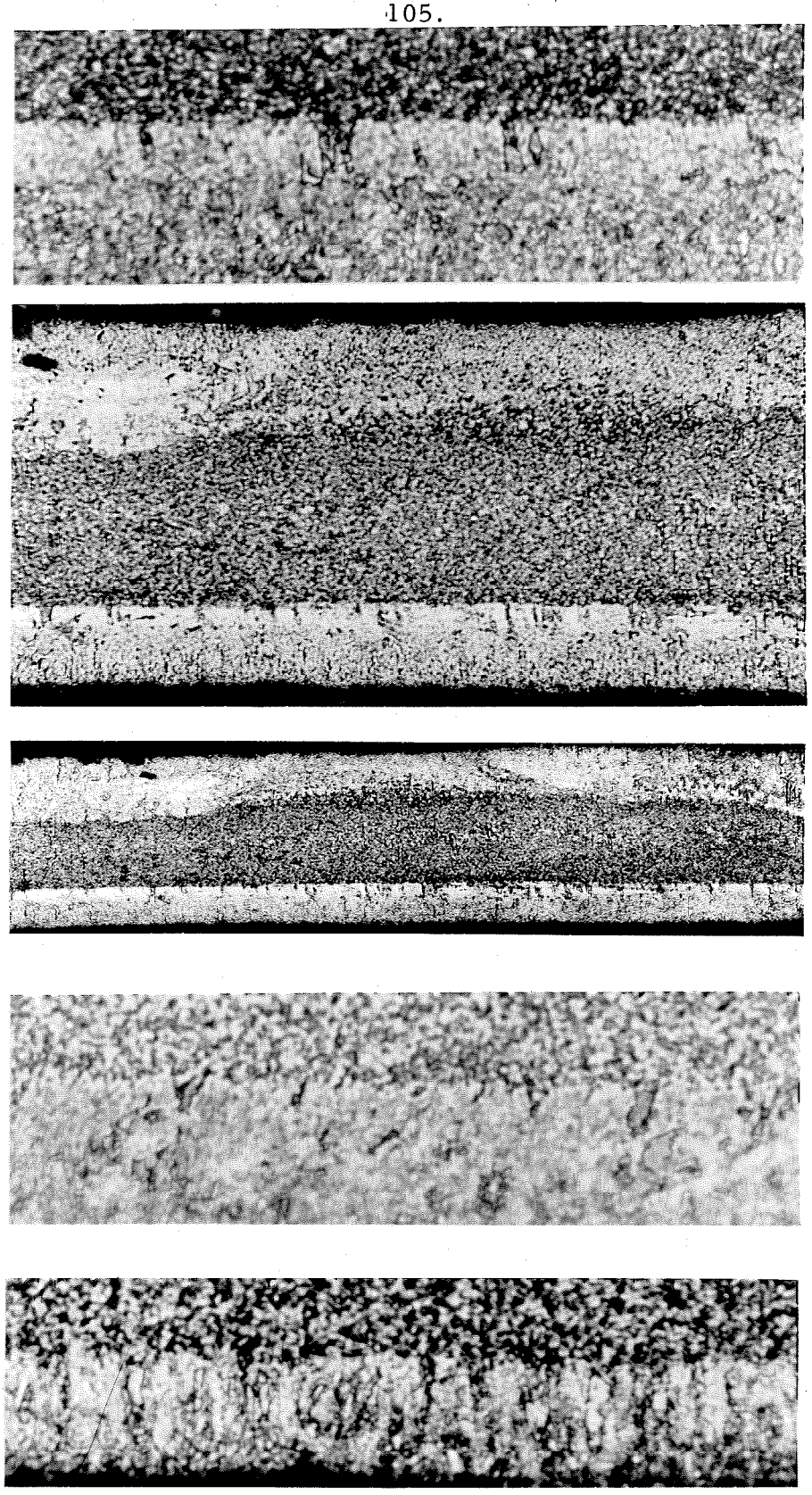

Figure 40. 75.0 at.% Ag;Cu rapid-quenched foils with various heat treatments: a) 1035 hr. at 162.0°C 1500x, b) 210 hr. at 205.5°C 1500x, c) 1100 hr. at 205.5°C 250x, d) 1100 hr. at 205.5°C 550x, e) 1100 hr. at 205.5°C 1500x.

to the photomicrographs of Figs. 40 and 41 and to the transformation curves of Fig. 24. The general trend to larger values of n at higher temperatures also supports the above picture, because localized depletion would have a greater relative effect on growth rates at lower temperatures.

As far as the second type of transformation equation is concerned, an equation of the same general form as the one developed by Austin and Rickett [81] was considered. The fraction transformed F (t) is defined by the equation

$$F(t) = \frac{C_o' - C'(t)}{C_o' - C_f'} , \qquad (6)$$

where C_o' is the initial concentration of solute atoms in the matrix, C_f' the final concentration, and $C'(t)$ the concentration at time t. Assuming that the ratio of the fraction transformed F (t) to the untransformed fraction $\left[1 - F(t)\right]$ is proportional to the precipitation time t raised to some power m, yields

$$\frac{F(t)}{1 - F(t)} = K\, t^m , \qquad (7)$$

where K is a constant. Substituting Equation 6 into Equation 7 and taking logarithms leads to the equation

$$\log \frac{C_o' - C'(t)}{C'(t) - C_f'} = m \log t - \log K. \qquad (8)$$

In the present investigation Equation 8 may be simplified by setting $C_f' = 0$, so that

$$\log \frac{1 - C'(t)/C_o'}{C'(t)/C_o'} = m \log t - \log K. \qquad (9)$$

(a)

(b)

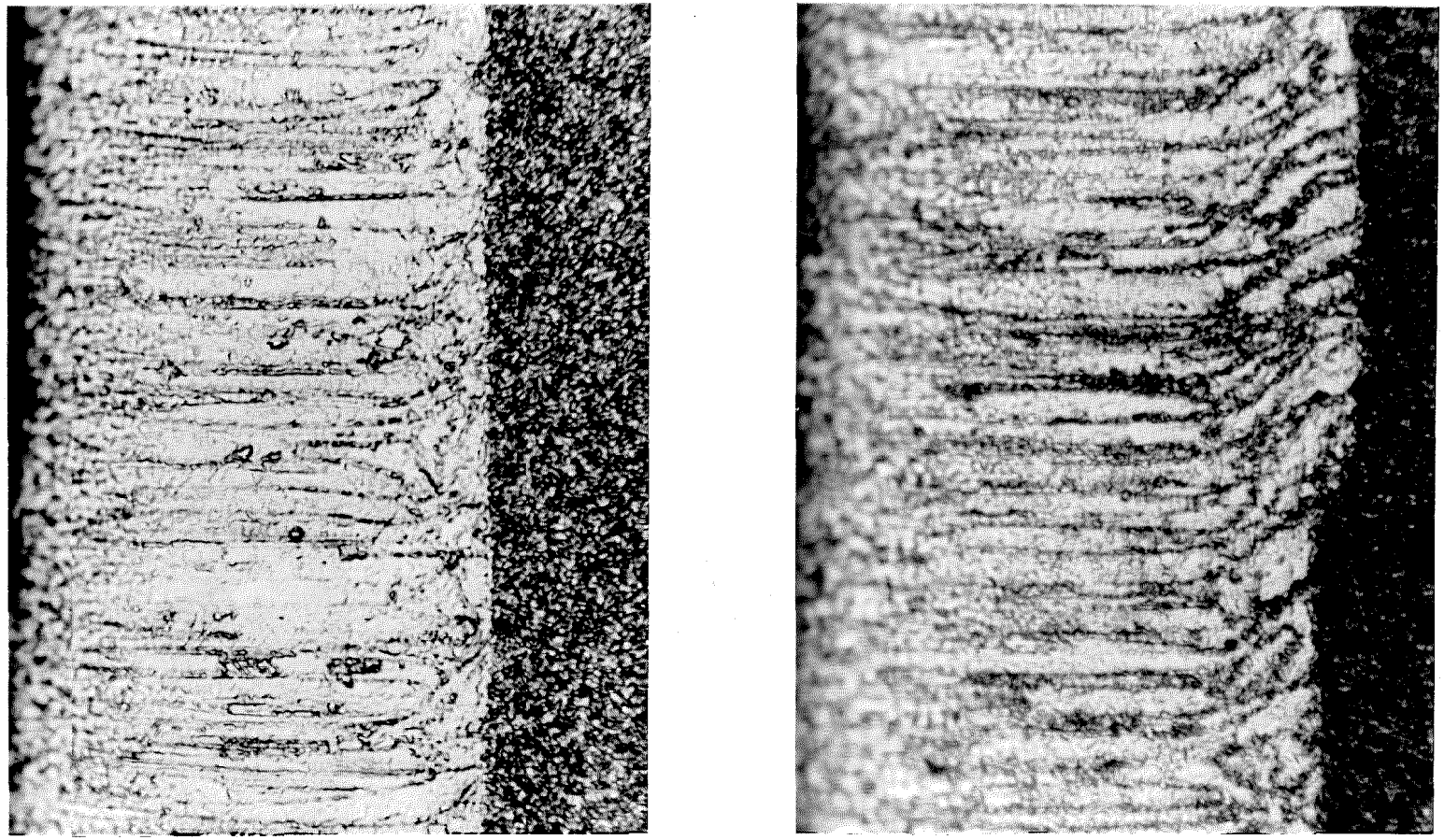

Figure 41. 75.0 at.% Ag;Cu rapid-quenched foil held at 162.0 °C for 120 hr: a) light etch 1500x, b) heavy etch 1500x.

Then m may be determined as the slope of a log-log plot of $\frac{1 - C'(t)/C'_o}{C'(t)/C'_o}$ vs. t, if Equation 9 is a valid transformation equation for the process under consideration. Using the notation of Chapter IV, I/I_o has been substituted for $C'(t)/C'_o$ in the plots of Figs. 42 and 43.

Mishima [61] has indicated that, in general, in connection with Equation 9, $m \simeq 1$ for plate-like precipitates, and $m \gtrsim 1.9$ for "three dimensional" precipitates. Furthermore, since $K^{1/m}$ corresponds to a rate constant, the activation energy Q for the transformation can be calculated from the equation

$$K^{1/m} = K_o^{1/m} e^{-Q/RT} \qquad (10)$$

where K is measured as the intercept on the $\frac{1 - C'(t)/C'_o}{C'(t)/C'_o}$ axis of the log-log plot of Equation 9. Q is then calculated as $(-\frac{R}{m})$ times the slope of a ln K vs. $1/T$ plot. The results from Figs. 42 and 43 are presented in Table IX.

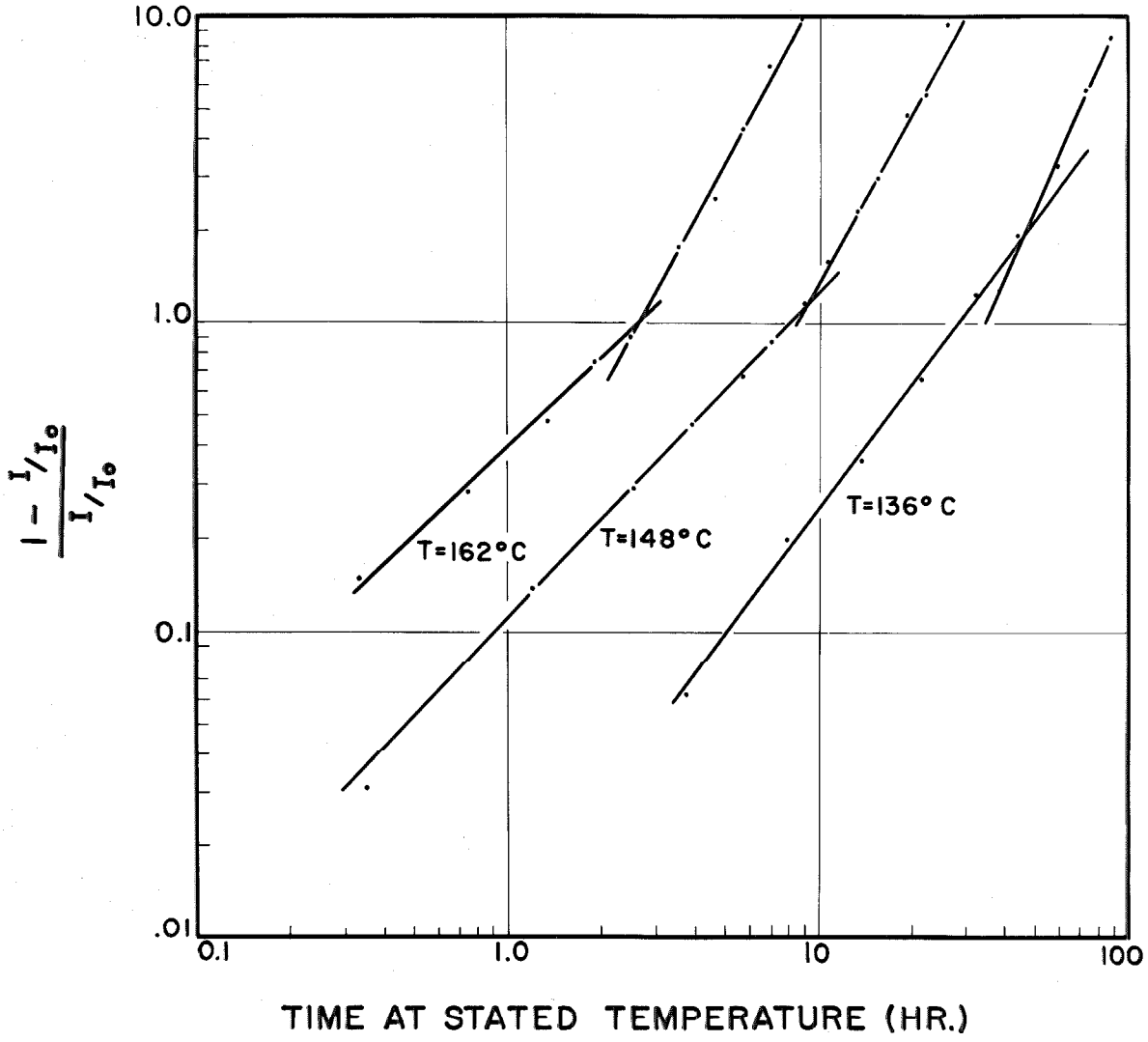

Figure 42. Determination of m of Equations 7 - 9 for the 60.1 at. % Ag;Cu composition, using x-ray diffraction data.

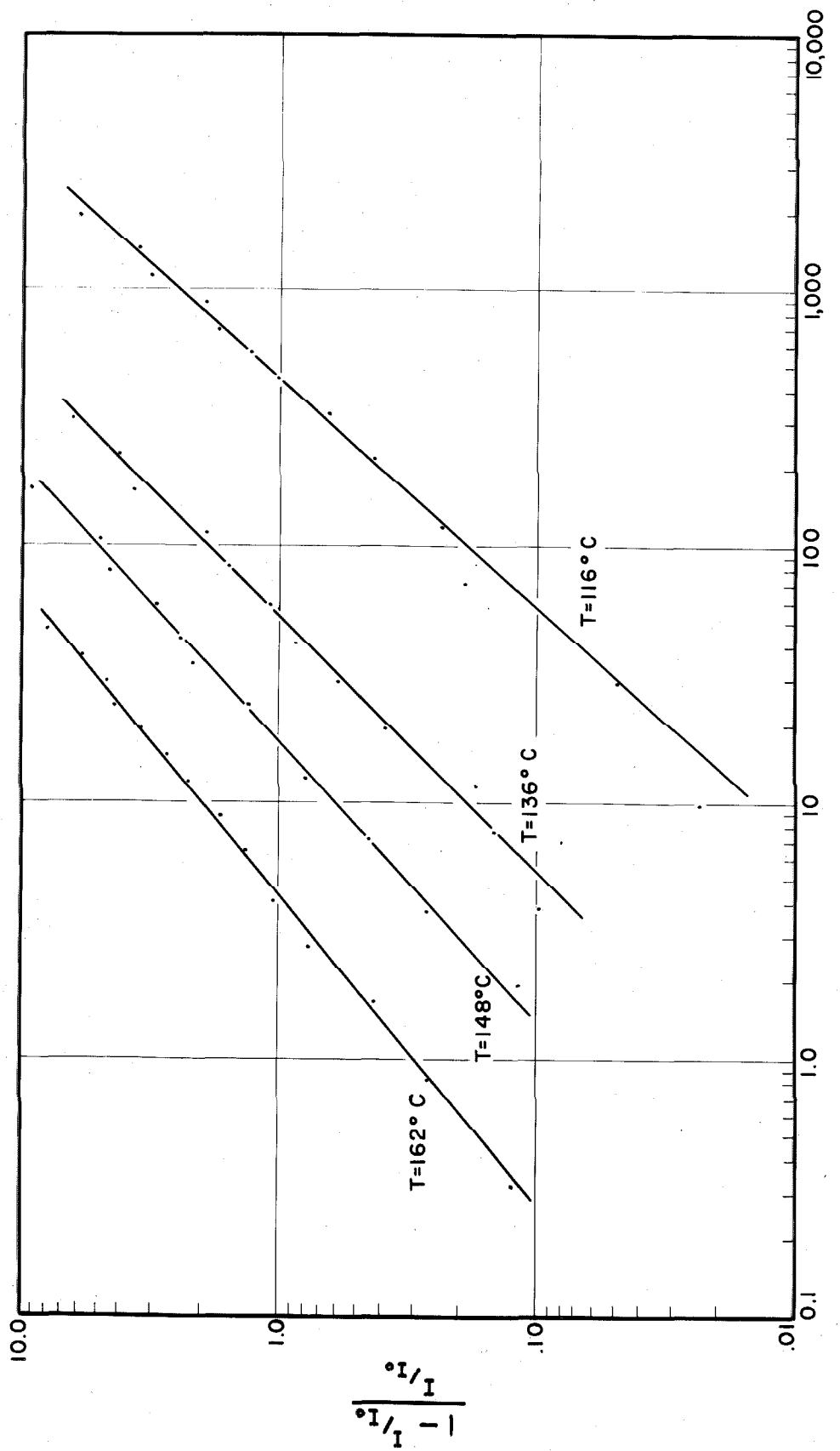

Figure 43. Determination of m of Equations 7 - 9 for the 75.0 at.% Ag;Cu composition, using x-ray diffraction data.

TABLE IX

EXPONENT m AS DETERMINED FROM FIGURES 42 AND 43.

Composition (at.% Ag)	Temperature (°C)	m (t = small)	m (t = large)
60.1	136.0 ± .2 °C	.77	.44
60.1	148.0 ± .2 °C	.95	.55
60.1	162.0 ± .2 °C	1.04	.57
	Average	.92	.52
75.0	116.0 ± .2 °C	.89	.89
75.0	136.0 ± .2 °C	.99	.99
75.0	148.0 ± .2 °C	1.09	1.09
75.0	162.0 ± .2 °C	1.20	1.20
	Average	1.04	1.04

Upon glancing at these results, one might be led to the conclusion that the precipitates are essentially disk-like. That this would be an erroneous conclusion is pointed out by the results obtained for the Johnson-Mehl equation. Since the latter equation demonstrated pronounced depletion effects, the result $m \simeq 1$ in the Austin-Rickett equation must also evidence these effects, due to the allowance which the Austin-Rickett equation makes for depletion and impingement. The only conclusion which can be drawn is that the precipitates must be "three dimensional" in general, with the possibility of some disk-like precipitates not discounted. The change in the value of m at large times may be associated with impingement

and additional depletion caused by adjacent transformed regions rather than just by the growth of nuclei within a given transforming region. It should be noted that, as expected, in this treatment the same type of temperature dependence of m was observed as was found for n previously. Values of Q calculated from a plot of Equation 10 were in general agreement with the values obtained in Chapter IV but involved sufficient scatter of points to make their usefulness dubious.

By way of comparison with studies of alloys quenched from the solid state, some comments about continuous and discontinuous precipitation as briefly referred to previously are held to be in order. As defined by Gayler,[82] discontinuous precipitation is characterized by a preferential precipitation in the grain boundaries, which then can spread inwards. Precipitation within the grains is nonuniform. X-ray diffraction records show the gradual appearance of faint lines belonging to the new phase (s), which increase in intensity as precipitation continues. The lines corresponding to the parent phase(s) correspondingly decrease in intensity without an appreciable shift in position. On the other hand, continuous precipitation is characterized by reasonably uniform precipitation throughout the grains at essentially the same rate everywhere, with no preference for grain boundaries. The x-ray lines shift regularly from those of the original phase(s) to those of the new phase(s). In this thesis the

stipulation of preferential precipitation in grain boundaries included in Gayler's definition has been removed in defining discontinuous precipitation.

Jones, Leech, and Sykes [83] have studied precipitation in Ag-Cu alloys and have concluded that for this system:

(1) Crystals undergoing discontinuous precipitation are composed mainly of regions in which precipitation either has not commenced or is completed.

(2) Discontinuous precipitation occurs when the degree of supersaturation is high and the temperature is low.

(3) Discontinuous precipitation is accompanied by fragmentation.

(4) Discontinuous precipitation may become catastrophic in small regions due to strain energy considerations, causing the precipitation to go very rapidly to completion in these regions.

Gayler and Carrington, [73] while lending support to the above conclusions, have further pointed out that a critical degree of supersaturation which varies with the time and temperature of ageing is the most important factor controlling the type of precipitation in Ag-Cu alloys.

It is evident that many of the original quenched-in nuclei would necessarily be localized in grain boundaries, but even for these nuclei

it is probable that their growth would so strain the surrounding lattices, that parts of the lattices of the neighboring grains would collapse under the strain, further enhancing the growth of these nuclei. This process, coupled with the previous conclusions of this chapter, would lead one to expect that the grain size in the fine-grained regions of foils should not have changed markedly after transformation at low temperatures of aging. The breakdown of the columnar structure has already been discussed.

The primary diffusion mechanism involved in the transformation of rapid-quenched foils is worthy of consideration. In general, for self-diffusion in metals like Ag and Cu the volume diffusion activation energy is about 2 or 3 times as large as the grain boundary diffusion activation energy. The volume diffusion activation energy may be lowered at low temperatures, however, by the presence of short-circuiting paths, such as dislocations. This effect is estimated by Hart [84] to yield an overall increase in the volume diffusion coefficient of only about 5% at 600 °C for dislocation densities which amount to about 10^7 cm./cm.^{3} However, in the present investigation not only is the temperature of aging considerably lower, but the density of quenched-in dislocations is likely to be very high. [45] The presence of additional quenched-in vacancies or interstitials may also have a considerable effect.

That neither grain boundary diffusion, nor diffusion enhancement by quenched-in defects could play a major role is demonstrated by the values of diffusion activation energies cited in Table VI and by a comparison of the results cited in this chapter for rapid-quenched foils and foils quenched from the solid state. It is apparent from Figs. 28 and 29 that, in view of the previously discussed grain size effects, the transformation rates for both types of foils are essentially the same. Furthermore, it is noteworthy from the photomicrographs of Figs. 30 - 34 that precipitation in foils quenched from the solid state appears to be uniform and without preference for grain boundaries. On the basis of these observations it is concluded that due to the very localized nature of the precipitation in rapid-quenched foils, diffusion along grain boundaries and other short circuiting paths does not contribute much.

The high values of Q obtained in Chapter IV for the transformation process make the above conclusions rather convincing, particularly since Q is essentially the activation energy for diffusion, most of the nuclei being present quite early in the transformation process. It should be noted that the values reported in Table VI for direct diffusion measurements were made at considerably higher temperatures than those of the present investigation. In general, for precipitation reactions $Q = A + B(T)$ where B is a temperature -

dependent activation energy which is small at low temperatures but increases as the temperature increases in cases where the supersaturation or driving force for the reaction decreases with increasing temperature. Then, for temperatures at which B(T) is not negligible,

$$\frac{\partial \ln t}{\partial (1/T)} = \frac{A}{R} + \frac{B}{R} + \frac{1}{RT}\frac{\partial B}{\partial (1/T)} .$$

Thus, the value of Q determined from the slope of a ln t vs. 1/T plot for higher temperatures may be somewhat less than the actual value of Q at low temperatures. The measured value of Q at low temperatures will be less than the measured value at high temperatures, provided that

$$\frac{B}{R}\Big|_{T_{low}}^{T_{high}} > \frac{1}{RT}\frac{\partial B}{\partial (1/T)}\Big|_{T_{low}}^{T_{high}} ,$$

which is generally the case. Thus, Q as measured in Chapter IV is rather close to the Q which might be expected for volume diffusion for the temperatures and solid solution compositions in question, particularly in view of the influences of alloying and of chemical driving force in the lowering of activation energies.

As an extention of this work, the study of short range clustering in the extended metastable solid solutions would undoubtedly prove to be of interest.

C. CONCLUSIONS

Results indicate that the transformation of metastable Ag-Cu solid solutions obtained by rapid quenching from the liquid state occurs by the growth of stable-phase nuclei, most of which are present immediately after solidification or soon thereafter. No pre-precipitation stage was observed. Precipitation of the stable phases takes place discontinuously, with small regions transforming completely, while the rest of the matrix remains unchanged; and this process continues until the entire matrix is finally transformed. Depletion effects are present very early in the process. Results show the role of quenched-in defects to be unimportant, at least after most of the nucleation has taken place. Volume diffusion, rather than grain boundary or short-circuit diffusion, is the primary mechanism for migration of atoms and controls the rate of transformation. Activation energies of $33,600 \pm 2500$ cal./g. mole and $33,100 \pm 2000$ cal./g. mole were obtained for the transformation of the 60.1 at.% Ag;Cu and 75.0 at.% Ag;Cu solid solutions, respectively.

In general, the microstructure of rapid-quenched foils consists of columnar regions near the surfaces of the foils, with a fine grained structure in the central portions of the foils. Occasionally, a coarser grained structural constituent was present between the columnar and fine grained regions. This microstructure can be

accounted for by considering relative rates of nucleation from the melt. Results indicate that with the present degree of undercooling the maximum rate of nucleation was not reached.

REFERENCES

(1) E. A. Smith, J. Inst. Metals, (1939), 65, 271-275.

(2) A. Mattheissen, Brit. Assoc. Advancement Sci., (1863), 37.

(3) A. Mattheissen and C. Vogt, Trans. Roy. Soc. London, (1865), A154, 167.

(4) W. C. Roberts-Austen, Proc. Roy. Soc. London, (1875), 23, 481 - 495.

(5) M. K. Arafa, Proc. Phys. Soc. London, (1949), B62, 238-241.

(6) C. H. Johansson and J. O. Linde, Z Metallkunde, (1928) 20, 443-444.

(7) A. L. Norbury, J. Inst. Metals, (1928), 39, 149-150.

(8) A. Wilm, Metallurgie, (1911), 8, 225-227.

(9) A. Wilm, J. Inst. Metals, (1912), 7, 274.

(10) P. D. Merica, R. G. Waltenberg, and H. Scott, Trans. A.I.M.E., (1920), 64, 41-77.

(11) M. Hansen and K. Anderko, Constitution of Binary Alloys, (1958), 18-20.

(12) Pol Duwez, R. H. Willens, and W. Klement, Jr., J. Appl. Phys., (1960), 31, 1136

(13) T. Banerjee and P.L. Ahuja, Mem. sci. rev. mét., (1961) 58.

(14) Paul Pietrokowsky, Rev. Sci. Inst., (1962), 34, 445-446.

(15) S. Mader, H. Widmer, F. M. d'Heurle, and A. S. Nowick, Appl. Phys. Let., (1963), 3, 201-203.

(16) W. Klement, Jr., Doctor's Thesis, Calif. Inst. of Technology, (1962).

(17) N. Ageew, M. Hanson, and G. Sachs, Z Physik, (1930), 66, 350-376.

(18) M. Cohen, Trans. A.I.M.E., (1937), 124, 138-157.

(19) W. F. Cox and C. Sykes, J. Inst. Metals, (1940), 66, (Part 11), 350-387.

(20) W. Koster and H. Dietrich, Z. Metallkunde, (1952), 43, 449-453.

(21) W. Koster and W. Knorr, Z.Metalkunde, (1954), 45, 350-356.

(22) P. Wiest, Metallwirtschaft, (1933), 12, 47-48.

(23) H. Pfister and P. Wiest, Metallwirtschaft, (1934), 13, 317-320.

(24) H. Bumm, Metallwirtschaft, (1935), 14, 429-431.

(25) M. Gayler and W. E. Carrington, J. Inst. Metals, (1947), 14, 625-639.

(26) O'Neill, Farnham, and Jackson, J. Inst. Metals, (1933), 52, 75-84.

(27) N. Swindells and C. Sykes, Proc. Roy. Soc. London, (1938), A168, 237-264.

(28) Pol Duwez and R. H. Willens, Trans. A.I.M.E. (Met.), (1962), 227, 362-365.

(29) E. A. Owen and J. Rogers, J. Inst. Metals, (1935), 57, 257-266.

(30) N. Ageev and G. Sachs, Z. Phys., (1930), 63, 293 - 303.

(31) H. D. Megaw, Phil. Mag., (1932), 14, 130-142.

(32) N. Ageev, M. Hansen, and G. Sachs, Z. Phys., (1930), 66, 360-376.

(33) R. A. Swalin, Thermodynamics of Solids, (1962).

(34) O. Kubaschewski and E. Evans, Metallurgical Thermochemistry, (1951).

(35) C. D. Hodgman (ed.), Handbook of Chemistry and Physics (CRC), 42nd Edition, (1960), 1882 - 1915.

(36) C. J. West and C. Hull (ed.) International Critical Tables (National Research Council), (1933), 5, 122.

(37) C. Kittel, Introduction to Solid State Physics, Second Edition, (1956), 132.

(38) E. Scheil, Z. Elektrochem., (1943), 49, 242-254.

(39) H. K. Hardy, Acta Met., (1953), 1, 202-209.

(40) T. Heumann, Z. Metallkunde, (1951), 42, 182-189.

(41) R. A. Oriani and W. K. Murphy, J. Phys. Chem., (1958), 62, 199-202.

(42) Orr and Hultgren, private communication cited in Reference (41).

(43) O. Kubaschewski and J. A. Catterall, Thermodynamic Data of Alloys, (1956), 60.

(44) S. H. Maron and C. F. Prutton, Principles of Physical Chemistry, (1958), 96.

(45) G. Thomas and R. H. Willens, Acta Met., (1964), 12, 191-196.

(46) T. Lyman (ed.), Metals Handbook (ASM), (1958), 617.

(47) F. Weinberg and B. Chalmers, Canad. J. Phys., (1952), 30, 488-502.

(48) C. A. Wert, J. Appl. Phys., (1949), 20, 943-949.

(49) H. K. Hardy and T. J. Heal, Ch. 4 in: B. Chalmers and R. King (ed.), Progress in Metal Physics, (1954), 5, 143-278.

(50) C. T. Tomizuka and E. Sonder, Phys. Rev., (1956), 103, 1182-1184.

(51) R. E. Joffman, D. Turnbull, and E. W. Hart, Acta Met., (1955), 3, 417-424.

(52) O. Kubaschewski, Trans. Faraday Soc., (1950), 46, 713-722.

(53) S. D. Gertsriken and A. L. Revo, Phys. Metals and Metallog., (1960), 9, (No. 4), 92-97.

(54) A. Sawatsky and F. E. Jaumot, Jr., Trans AIMA, (1957), 209, 1207-1210.

(55) W. Seith and E. Peretti, Z. Elecktrochem, (1936), 42, 570-579.

(56) A. Kuper, H. Letaw, L. Slifkin, E. Sonder and C. T. Tomizuka, Phys. Rev., (1954), 96, 1224-1445.

(57) R. E. Hoffman and D. Turnbull, J. Appl. Phys., (1951), 22, 634-639.

(58) D. Turnbull and R. E. Hoffman, Acta Met., (1954), 2, 419-426.

(59) H. Margolin, Doctor's Thesis, Yale University, (1950).

(60) Y. Mishima, Rept. Inst. Sci. and Technol. Univ. Tokyo, (1949), 3, 210-213.

(61) Y. Mishima, "Study on Age-Hardening" in: W. M. Baldwin (ed.), Proc. First World Metallurgical Congress, 1951 (ASM), (Pub. 1952), 668-681.

(62) C. D. Hodgman (ed.), Handbook of Chemistry and Physis (CRC), 42nd Edition, (1960), 2589-2595.

(63) D. Turnbull, J. Chem. Phys., (1950), 18, 769.

(64) D. Turnbull and J. C. Fisher, J. Chem. Phys., (1949), 17, 71-73.

(65) S. Glasstone, K. J. Laidler, and H. Eyring, The Theory of Rate Processes, (1941), 496.

(66) K. A. Jackson, Liquid Metals and Solidification (ASM), (1958), 174-186.

(67) G. A. Colligan and B. J. Bayles, Acta Met., (1962), 10, 895-897.

(68) A. Rosenberg and W. C. Winegard, Acta Met., (1954), 2, 342-343.

(69) W. Humme-Rothery, J. Phys. Chem., (1940), 44, 808-824.

(70) H. Suzuki, Tohoku Univ. Sci. Repts., (1952), A4, 455-463.

(71) R. D. Heidenreich and W. Shockley, Strength of Solids (Bristol Conference), (1948), 57-75.

(72) C. S. Barrett, H. F. Kaiser, and R. F. Mehl, Trans AIME (Met), (1935), 117, 39-57.

(73) M. L. V. Gayler and W. E. Carrington, J. Inst. Metals, (1947), 73, 625-639.

(74) F. R. N. Nabarro, Proc. Phys. Soc. London, (1940), 52, 90-104.

(75) A. Opinsky and R. Smoluchowski, Phys. Rev., (1948), 74, 343.

(76) A. G. Geisler, Ch. 15 in: R. Smoluchowski, J. E. Mayer, W. A. Weyl, (editors), Phase Transformations in Solids (Cornell Symposium - 1948), (Pub. 1951), 387-536.

(77) C.S. Barrett, Discussion to reference (76), 536-537.

(78) W. A. Johnson and R. F. Mehl, Trans AIME (Iron and Steel Div.), (1939), 135, 416-458.

(79) C. Wert and C. Zener, J. Appl. Phys., (1950), 21, 5-8.

(80) C. Zener, J. Appl. Phys., (1949), 20, 950-953.

(81) J. B. Austin and R. L. Rickett, Trans AIME (Iron and Steel Div.), (1939), 135, 396-415.

(82) M. L. V. Gayler, J. Inst. Metals, (1947), 73, 681-691.

(83) F. W. Jones, P. Leech and C. Sykes, Proc. Roy. Soc. London, (1942), A181, 154-168.

(84) E. W. Hart, Acta Met., (1957), 5, 597.

(85) C. D. Hodgman (ed.) Handbook of Chemistry and Physics (CRC), 42nd Edition, (1960), 2130-2132.

(86) D. Turnbull and R. E. Cech, J. Appl. Phys., (1950), 21, 804-810.

(87) R. E. Cech and D. Turnbull, J. Metals, (1951), 3, 242-243.

APPENDIX

DETERMINATION OF ΔF_c FOR FORMATION OF 75.0 at.% Ag;Cu NUCLEI FROM THE LIQUID STATE

As discussed in Chapter V, for a spherical nucleus

$$\Delta F = \Delta F_V \left(\frac{4}{3}\pi r^3\right) + \Delta F_S \left(4\pi r^2\right).$$

Imposing the condition that $\left.\frac{\partial(\Delta F)}{\partial r}\right|_{r_c} = 0$ leads to:

$$r_c = -\frac{2(\Delta F_S)}{\Delta F_V}$$

so that

$$\Delta F_C = \frac{\frac{16}{3}\pi(\Delta F_S)^3}{(\Delta F_V)^2} \quad . \tag{11}$$

In the ensuing discussion the following new symbols, subscripts, and definitions will be used:

SYMBOL	DEFINITION
α	composition of maximum equilibrium primary solid solubility of Ag in Cu, which is a function of temperature
α'	composition of maximum equilibrium primary solid solubility of Ag in Cu at 779 °C
β	composition of maximum equilibrium primary solid solubility of Cu in Ag, which is a function of temperature
β'	composition of maximum equilibrium primary solid solubility of Cu in Ag at 779 °C
$(F_V)_{\alpha+\beta}$	chemical free energy of amount of solid ($\alpha+\beta$) which would be needed to form exactly one cm.^{3} of 75.0 at.% Ag;Cu solid solution (cal./cm.^{3})

SYMBOL	DEFINITION
$(F_v)_l$	chemical free energy of liquid containing same number of atoms as one $cm.^3$ of solid of the same composition ($cal./cm.^3$)
ΔH_γ	integral enthalpy of solution per g. mole of γ (cal./g. mole)
$\Delta H_{\alpha+\beta}$	integral enthalpy of solution of amount of solid ($\alpha+\beta$) which forms from one g. mole of 75.0 at.% Ag;Cu liquid (cal./g. mole)
l	liquid
L_f	latent heat of fusion (cal./g. mole)
L'_f	weighted average of the latent heats of fusion of the elements in a binary mixture (cal./g. mole of mixture)
μ	metastable 75.0 at.% Ag;Cu composition
S_M	entropy of mixing (cal./g. mole - ^oK)
$(S_M)_{\alpha+\beta}$	entropy of mixing of amount of solid ($\alpha+\beta$) which forms from one g. mole of 75.0 at.% Ag;Cu liquid (cal./g.mole - ^oK)
σ	solid
V	specific volume of 75.0 at.% Ag;Cu solid solution ($cm.^3$/g. mole)

For pure metals $\Delta F_v = 0$ at the melting point T_m. On the other hand, for the alloy in question (75.0 at .% Ag;Cu) there is no distinct melting point; however, the chemical free energy $(F_v)_{\ell\mu}$ must be equal to $(F_v)_{\alpha'+\beta'}$ at a temperature somewhere between $T_{\text{liquidus}\,(\mu)}$ and 779°C (refer to Fig. 1), since the free energy of a phase is a continuous function of temperature and $(F_v)_{\ell\mu} < (F_v)_{\alpha'+\beta'}$ at $T_{\text{liquidus}\,(\mu)}$, while $(F_v)_{\ell\mu} > (F_v)_{\alpha'+\beta'}$ at 779°C. Therefore, no great error is introduced by choosing a temperature midway between 1052°K (779°C) and $T_{\text{liquidus}\,(\mu)}$ to represent T_m. This results in an effective value of $T_m = 1079$°K (806°C).

Now, $\left(\frac{\partial(\Delta F_v)}{\partial T}\right)_p = -\Delta S$ and $\Delta S\Big|_{T_m} = \frac{(\Delta H)_{\ell\to\sigma}}{T_m} = \frac{L_f}{T_m V}$

Then, since changes in vibrational entropy with composition should be small in view of the small deviation from Vegard's law found in Chapter II,

$$(-V)(\Delta F_v)_{\ell\mu\to\alpha+\beta} = \int_T^{T_m} \Delta S\, dT$$

$$\simeq \frac{T_m - T}{T_m}\left[L_f' + (\Delta H_{\ell\mu} - \Delta H_{\alpha'+\beta'})\right] + \int_T^{T_m}\left[(S_M)_{\alpha+\beta} - (S_M)_{\ell\mu}\right] dT,$$

and $(-V)(\Delta F_v)_{\alpha+\beta\to\sigma\mu} \simeq -\left[\Delta H_{\sigma\mu} - \Delta H_{\alpha+\beta}\right] + T\left[(S_M)_{\sigma\mu} - (S_M)_{\alpha+\beta}\right]$;

thus, $(-V)(\Delta F_v)_{\ell\mu\to\sigma\mu} \simeq \frac{T_m - T}{T_m}\left[L_f' + (\Delta H_{\ell\mu} - \Delta H_{\alpha'+\beta'})\right] - \int_T^{T_m}\left[(S_M)_{\ell\mu} - (S_M)_{\alpha+\beta}\right] dT$

$$- \left[\Delta H_{\sigma\mu} - \Delta H_{\alpha+\beta}\right] + T\left[(S_M)_{\sigma\mu} - (S_M)_{\alpha+\beta}\right] \qquad (12)$$

Using 1) Hume-Rothery's values of the latent heats of fusion[64] $(L_f)_{Ag} = 2,690$ cal./g. mole and $(L_f)_{Cu} = 3,100$ cal./g. mole,

2) $V = 9.5\ \text{cm}^3$/g. mole, as computed from density values[85] and Fig. 3,

3) the solid solubility data compiled by Hansen and Anderko, [12]

4) the integral enthalpies of solution calculated by Scheil, [38] and

5) the assumption of a regular solution, as was found to be valid for the liquid state, [43]

The value of $(\Delta F_V)_{l \rightarrow \sigma\mu}$ could be determined as a function of temperature from Equation 12. To this end, the following expressions were obtained by a least squares fit to values computed from data presented in the above mentioned sources:

$$(S_M)_{\alpha+\beta} = \left[3.99\times10^{-11}T^3 + 1.73\times10^{-7}T^2 - 7.22\times10^{-5}T + 1.02\right] \text{cal./cm.}^3\text{-}^\circ\text{K}$$

and

$$\Delta H_{\alpha+\beta} = \left[-5.42\times10^{-8}T^3 + 2.71\times10^{-4}T^2 - 1.09\times10^{-1}T + 1.33\times10^{1}\right] \text{cal./cm.}^3$$

As far as ΔF_S is concerned, a weighted average of Turnbull's values for pure Ag and pure Cu [63] calculated from the data of Turnbull and Cech [86] could be used and should not be too poor an estimate in view of the approximate nature of this calculation. This assumption is supported by the data of Cech and Turnbull for the Cu-Ni system. [87] Turnbull's values of ΔF_S are 126 ergs/cm.^{2} for Ag and 177 ergs/cm.^{2} for Cu, which yield a weighted average of 139 ergs/cm.^{2} = 3.32×10^{-6} cal./cm.^{2} for the alloy in question. It was found that even if this estimate of ΔF_S is off by a factor of two in either direction, the conclusions of Chapter V are not affected, although any estimate of the absolute nucleation rate would change by several orders of magnitude and the shapes of the

peaks of Fig. 37 would change slightly. This serves also to point out the fact that deviations from the spherical shape of nuclei should not affect the conclusions.